From Molecule to Movement: An Integrated Multiscale Study of Age-Related Human Skeletal Muscle Dysfunction

By

Justin Ray Lopez

A dissertation submitted in partial fulfillment of

the requirements for the degree of

Doctor of Philosophy

(Kinesiology)

at the

UNIVERSITY OF WISCONSIN-MADISON

2026

Date of final oral examination: 04/29/2026

The dissertation is approved by the following members of the Final Oral Committee:

Gary M. Diffee, Professor, Kinesiology
William G. Schrage, Professor, Kinesiology
Janet L. Branchaw, Associate Professor, Kinesiology
Jill N. Barnes, Associate Professor, Kinesiology
Adam R. Konopka, Assistant Professor, Medicine

Acknowledgements

It's nice not having to write something in such an academic and formal tone after all the scientific writing the last few months. I probably shouldn't have waited last minute to write this section either. After spending months writing and revising, the last thing I want to do is write more, and the last thing my committee probably wanted was another page to read. So, to my committee, thank you for your patience, including now, when I was supposed to have sent this out to you yesterday.

To my mentor, Dr. Diffee, do I still need to call you that once I earn my PhD, or do you start calling me Dr. Lopez? There are many things I could thank you for, but I will keep it to what I think has helped me most in navigating this process and becoming a better scientist: your patience. I'm still not entirely sure why you welcomed me into your lab with absolutely zero wet-lab experience after little more than an email and a phone call, but I'm glad you did. One of my favorite memories from my time in the lab goes all the way back to the Natatorium when I first started, and I'll start with saying it's not when I packed up the lab for the move to MSC, or when you said you had something to teach me and then handed me forceps and dental floss to tie some loops under a microscope. Nope, it was after you spent time teaching me how to run zymography gels, and then eventually had me run them on my own. After a few weeks of getting absolutely no results, I was convinced I had tried everything possible and the results were still null. One day you came in to check things out, and within ten seconds you unplugged the gel lid from the power pack, flipped the leads, plugged them back in, and the gel started working normally. You looked at me and then walked out. Good times. At that point, I wasn't entirely sure whether I had already worn out your patience after only a couple of

months in the lab, or asking if I needed some type of training to use liquid nitrogen, or even how to dilute a 4× buffer with water, but here I am seven years later getting ready to defend. All of that is to say, thank you for your patience, your guidance, and for the opportunity to grow into a scientist in your lab. Jokes aside, thank you for your mentorship and guidance, Dr. Diffee, I hope to one day be as patient and open-minded a mentor as you have been to me. There is much more I could say, but your training taught me to be concise in writing, so I will leave it there and let you decide how well that training worked.

Thank you to my committee, your mentorship, guidance, feedback, and thoughtfulness in both your questions and discussions have made me a better scientist. Dr. Schrage, thank you for always having an analogy for just about anything in science. I have tried to take that with me and become better at communicating science, especially in my teaching. Dr. Branchaw, thank you not only for your scientific mentorship, but also for your mentorship in teaching. I can only hope to become even a fraction as effective an educator as you are. I will also always appreciate all of the conversations we had walking back from College Library. Dr. Barnes and Dr. Konopka, thank you for asking the kinds of questions that genuinely made me pause and think more deeply about my work and viewing it from different angles than I otherwise would have. Your suggestions on research design and how to look at data and what logical steps to take next sent me down rabbit holes of reanalyzing data and looking at things from entirely different perspectives, usually by spending more time in GraphPad and delaying my writing even further (Dr. Diffee, you can blame them for that). Genuinely, thank you all. Without your feedback and constructive criticism, I would not have

developed into the scientist I am today and I will continue to try and improve to be an asset to students like you have been to me. I will take something I learned from each of you with me into whatever comes next.

To all the Diffee Lab members: Jared… But also the undergrads, Nolan, Zach, Rasmus, Eli, and everyone else who has been part of the lab along the way, thanks for making it such an enjoyable process. It's not uncommon to hear horror stories about graduate school, but honestly, this has been the most fun "job" I've ever had. And I have all of you to thank for that.

To my past mentors, Dr. Alvar, Dr. Lewis and Dr. Dondzila, thank you for allowing me as an undergrad to get my feet wet in research. It directly set me on the path to where I am now, and I'm especially grateful for that. Dr. Alvar, thank you as well for your mentorship during my master's, and for helping shape the certainty that I knew a PhD was exactly what I wanted to do next.

To my family and friends. Thank you for your never-ending support, and being a space away from science, but also allowing me to nerd out and talk your ears off about what I think is awesome.

Sarah, this was something I was able to do because of you. Your unrelenting support meant there was no way I could not see this through. More than a decade ago, I told you that I wanted to earn my PhD, and you were all for it. Thank you for letting me practice teaching content with you at random, for letting me talk through conceptual experimental thoughts, and for showing up to my poster presentations just because you wanted a picture of me in front of the poster (but really it was probably the cool plots and graphs). Thank you for surprising me during long days with Enzo and Poppy

throughout my MS and PhD and thank you for being my biggest supporter through all of it. And they deserve their own thanks too: thank you Enzo, Bullwinkle, and Poppy.

ABSTRACT

Sarcopenia is characterized by age-related declines in skeletal muscle mass and function, yet losses in strength and especially power exceed the loss of muscle tissue alone, suggesting that intrinsic contractile dysfunction contributes to impaired performance. The central premise of this dissertation was that age-related muscle dysfunction reflects integrated impairments across biological scales, such that whole-muscle deficits are linked to fiber-type-specific alterations in single muscle fiber mechanics, which are in turn associated with molecular changes within the sarcomeric contractile apparatus. To test this premise, a multiscale approach was employed in younger and older men and women that combined whole-muscle knee extensor function and body composition testing, fiber-type-stratified single muscle fiber mechanical experiments from the vastus lateralis, and paired top-down proteomic characterization of the same individual fibers that completed mechanical testing.

Chapter II (Aim 1) examined age-related alterations in single muscle fiber contractile properties across fiber types. Peak power was approximately 32% lower in older adults in both Type I and Type II fibers. This deficit was not attributable to slower shortening velocity, which was preserved with aging in both fiber types, indicating that the reduction in power was primarily force related. Type I fibers exhibited lower absolute peak force with preserved specific force, whereas Type II fibers exhibited lower specific force and normalized power, indicating intrinsic contractile dysfunction. Notably, Type II dysfunction occurred without a significant reduction in fiber cross-sectional area, demonstrating that impaired muscle quality can emerge independently of overt atrophy.

Chapter III (Aim 2) determined the relationship between single muscle fiber mechanics and whole-muscle function. Type II fiber force, power, and size emerged as the principal cellular correlates of whole-muscle performance, whereas Type I associations were weaker and largely explained by shared age-related decline. Whole-muscle peak power was the outcome most tightly coupled to Type II fiber mechanics and the specific outcome for which aging attenuated the cellular-to-whole-muscle relationship. Absolute Type II properties retained independent predictive value after age adjustment, indicating a genuine cellular contribution to whole-muscle performance beyond shared age-related covariation.

Chapter IV (Aim 3) identified molecular correlates of single muscle fiber contractile function using top-down proteomics performed on the exact same fibers that completed mechanical testing. Fast-associated isoforms, including MLC1F, MLC2F, and fsTnC, were strongly associated with maximal shortening velocity, while α-tropomyosin, β-tropomyosin ratio, and MLC2F-related proteoforms tracked absolute peak power. Together, these findings demonstrate that age-related muscle dysfunction is an integrated, multiscale phenomenon linking whole-muscle deficits, intrinsic single-fiber dysfunction, and candidate molecular features of the sarcomeric proteome.

Table of Contents

CHAPTER I

REVIEW OF THE LITERATURE

INTRODUCTION

Sarcopenia, the age-related progressive loss of skeletal muscle mass and function, is a defining feature of biological aging and a major contributor to frailty, falls, loss of independence, and mortality in older adults (1–5). Although reductions in muscle mass are the most readily measured hallmark of sarcopenia, the disproportionate decline in strength and, especially, power relative to the loss of mass has been recognized for more than three decades and remains incompletely explained (6–14). This discrepancy indicates that age-related muscle dysfunction cannot be attributed to atrophy alone; rather, it reflects integrated impairments across whole-muscle, cellular, and molecular levels of organization. The central premise of this dissertation was that the age-related muscle dysfunction reflects integrated impairments across biological scales: whole muscle contractile deficits are linked to fiber-type-specific alterations in single muscle fiber mechanics, and those cellular deficits are in turn associated with molecular changes within the sarcomeric contractile apparatus. To test this premise, a multiscale experimental approach was employed in younger and older men and women, combining whole-muscle knee extensor function and body composition testing, fiber-type-stratified single muscle fiber mechanical experiments from the vastus lateralis, and paired top-down proteomic characterization of the same individual fibers that had completed mechanical testing. The three experimental chapters addressed this premise in sequence, progressing from the cellular phenotype (Chapter II), to its translation to whole-muscle function (Chapter III), and finally to its molecular correlates (Chapter IV).

Clinical Significance

Sarcopenia affects an estimated 10–16% of adults worldwide, and its prevalence is climbing in parallel with global population aging; by 2050, approximately one in six people will be over the age of 60, placing an unprecedented burden on healthcare systems and long-term care infrastructure (1–5). After the third decade of life, skeletal muscle mass declines at roughly 3–8% per decade, accelerating after age 60, while strength declines at 1–3% per year and power declines earlier and more precipitously still, as much as 3–4% per year beginning in the fourth decade (1–4, 15, 16). The clinical consequences of these changes are substantial. Low muscle strength and low muscle power independently predict mobility limitation, hospitalization, disability, and all-cause mortality, and their prognostic value often exceeds that of muscle mass itself (11–14, 17–22). Direct healthcare costs attributable to sarcopenia in the United States have risen from approximately $18.5 billion in 2000 to an estimated $40.4 billion by 2019, and these figures substantially underestimate the true economic burden once indirect costs from caregiving, lost productivity, and long-term care are included (5–10). Importantly, the clinical trajectory of sarcopenia is not driven primarily by loss of muscle size; it is driven by loss of muscle function, and particularly by loss of the rapid, forceful contractions required for daily mobility, balance recovery, and fall prevention. This clinical reality motivates the present dissertation’s focus on the contractile determinants of age-related muscle dysfunction across progressively finer levels of biological resolution.

Whole-Muscle Contractile Dysfunction in Aging

The functional consequences of sarcopenia are routinely documented in the clinical literature through performance-based assessments, gait speed, grip strength, chair-rise time, and the short physical performance battery, all of which are associated with adverse health outcomes (11–14, 17–19, 21, 22). These measures are pragmatic and prognostically valuable, but they capture the downstream consequences of muscle dysfunction rather than the contractile mechanisms responsible for it. They cannot resolve whether impaired performance arises from deficits in force, velocity, or power, nor can they distinguish atrophy-driven losses from intrinsic impairments of the contractile machinery. This mechanistic limitation underscores the value of direct contractile assessment through isokinetic dynamometry, which provides criterion-standard measurement of torque, shortening velocity, and power under controlled conditions and permits identification of the specific contractile properties most affected by aging (23–28).

Cross-sectional and longitudinal studies using these laboratory approaches consistently document significant age-related declines in peak torque, maximal shortening velocity, rate of force development, and power, particularly in the knee extensors, which are central to gait, stair climbing, chair rise, and fall recovery (7, 11, 15, 29–38). Peak torque is reduced by approximately 8–47% across isokinetic velocities in older compared to younger adults, with larger deficits at higher contraction speeds, a velocity-dependent pattern consistent with preferential compromise of Type II fiber-dependent contractions (31–33, 39, 40). Rate of force development, the speed of early-phase force generation essential to balance recovery, declines to a proportionally

greater degree than peak torque (16, 41–49). Power, the product of force and velocity, is the most sensitive and clinically consequential contractile property affected by aging and is the strongest contractile predictor of mobility limitation and all-cause mortality in older adults (3). Previous cross-sectional studies have reported reductions of 20–60% relative to younger adults with longitudinal rates of decline reaching 3–4% per year (2, 3, 15, 16, 29, 39, 43, 50–53). Critically, these deficits in strength and power persist in many studies after normalization to muscle size or lean mass, indicating that muscle quality, force and power per unit of muscle tissue, also deteriorates with aging and that intrinsic impairments of the contractile apparatus contribute independently to functional decline (7, 14, 31, 33, 35, 36, 43, 50). Whole-muscle testing therefore establishes both the magnitude of the problem and its central paradox: the loss of function outpaces the loss of tissue, and the excess cannot be explained by mass alone.

Mechanisms of Age-Related Muscle Dysfunction

The mechanisms proposed to underlie age-related muscle dysfunction span multiple physiological systems, and each contributes meaningfully to the whole-body phenotype. Aging disrupts the neural control of muscle through preferential loss of large, fast-conducting motor neurons that innervate Type II fibers, with repeated cycles of denervation and incomplete reinnervation driving both fiber loss and fiber-type grouping (5, 26, 54–64). Neuromuscular junction remodeling further impairs signal transmission efficiency, and reductions in cortical excitability limit the recruitment of high-threshold motor units during voluntary contractions. Systemic hormonal changes, declining circulating testosterone, growth hormone, and IGF-1, together with the increasingly recognized phenomenon of anabolic resistance to both feeding and

loading, blunt the normal stimuli for protein accretion and contribute to a chronic imbalance between muscle protein synthesis and degradation (5, 26). Chronic low-grade inflammation, or inflammaging, and the accompanying elevations in circulating cytokines have been linked to accelerated proteolysis and impaired regeneration, while satellite cell numbers and regenerative capacity decline progressively in aged muscle (26). Metabolically, impaired mitochondrial function, elevated reactive oxygen species production, and disrupted calcium handling reduce contractile efficiency and increase susceptibility to fatigue (26, 65–68).

These systemic contributors are essential context for understanding the aging phenotype, and each contributes meaningfully to the clinical trajectory of sarcopenia. However, they share a common analytical limitation, they describe the environment in which aging muscle operates, while leaving the condition of the contractile machinery itself as a separate mechanistic question. They explain, in broad terms, why aged muscle atrophies, why it is less well recruited, and why it is metabolically compromised, but they do not explain what has happened to the basic functional unit of muscle, the sarcomere, or how those sarcomere-level changes translate into the fiber-level and whole-muscle deficits that define the clinical phenotype. Put plainly, work on neural, hormonal, inflammatory, and metabolic contributors to sarcopenia has identified important components of the aging phenotype but has not addressed a distinct mechanistic question: what is the contribution of the single muscle fiber and its contractile apparatus to age-related whole-muscle dysfunction, and what molecular alterations of the sarcomere underlie it. The disproportionate rate of functional decline relative to mass loss points to intrinsic alterations within the contractile apparatus as an

additional, independent, and mechanistically distinct contributor to dysfunction (51). Resolving these intrinsic changes requires isolating the contractile machinery from the neural, architectural, hormonal, and metabolic confounders that shape muscle function in vivo, a capability uniquely provided by the permeabilized single muscle fiber approach, and, at finer resolution still, by direct molecular characterization of the sarcomere.

Single Muscle Fiber Contractile Properties in Human Aging

The permeabilized, or chemically skinned, single muscle fiber technique removes the sarcolemmal membrane while preserving myofilament lattice integrity, enabling direct measurement of intrinsic contractile properties, cross-sectional area (CSA), peak isometric force (P_0), specific force (SF, defined as P_0 normalized to CSA), maximal shortening velocity (V_{max}), peak power output (PPO), and normalized power output (NPO, defined as PPO normalized to CSA), under conditions free from neural, tendinous, and architectural confounders (6, 12, 44–46, 69, 70). Force and power measurements from skinned fibers closely approximate those obtained from intact muscle preparations once normalized to fiber size, validating the physiological relevance of the approach (24, 71). In the context of aging, single fiber experiments provide the mechanistic resolution to identify intrinsic contractile impairments that may precede, exceed, or differ qualitatively from those evident at the whole-muscle level.

Human aging studies using this technique have converged on a fiber-type-specific pattern of vulnerability. Type I fibers demonstrate substantial resilience: the preponderance of evidence shows preserved CSA, P_0, and SF, with only limited and variable evidence of modest shortening velocity decline, and recent work suggests that

absolute and normalized Type I power output may be preserved or even enhanced in older adults, particularly in women (72). This preservation has been attributed to the habitual recruitment of Type I fibers across daily activities, which provides a chronic adaptive stimulus against structural and functional decline, and it carries the important implication that the oxidative, slow phenotype is not inevitably compromised by aging but may instead reflect use-dependent protection. The same conclusion does not extend to Type II fibers, which depend on higher-threshold recruitment that occurs far less frequently in the daily activities of older adults. In contrast, Type II fibers exhibit greater vulnerability across multiple contractile properties. Type II CSA is consistently and significantly reduced in older adults, confirmed by pooled analyses in both sexes (72). Absolute P_0 is reduced in the majority of studies; SF is more variable, with roughly half of published studies reporting significant age-related differences, and those differences split between lower and higher values in older adults, a pattern implicating a complex mix of atrophy-dependent and intrinsic molecular contributors (31, 73–78). Absolute PPO reductions in Type II fibers are largely proportional to CSA reductions, consistent with the dominant role of atrophy in driving absolute power loss; however, NPO is preserved or enhanced in several cohorts, suggesting that the intrinsic power-generating quality per unit of fiber area is not inevitably compromised and may be subject to compensatory adaptation (72). The literature also remains under-powered for sex as a biological variable, and the few studies that have stratified by sex report findings that are not always concordant between men and women.

Despite this growing cellular literature, its translation to whole-muscle function in the same individuals remains poorly characterized. To our knowledge, only a handful of

studies have attempted paired correlations between single fiber contractile properties and whole-muscle performance in the same participants, and these are constrained by important methodological limitations: incomplete measurement of contractile parameters, pooling of fiber types in ways that obscure fiber-specific contributions, variation across contraction modes, and in several cases mismatched muscles between cellular and whole-muscle assessments (31–33, 79–81). As a result, it remains unclear which specific fiber-level properties most robustly predict whole-muscle performance, which fiber type contributes most to that prediction, and whether those cellular-to-whole-muscle relationships are altered by aging or modified by structural variables such as thigh lean mass. This gap is not peripheral, it is central to any mechanistic account of sarcopenia because the cellular-to-whole-muscle translation is the precise link required to move from descriptive cellular findings to a mechanistic understanding of clinical functional decline. Addressing this gap, with a fiber-type-stratified, paired design in the same muscle and the same individuals across age groups and sexes, was a central motivation for the studies presented in Chapters 2 and 3.

Molecular Determinants of Single Fiber Contractile Dysfunction

The observation that specific force and normalized power are altered in aged single fibers, in directions and magnitudes not fully predicted by changes in fiber size, points directly toward molecular alterations within the sarcomere as additional contributors to age-related dysfunction. The sarcomere is the basic contractile unit of muscle, and its proteins exist not as single uniform species but as proteoforms: distinct molecular forms of a protein arising from alternative splicing, genetic variation, and post-translational modification (82–85). Each of these proteoform dimensions carries

functional consequences for force, velocity, and power generation, and the collective proteoform landscape of aged human muscle is only beginning to be mapped. Characterizing that landscape is essential because the functional behavior of a fiber reflects not only how many contractile proteins it contains, but which specific molecular forms of those proteins are present and in what modification state.

Several specific molecular mechanisms have been implicated. Reduced myosin heavy chain (MHC) content has been identified as a direct correlate of specific force decline in aged Type II fibers, with fewer available cross-bridges producing lower force per unit cross-sectional area (75). Oxidative post-translational modifications, particularly MHC carbonylation, which accumulates with aging due to the long half-life of myosin and sustained redox imbalance, impair actin-myosin interactions and cross-bridge cycling independent of protein content (76, 86). Regulatory protein changes, including downregulation of fast isoforms of troponin T and tropomyosin and reduced thin-filament calcium sensitivity, further compromise force generation in ways that may be especially consequential under the reduced calcium availability that characterizes aging muscle in vivo (76, 78, 87–89). Myosin light chain (MLC) isoforms represent an additional regulatory point with direct implications for contractile velocity, in human skeletal muscle, the slow (MLC2S) and fast (MLC2F) regulatory isoforms modulate actomyosin interactions and shortening velocity through isoform-specific phosphorylation, and elevated MLC2S phosphorylation has been linked to slowed velocity in aged muscle (82, 90–93). Non-canonical co-expression of slow MLC isoforms in nominally fast fibers has been documented in humans, and rodent evidence suggests that this heterogeneity influences contractile properties in ways that cannot be predicted from MHC isoform

typing alone, a finding with direct relevance to proteoform-level interpretation (82, 90–93).

Recent advances in top-down liquid chromatography-mass spectrometry now permit intact proteoform profiling at single-fiber resolution, enabling simultaneous identification of isoform identity and post-translational modification state without the protein digestion that limits bottom-up approaches (82, 93). This methodology has been applied to rodent single fibers in collaborative work from our group, revealing MHC isoform-specific molecular signatures correlated with contractile function (82). However, prior to the work reported in Chapter 4, no prior studies in humans had performed paired molecular and mechanical characterization of the same individual fibers, the direct linkage required to establish interpretable structure-function relationships and to identify the molecular correlates of contractile impairment in human aging.

SPECIFIC AIMS

The literature reviewed above converges on a single unresolved problem. Whole-muscle studies demonstrate that aged muscle loses disproportionately more function than mass, implicating intrinsic contractile dysfunction. Single fiber studies localize that dysfunction preferentially to Type II fibers and suggest that atrophy alone does not account for the full magnitude of age-related deficits. Molecular studies point to sarcomeric proteoform alterations, including changes in myosin content and oxidative state, regulatory protein composition, and light-chain isoform expression and phosphorylation, as candidate contributors. Yet these three bodies of work have remained largely parallel rather than integrated: (1) whole-muscle contractile studies have not consistently linked their findings to fiber-level mechanisms within the same individuals; (2) single-fiber studies have rarely been paired with whole-muscle assessments in the same cohort; and (3) molecular characterization of the sarcomere has rarely been performed on the same fibers whose contractile properties were measured. No prior human study has combined all three. The central premise of this dissertation is that age-related muscle dysfunction reflects integrated impairments across biological scales: whole-muscle contractile deficits are linked to fiber-type-specific alterations in single muscle fiber mechanics, which are in turn associated with molecular changes in the sarcomeric contractile apparatus. To test this premise, a multiscale approach was employed in younger and older men and women that combined whole-muscle functional and compositional testing, single muscle fiber mechanical experiments, and paired top-down proteomic characterization of the same

fibers that completed mechanical testing. The dissertation was guided by the following specific aims:

Aim 1. Identify age-related, fiber-type-specific alterations in single muscle fiber contractile properties in young and older adults (Chapter 2).

Peak isometric force (P_0), specific force (SF), maximal shortening velocity (V_{max}), peak power output (PPO), normalized power output (NPO), and cross-sectional area (CSA) were determined in both Type I and Type II fibers from younger and older men and women, enabling assessment of absolute and intrinsic contractile function across fiber types and sexes.

We hypothesized that Type I fibers would exhibit no significant age-related differences in CSA or contractile properties. We hypothesized that aging would preferentially impair Type II fibers, resulting in smaller CSA and reduced absolute P_0, PPO, and SF compared to younger adults, while Type II NPO would be preserved or greater in older adults. Type II V_{max} was hypothesized not to differ significantly between age groups.

Aim 2. Determine the relationship between single muscle fiber contractile properties and whole-muscle function and composition, and identify the fiber-level predictors of whole-muscle function that remain significant independent of age (Chapter 3).

Single fiber properties from the vastus lateralis were evaluated for their associations with knee extensor peak torque, shortening velocity, and peak power measured by isokinetic dynamometry, and with thigh and whole-body composition determined by dual-energy X-ray absorptiometry. Fiber-type-stratified regression

analyses were performed across the full cohort, within age groups, and after age adjustment, and an ANCOVA was used to test whether the slopes of cellular-to-whole-muscle relationships differed between young and older adults.

We hypothesized that older adults would exhibit reduced whole-muscle function and thigh lean mass relative to younger adults. We hypothesized that Type II fiber contractile properties, in particular absolute P_0, PPO, and CSA, would demonstrate the strongest and most independent associations with whole-muscle torque and power, and that age-related whole-muscle deficits would be linked to cellular-level impairments in Type II fibers beyond what is explained by reductions in muscle size alone.

Aim 3. Identify molecular correlates of single muscle fiber contractile function in aging using top-down proteomics performed on the same fibers that completed mechanical experiments (Chapter 4).

Permeabilized human single muscle fibers from young and older adults underwent paired top-down liquid chromatography-mass spectrometry analysis following mechanical testing, enabling direct correlation of isoform- and proteoform-level molecular measurements with P_0, SF, V_{max}, PPO, NPO, and CSA in the same individual fibers.

We hypothesized that specific sarcomeric proteoform characteristics, including MLC isoform identity and phosphorylation state, would correlate with single fiber force, velocity, and power. We further hypothesized that older adults would exhibit differences in their sarcomeric proteome that corresponded to their contractile impairments relative to younger adults.

REFERENCES

1. **Volpi E**, **Nazemi R**, **Fujita S**. Muscle tissue changes with aging. *Curr Opin Clin Nutr Metab Care* 7: 405–410, 2004.

2. **Kennis E**, **Verschueren S**, **Van Roie E**, **Thomis M**, **Lefevre J**, **Delecluse C**. Longitudinal impact of aging on muscle quality in middle-aged men. *AGE* 36: 9689, 2014. doi: 10.1007/s11357-014-9689-1.

3. **Reid KF**, **Fielding RA**. Skeletal Muscle Power: A Critical Determinant of Physical Functioning in Older Adults. *Exerc Sport Sci Rev* 40: 4, 2012. doi: 10.1097/JES.0b013e31823b5f13.

4. **Skelton DA**, **Greig CA**, **Davies JM**, **Young A**. Strength, power and related functional ability of healthy people aged 65-89 years. *Age Ageing* 23: 371–377, 1994. doi: 10.1093/ageing/23.5.371.

5. **Xu J**, **Wan CS**, **Ktoris K**, **Reijnierse EM**, **Maier AB**. Sarcopenia Is Associated with Mortality in Adults: A Systematic Review and Meta-Analysis. *Gerontology* 68: 361–376, 2021. doi: 10.1159/000517099.

6. **Koon-Yee Lee G**, **Chun-Ming Au P**, **Hoi-Yee Li G**, **Chan M**, **Li H-L**, **Man-Yung Cheung B**, **Chi-Kei Wong I**, **Ho-Fun Lee V**, **Mok J**, **Hon-Kei Yip B**, **King-Yip Cheng K**, **Wu C-H**, **Cheung C-L**. Sarcopenia and mortality in different clinical conditions: A meta-analysis. *Osteoporos Sarcopenia* 7: S19–S27, 2021. doi: 10.1016/j.afos.2021.02.001.

7. **Pacifico J**, **Reijnierse EM**, **Lim WK**, **Maier AB**. The Association between Sarcopenia as a Comorbid Disease and Incidence of Institutionalisation and Mortality in Geriatric Rehabilitation Inpatients: REStORing health of acutely unwell adulTs (RESORT). *Gerontology* 68: 498–508, 2022. doi: 10.1159/000517461.

8. **Pacifico J**, **Geerlings MAJ**, **Reijnierse EM**, **Phassouliotis C**, **Lim WK**, **Maier AB**. Prevalence of sarcopenia as a comorbid disease: A systematic review and meta-analysis. *Exp Gerontol* 131: 110801, 2020. doi: 10.1016/j.exger.2019.110801.

9. **Janssen I**, **Shepard DS**, **Katzmarzyk PT**, **Roubenoff R**. The healthcare costs of sarcopenia in the United States. *J Am Geriatr Soc* 52: 80–85, 2004. doi: 10.1111/j.1532-5415.2004.52014.x.

10. **Goates S**, **Du K**, **Arensberg MB**, **Gaillard T**, **Guralnik J**, **Pereira SL**. Economic Impact of Hospitalizations in US Adults with Sarcopenia. *J Frailty Aging* 8: 93–99, 2019. doi: 10.14283/jfa.2019.10.

11. **Guttikonda D**, **Smith AL**. Sarcopenia Assessment Techniques. *Clin Liver Dis* 18: 189, 2021. doi: 10.1002/cld.1111.

12. **Lee SH**, **Gong HS**. Measurement and Interpretation of Handgrip Strength for Research on Sarcopenia and Osteoporosis. *J Bone Metab* 27: 85–96, 2020. doi: 10.11005/jbm.2020.27.2.85.

13. **Prado CM**, **Lieffers JR**, **Bowthorpe L**, **Baracos VE**, **Mourtzakis M**, **McCargar LJ**. Sarcopenia and Physical Function: In Overweight Patients with Advanced Cancer. *Can J Diet Pract Res* 74: 69–74, 2013. doi: 10.3148/74.2.2013.69.

14. **Lima AB de**, **Henrinques-Neto D**, **Scott D**, **de Araújo Pinto A**, **Dos Santos Ribeiro G**, **Peralta M**, **Miranda KA**, **Campos P**, **Gouveia ER**. Relationship between physical function and sarcopenia in the older adults from Amazonas: A cross-sectional study. *PloS One* 20: e0320079, 2025. doi: 10.1371/journal.pone.0320079.

15. **Sundberg CW**, **Hunter SK**, **Trappe SW**, **Smith CS**, **Fitts RH**. Effects of elevated H+ and Pi on the contractile mechanics of skeletal muscle fibres from young and old men: implications for muscle fatigue in humans. *J Physiol* 596: 3993–4015, 2018. doi: 10.1113/JP276018.

16. **Trappe S**, **Gallagher P**, **Harber M**, **Carrithers J**, **Fluckey J**, **Trappe T**. Single Muscle Fibre Contractile Properties in Young and Old Men and Women. *J Physiol* 552: 47–58, 2003. doi: 10.1113/jphysiol.2003.044966.

17. **Woods JL**, **Iuliano-Burns S**, **King SJ**, **Strauss BJ**, **Walker KZ**. Poor physical function in elderly women in low-level aged care is related to muscle strength rather than to measures of sarcopenia. *Clin Interv Aging* 6: 67–76, 2011. doi: 10.2147/CIA.S16979.

18. **Ooi H**, **Welch C**. Obstacles to the Early Diagnosis and Management of Sarcopenia: Current Perspectives. *Clin Interv Aging* 19: 323–332, 2024. doi: 10.2147/CIA.S438144.

19. **Li R**, **Xia J**, **Zhang X**, **Gathirua-Mwangi WG**, **Guo J**, **Li Y**, **McKenzie S**, **Song Y**. Associations of Muscle Mass and Strength with All-Cause Mortality among US Older Adults. *Med Sci Sports Exerc* 50: 458–467, 2018. doi: 10.1249/MSS.0000000000001448.

20. Association of Muscle Strength With All-Cause Mortality in the Oldest Old: Prospective Cohort Study From 28 Countries - Andersen - 2024 - Journal of Cachexia, Sarcopenia and Muscle - Wiley Online Library [Online]. [date unknown]. https://onlinelibrary.wiley.com/doi/full/10.1002/jcsm.13619 [9 June 2025].

21. **Michel E**, **Zory R**, **Guerin O**, **Prate F**, **Sacco G**, **Chorin F**. Assessing muscle quality as a key predictor to differentiate fallers from non-fallers in older adults. *Eur Geriatr Med* 15: 1301–1311, 2024. doi: 10.1007/s41999-024-01020-y.

22. **Araújo CGS**, **Kunutsor SK**, **Eijsvogels TMH**, **Myers J**, **Laukkanen JA**, **Hamar D**, **Niebauer J**, **Bhattacharjee A**, **Silva CG de S e**, **Franca JF**, **Castro CLB**. Muscle

Power Versus Strength as a Predictor of Mortality in Middle-Aged and Older Men and Women. *Mayo Clin Proc* 0, 2025. doi: 10.1016/j.mayocp.2025.02.015.

23. **Lim J-Y**, **Frontera WR**. Skeletal muscle aging and sarcopenia: perspectives from mechanical studies of single permeabilized muscle fibers. *J Biomech* 152: 111559, 2023. doi: 10.1016/j.jbiomech.2023.111559.

24. **Lim J-Y**, **Frontera WR**. Single skeletal muscle fiber mechanical properties: a muscle quality biomarker of human aging. *Eur J Appl Physiol* 122: 1383–1395, 2022. doi: 10.1007/s00421-022-04924-4.

25. **Keller K**, **Engelhardt M**. Strength and muscle mass loss with aging process. Age and strength loss. *Muscles Ligaments Tendons J* 3: 346–350, 2014.

26. **Larsson L**, **Degens H**, **Li M**, **Salviati L**, **Lee YI**, **Thompson W**, **Kirkland JL**, **Sandri M**. Sarcopenia: Aging-Related Loss of Muscle Mass and Function. *Physiol Rev* 99: 427–511, 2019. doi: 10.1152/physrev.00061.2017.

27. **Grgic J**, **Lazinica B**, **Schoenfeld BJ**, **Pedisic Z**. Test-Retest Reliability of the One-Repetition Maximum (1RM) Strength Assessment: a Systematic Review. *Sports Med - Open* 6: 31, 2020. doi: 10.1186/s40798-020-00260-z.

28. **Cruz-Jentoft AJ**, **Bahat G**, **Bauer J**, **Boirie Y**, **Bruyère O**, **Cederholm T**, **Cooper C**, **Landi F**, **Rolland Y**, **Sayer AA**, **Schneider SM**, **Sieber CC**, **Topinkova E**, **Vandewoude M**, **Visser M**, **Zamboni M**, **Writing Group for the European Working Group on Sarcopenia in Older People 2 (EWGSOP2) and the EG for E**. Sarcopenia: revised European consensus on definition and diagnosis. *Age Ageing* 48: 16–31, 2019. doi: 10.1093/ageing/afy169.

29. **Sundberg CW**, **Teigen LE**, **Hunter SK**, **Fitts RH**. Cumulative effects of H+ and Pi on force and power of skeletal muscle fibres from young and older adults. *J Physiol* 603: 187–209, 2025. doi: 10.1113/JP286938.

30. **Trombetti A**, **Reid KF**, **Hars M**, **Herrmann FR**, **Pasha E**, **Phillips EM**, **Fielding RA**. Age-associated declines in muscle mass, strength, power, and physical performance: impact on fear of falling and quality of life. *Osteoporos Int J Establ Result Coop Eur Found Osteoporos Natl Osteoporos Found USA* 27: 463–471, 2016. doi: 10.1007/s00198-015-3236-5.

31. **Frontera WR**, **Suh D**, **Krivickas LS**, **Hughes VA**, **Goldstein R**, **Roubenoff R**. Skeletal muscle fiber quality in older men and women. *Am J Physiol Cell Physiol* 279: C611-618, 2000. doi: 10.1152/ajpcell.2000.279.3.C611.

32. **Miller MS**, **Bedrin NG**, **Callahan DM**, **Previs MJ**, **Jennings ME**, **Ades PA**, **Maughan DW**, **Palmer BM**, **Toth MJ**. Age-related slowing of myosin actin cross-bridge kinetics is sex specific and predicts decrements in whole skeletal muscle performance in humans. *J Appl Physiol* 115: 1004–1014, 2013. doi: 10.1152/japplphysiol.00563.2013.

33. **Straight CR**, **Ades PA**, **Toth MJ**, **Miller MS**. Age-related reduction in single muscle fiber calcium sensitivity is associated with decreased muscle power in men and women. *Exp Gerontol* 102: 84–92, 2018. doi: 10.1016/j.exger.2017.12.007.

34. **Wrucke DJ**, **Kuplic A**, **Adam MD**, **Hunter SK**, **Sundberg CW**. Neural and muscular contributions to the age-related differences in peak power of the knee extensors in men and women. *J Appl Physiol Bethesda Md 1985* 137: 1021–1040, 2024. doi: 10.1152/japplphysiol.00773.2023.

35. **Delgadillo JD**, **Sundberg CW**, **Kwon M**, **Hunter SK**. Fatigability of the knee extensor muscles during high-load fast and low-load slow resistance exercise in young and older adults. *Exp Gerontol* 154: 111546, 2021. doi: 10.1016/j.exger.2021.111546.

36. **Thompson BJ**, **Whitson M**, **Sobolewski EJ**, **Stock MS**. The Influence of Age, Joint Angle, and Muscle Group on Strength Production Characteristics at the Knee Joint. *J Gerontol A Biol Sci Med Sci* 73: 603–607, 2018. doi: 10.1093/gerona/glx156.

37. **de Sousa AMM**, **Cavalcante JGT**, **Bottaro M**, **Vieira DCL**, **Babault N**, **Geremia JM**, **Corrigan P**, **Silbernagel KG**, **Durigan JLQ**, **Marqueti R de C**. The Influence of Hip and Knee Joint Angles on Quadriceps Muscle-Tendon Unit Properties during Maximal Voluntary Isometric Contraction. *Int J Environ Res Public Health* 20: 3947, 2023. doi: 10.3390/ijerph20053947.

38. **Rassier DE**, **MacIntosh BR**, **Herzog W**. Length dependence of active force production in skeletal muscle. *J Appl Physiol Bethesda Md 1985* 86: 1445–1457, 1999. doi: 10.1152/jappl.1999.86.5.1445.

39. **Petrella JK**, **Kim J**, **Tuggle SC**, **Hall SR**, **Bamman MM**. Age differences in knee extension power, contractile velocity, and fatigability. *J Appl Physiol* 98: 211–220, 2005. doi: 10.1152/japplphysiol.00294.2004.

40. **Baron R**. Normative data for muscle strength in relation to age, knee angle and velocity. *Wien Med Wochenschr 1946* 145: 600–606, 1995.

41. **Lanza IR**, **Towse TF**, **Caldwell GE**, **Wigmore DM**, **Kent-Braun JA**. Effects of age on human muscle torque, velocity, and power in two muscle groups. *J Appl Physiol Bethesda Md 1985* 95: 2361–2369, 2003. doi: 10.1152/japplphysiol.00724.2002.

42. **Ng AV**, **Kent-Braun JA**. Slowed muscle contractile properties are not associated with a decreased EMG/force relationship in older humans. *J Gerontol A Biol Sci Med Sci* 54: B452-458, 1999. doi: 10.1093/gerona/54.10.b452.

43. **Reid KF**, **Doros G**, **Clark DJ**, **Patten C**, **Carabello RJ**, **Cloutier GJ**, **Phillips EM**, **Krivickas LS**, **Frontera WR**, **Fielding RA**. Muscle power failure in mobility-limited older adults: preserved single fiber function despite lower whole muscle size,

quality and rate of neuromuscular activation. *Eur J Appl Physiol* 112: 2289–2301, 2012. doi: 10.1007/s00421-011-2200-0.

44. **Raj IS**, **Bird SR**, **Shield AJ**. Aging and the force-velocity relationship of muscles. *Exp Gerontol* 45: 81–90, 2010. doi: 10.1016/j.exger.2009.10.013.

45. **Alcazar J**, **Rodriguez-Lopez C**, **Ara I**, **Alfaro-Acha A**, **Rodríguez-Gómez I**, **Navarro-Cruz R**, **Losa-Reyna J**, **García-García FJ**, **Alegre LM**. Force-velocity profiling in older adults: An adequate tool for the management of functional trajectories with aging. *Exp Gerontol* 108: 1–6, 2018. doi: 10.1016/j.exger.2018.03.015.

46. **Thompson BJ**, **Ryan ED**, **Herda TJ**, **Costa PB**, **Herda AA**, **Cramer JT**. Age-related changes in the rate of muscle activation and rapid force characteristics. *Age* 36: 839–849, 2014. doi: 10.1007/s11357-013-9605-0.

47. **Thompson BJ**, **Ryan ED**, **Sobolewski EJ**, **Conchola EC**, **Cramer JT**. Age related differences in maximal and rapid torque characteristics of the leg extensors and flexors in young, middle-aged and old men. *Exp Gerontol* 48: 277–282, 2013. doi: 10.1016/j.exger.2012.10.009.

48. **Ditroilo M**, **Forte R**, **Benelli P**, **Gambarara D**, **De Vito G**. Effects of age and limb dominance on upper and lower limb muscle function in healthy males and females aged 40-80 years. *J Sports Sci* 28: 667–677, 2010. doi: 10.1080/02640411003642098.

49. **Varesco G**, **Espeit L**, **Feasson L**, **Lapole T**, **Rozand V**. Rate of force development and rapid muscle activation characteristics of knee extensors in very old men. *Exp Gerontol* 124: 110640, 2019. doi: 10.1016/j.exger.2019.110640.

50. **Alcazar J**, **Rodriguez-Lopez C**, **Delecluse C**, **Thomis M**, **Van Roie E**. Ten-year longitudinal changes in muscle power, force, and velocity in young, middle-aged, and older adults. *J Cachexia Sarcopenia Muscle* 14: 1019–1032, 2023. doi: 10.1002/jcsm.13184.

51. **Goodpaster BH**, **Park SW**, **Harris TB**, **Kritchevsky SB**, **Nevitt M**, **Schwartz AV**, **Simonsick EM**, **Tylavsky FA**, **Visser M**, **Newman AB**. The loss of skeletal muscle strength, mass, and quality in older adults: the health, aging and body composition study. *J Gerontol A Biol Sci Med Sci* 61: 1059–1064, 2006. doi: 10.1093/gerona/61.10.1059.

52. **Reid KF**, **Pasha E**, **Doros G**, **Clark DJ**, **Patten C**, **Phillips EM**, **Frontera WR**, **Fielding RA**. Longitudinal decline of lower extremity muscle power in healthy and mobility-limited older adults: influence of muscle mass, strength, composition, neuromuscular activation and single fiber contractile properties. *Eur J Appl Physiol* 114: 29–39, 2014. doi: 10.1007/s00421-013-2728-2.

53. **Freitas SR**, **Cruz-Montecinos C**, **Ratel S**, **Pinto RS**. Powerpenia Should be Considered a Biomarker of Healthy Aging. *Sports Med - Open* 10: 27, 2024. doi: 10.1186/s40798-024-00689-6.

54. **Clark DJ**, **Patten C**, **Reid KF**, **Carabello RJ**, **Phillips EM**, **Fielding RA**. Impaired Voluntary Neuromuscular Activation Limits Muscle Power in Mobility-Limited Older Adults. *J Gerontol A Biol Sci Med Sci* 65A: 495–502, 2010. doi: 10.1093/gerona/glq012.

55. **Clark BC**, **Taylor JL**, **Hong SL**, **Law TD**, **Russ DW**. Weaker Seniors Exhibit Motor Cortex Hypoexcitability and Impairments in Voluntary Activation. *J Gerontol A Biol Sci Med Sci* 70: 1112–1119, 2015. doi: 10.1093/gerona/glv030.

56. **Rozand V**, **Sundberg CW**, **Hunter SK**, **Smith AE**. Age-related Deficits in Voluntary Activation: A Systematic Review and Meta-analysis. *Med Sci Sports Exerc* 52: 549, 2020. doi: 10.1249/MSS.0000000000002179.

57. **Clark LA**, **Manini TM**, **Wages NP**, **Simon JE**, **Russ DW**, **Clark BC**. Reduced Neural Excitability and Activation Contribute to Clinically Meaningful Weakness in Older Adults. *J Gerontol A Biol Sci Med Sci* 76: 692–702, 2021. doi: 10.1093/gerona/glaa157.

58. **Cespón J**, **Pellicciari MC**, **Casula EP**, **Miniussi C**. Age-related Changes in Cortical Excitability Linked to Decreased Attentional and Inhibitory Control. *Neuroscience* 495: 1–14, 2022. doi: 10.1016/j.neuroscience.2022.05.021.

59. **Geiger PC**, **Bailey JP**, **Zhan W-Z**, **Mantilla CB**, **Sieck GC**. Denervation-induced changes in myosin heavy chain expression in the rat diaphragm muscle. *J Appl Physiol Bethesda Md 1985* 95: 611–619, 2003. doi: 10.1152/japplphysiol.00862.2002.

60. **Gauthier GF**, **Hobbs AW**. Effects of denervation on the distribution of myosin isozymes in skeletal muscle fibers. *Exp Neurol* 76: 331–346, 1982. doi: 10.1016/0014-4886(82)90213-8.

61. **Bergmeister KD**, **Aman M**, **Muceli S**, **Vujaklija I**, **Manzano-Szalai K**, **Unger E**, **Byrne RA**, **Scheinecker C**, **Riedl O**, **Salminger S**, **Frommlet F**, **Borschel GH**, **Farina D**, **Aszmann OC**. Peripheral nerve transfers change target muscle structure and function. *Sci Adv* 5: eaau2956, 2019. doi: 10.1126/sciadv.aau2956.

62. **Castro RW**, **Lopes MC**, **Settlage RE**, **Valdez G**. Aging alters mechanisms underlying voluntary movements in spinal motor neurons of mice, primates, and humans. *JCI Insight* 8, 2023. doi: 10.1172/jci.insight.168448.

63. **Oda K**. Age changes of motor innervation and acetylcholine receptor distribution on human skeletal muscle fibres. *J Neurol Sci* 66: 327–338, 1984. doi: 10.1016/0022-510X(84)90021-2.

64. **Wokke JHJ**, **Jennekens FGI**, **van den Oord CJM**, **Veldman H**, **Smit LME**, **Leppink GJ**. Morphological changes in the human end plate with age. *J Neurol Sci* 95: 291–310, 1990. doi: 10.1016/0022-510X(90)90076-Y.

65. **Sundberg CW**, **Prost RW**, **Fitts RH**, **Hunter SK**. Bioenergetic basis for the increased fatigability with ageing. *J Physiol* 597: 4943–4957, 2019. doi: 10.1113/JP277803.

66. **Conley KE**, **Jubrias SA**, **Esselman PC**. Oxidative capacity and ageing in human muscle. *J Physiol* 526: 203–210, 2000. doi: 10.1111/j.1469-7793.2000.t01-1-00203.x.

67. **Peterson CM**, **Johannsen DL**, **Ravussin E**. Skeletal Muscle Mitochondria and Aging: A Review. *J Aging Res* 2012: 194821, 2012. doi: 10.1155/2012/194821.

68. **Michelucci A**, **Liang C**, **Protasi F**, **Dirksen RT**. Altered Ca2+ Handling and Oxidative Stress Underlie Mitochondrial Damage and Skeletal Muscle Dysfunction in Aging and Disease. *Metabolites* 11: 424, 2021. doi: 10.3390/metabo11070424.

69. **Wood DS**, **Zollman J**, **Reuben JP**, **Brandt PW**. Human Skeletal Muscle: Properties of the “Chemically Skinned” Fiber. *Science* 187: 1075–1076, 1975.

70. **Eastwood AB**, **Wood DS**, **Bock KL**, **Sorenson MM**. Chemically skinned mammalian skeletal muscle. I. The structure of skinned rabbit psoas. *Tissue Cell* 11: 553–566, 1979. doi: 10.1016/0040-8166(79)90062-4.

71. **Curtin NA**, **Diack RA**, **West TG**, **Wilson AM**, **Woledge RC**. Skinned fibres produce the same power and force as intact fibre bundles from muscle of wild rabbits. *J Exp Biol* 218: 2856–2863, 2015. doi: 10.1242/jeb.121897.

72. **Grosicki GJ**, **Zepeda CS**, **Sundberg CW**. Single muscle fibre contractile function with ageing. *J Physiol* 600: 5005–5026, 2022. doi: 10.1113/JP282298.

73. **Larsson L**, **Li X**, **Frontera WR**. Effects of aging on shortening velocity and myosin isoform composition in single human skeletal muscle cells. *Am J Physiol-Cell Physiol* 272: C638–C649, 1997. doi: 10.1152/ajpcell.1997.272.2.C638.

74. **Ochala J**, **Frontera WR**, **Dorer DJ**, **Hoecke JV**, **Krivickas LS**. Single Skeletal Muscle Fiber Elastic and Contractile Characteristics in Young and Older Men. *J Gerontol Ser A* 62: 375–381, 2007. doi: 10.1093/gerona/62.4.375.

75. **D’Antona G**, **Pellegrino MA**, **Adami R**, **Rossi R**, **Carlizzi CN**, **Canepari M**, **Saltin B**, **Bottinelli R**. The effect of ageing and immobilization on structure and function of human skeletal muscle fibres. *J Physiol* 552: 499–511, 2003. doi: 10.1113/jphysiol.2003.046276.

76. **Brocca L**, **McPhee JS**, **Longa E**, **Canepari M**, **Seynnes O**, **De Vito G**, **Pellegrino MA**, **Narici M**, **Bottinelli R**. Structure and function of human muscle fibres and

muscle proteome in physically active older men. *J Physiol* 595: 4823–4844, 2017. doi: 10.1113/JP274148.

77. **Hvid LG**, **Suetta C**, **Aagaard P**, **Kjaer M**, **Frandsen U**, **Ørtenblad N**. Four days of muscle disuse impairs single fiber contractile function in young and old healthy men. *Exp Gerontol* 48: 154–161, 2013. doi: 10.1016/j.exger.2012.11.005.

78. **Lamboley CR**, **Wyckelsma VL**, **Dutka TL**, **McKenna MJ**, **Murphy RM**, **Lamb GD**. Contractile properties and sarcoplasmic reticulum calcium content in type I and type II skeletal muscle fibres in active aged humans. *J Physiol* 593: 2499–2514, 2015. doi: 10.1113/JP270179.

79. **Jeon Y-N**, **Kim H-J**, **Yang S-Y**, **Lee S-H**, **Kim D-Y**, **Bae J-H**, **Lee H-J**, **Lim J-Y**, **Choi S-J**. Contractile Properties of Single Muscle Fiber and Their Relations to Whole Muscle Strength in Korean Young Male. *Exerc Sci* 27: 23–31, 2018. doi: 10.15857/ksep.2018.27.1.23.

80. **Jeon Y**, **Choi J**, **Kim HJ**, **Lee H**, **Lim J-Y**, **Choi S-J**, **Jeon Y**, **Choi J**, **Kim HJ**, **Lee H**, **Lim J-Y**, **Choi S-J**. Sex- and fiber-type-related contractile properties in human single muscle fiber. *J Exerc Rehabil* 15: 537–545, 2019. doi: 10.12965/jer.1938336.168.

81. **Wang Z-M**, **Leng X**, **Messi ML**, **Choi SJ**, **Marsh AP**, **Nicklas B**, **Delbono O**. Relationship of Physical Function to Single Muscle Fiber Contractility in Older Adults: Effects of Resistance Training With and Without Caloric Restriction. *J Gerontol Ser A* 74: 412–419, 2019. doi: 10.1093/gerona/gly047.

82. **Melby JA**, **Brown KA**, **Gregorich ZR**, **Roberts DS**, **Chapman EA**, **Ehlers LE**, **Gao Z**, **Larson EJ**, **Jin Y**, **Lopez JR**, **Hartung J**, **Zhu Y**, **McIlwain SJ**, **Wang D**, **Guo W**, **Diffee GM**, **Ge Y**. High sensitivity top–down proteomics captures single muscle cell heterogeneity in large proteoforms. *Proc Natl Acad Sci* 120: e2222081120, 2023. doi: 10.1073/pnas.2222081120.

83. **Fields S**. Proteomics in Genomeland. *Science* 291: 1221–1224, 2001. doi: 10.1126/science.291.5507.1221.

84. **Smith LM**, **Kelleher NL**. Proteoform: a single term describing protein complexity. *Nat Methods* 10: 186–187, 2013. doi: 10.1038/nmeth.2369.

85. **Carbonara K**, **Andonovski M**, **Coorssen JR**. Proteomes Are of Proteoforms: Embracing the Complexity. *Proteomes* 9: 38, 2021. doi: 10.3390/proteomes9030038.

86. **Day NJ**, **Kelly SS**, **Lui L**, **Mansfield TA**, **Gaffrey MJ**, **Trejo JB**, **Sagendorf TJ**, **Attah IK**, **Moore RJ**, **Douglas CM**, **Newman AB**, **Kritchevsky SB**, **Kramer PA**, **Marcinek DJ**, **Coen PM**, **Goodpaster BH**, **Hepple RT**, **Cawthon PM**, **Petyuk VA**, **Esser KA**, **Qian W**, **Cummings SR**. Signatures of cysteine oxidation on muscle structural and contractile proteins are associated with physical performance and

muscle function in older adults: Study of Muscle, Mobility and Aging (SOMMA). *Aging Cell* 23: e14094, 2024. doi: 10.1111/acel.14094.

87. **Prochniewicz E**, **Thompson LV**, **Thomas DD**. Age-Related Decline in Actomyosin Structure and Function. *Exp Gerontol* 42: 931–938, 2007. doi: 10.1016/j.exger.2007.06.015.

88. **Mollica JP**, **Dutka TL**, **Merry TL**, **Lamboley CR**, **McConell GK**, **McKenna MJ**, **Murphy RM**, **Lamb GD**. S-Glutathionylation of troponin I (fast) increases contractile apparatus Ca2+ sensitivity in fast-twitch muscle fibres of rats and humans. *J Physiol* 590: 1443–1463, 2012. doi: 10.1113/jphysiol.2011.224535.

89. **Lamb GD**, **Posterino GS**. Effects of oxidation and reduction on contractile function in skeletal muscle fibres of the rat. *J Physiol* 546: 149–163, 2003. doi: 10.1113/jphysiol.2002.027896.

90. **Larsson L**, **Moss RL**. Maximum velocity of shortening in relation to myosin isoform composition in single fibres from human skeletal muscles. *J Physiol* 472: 595–614, 1993. doi: 10.1113/jphysiol.1993.sp019964.

91. **Bottinelli R**, **Reggiani C**. Human skeletal muscle fibres: molecular and functional diversity. *Prog Biophys Mol Biol* 73: 195–262, 2000. doi: 10.1016/S0079-6107(00)00006-7.

92. **D'Antona G**, **Megighian A**, **Bortolotto S**, **Pellegrino MA**, **Marchese-Ragona R**, **Staffieri A**, **Bottinelli R**, **Reggiani C**. Contractile properties and myosin heavy chain isoform composition in single fibre of human laryngeal muscles. *J Muscle Res Cell Motil* 23: 187–195, 2002. doi: 10.1023/a:1020963021105.

93. **Gregorich ZR**, **Peng Y**, **Cai W**, **Jin Y**, **Wei L**, **Chen AJ**, **McKiernan SH**, **Aiken JM**, **Moss RL**, **Diffee GM**, **Ge Y**. Top-Down Targeted Proteomics Reveals Decrease in Myosin Regulatory Light-Chain Phosphorylation That Contributes to Sarcopenic Muscle Dysfunction. *J Proteome Res* 15: 2706–2716, 2016. doi: 10.1021/acs.jproteome.6b00244.

CHAPTER II

Age-related Alterations in Human Single Muscle Fiber Contractile Properties Across Fiber Types

INTRODUCTION

Age-related declines in skeletal muscle function are a major contributor to mobility loss, physical disability, and loss of independence in older adults. Although these impairments are often discussed in the context of sarcopenia and reduced muscle mass, functional decline cannot be explained by atrophy alone. Muscle power declines earlier and more precipitously than muscle strength with advancing age and is a stronger predictor of mobility limitation, falls, and mortality than force production alone (1, 2). These observations suggest that age-related muscle dysfunction reflects not only a loss of muscle quantity, but also a deterioration in muscle quality. Defining the cellular basis of this decline is therefore critical for understanding the mechanisms of sarcopenia and age-related loss of function.

Whole-muscle performance depends on the integrated behavior of individual muscle fibers, their size, fiber type distribution, and the intrinsic properties of the contractile apparatus. Age-related reductions in force and power may arise from several non-mutually exclusive mechanisms, including fiber loss, selective atrophy of fast fibers, fiber-type remodeling, and impairments in myofilament function. Because Type II fibers produce greater force, shorten more rapidly, and generate more power than Type I fibers, they have generally been considered vulnerable to aging and central to the loss of whole-muscle performance (3, 4). However, the larger decline in strength and power relative to muscle mass suggests that intrinsic contractile deficits may also contribute to the aging phenotype (4, 5).

A major limitation of in vivo measurements is that they cannot readily distinguish whether impaired muscle performance reflects altered neural activation, changes in

muscle architecture, shifts in fiber-type composition, or dysfunction within the sarcomere itself. Chemically skinned single-fiber preparations overcome many of these limitations by allowing direct assessment of contractile properties under tightly controlled conditions, independent of neural and tendon-related influences. This approach permits measurement of fiber cross-sectional area (CSA), peak isometric force (P_0), specific force, shortening velocity, and power at the level of the individual fiber, thereby providing a more direct index of intrinsic muscle function (4–6). Prior work has shown that certain single-fiber related properties are associated with whole-muscle performance in older adults, suggesting that fiber-level deficits may contribute to broader functional decline (7). More recently, molecular studies have further implicated qualitative alterations in contractile proteins, including oxidative modifications, as potential contributors to age-related reductions in muscle function (8, 9).

Human single-fiber studies have provided important but incomplete insight into how aging affects contractile function across fiber types. The prevailing view is that Type I fibers are relatively resistant to age-related decline, with most studies reporting preserved CSA, force, and power, whereas Type II fibers exhibit more consistent reductions in size and function (3, 4, 10). Trappe, et al. (2003) showed that aging is associated with lower power in fast fibers, whereas age-related effects in slow fibers were less evident and appeared to be influenced by sex and training status (10). Likewise, Frontera et al. (2000) reported lower specific force in single fibers from older adults, supporting the concept of reduced fiber quality independent of size alone (5). D’Antona et al. (2003) further demonstrated that lower myosin heavy chain content in older fibers was associated with reduced specific force, suggesting that loss of

contractile protein may contribute to intrinsic dysfunction even when overt atrophy is limited (6). Brocca et al. (2017) extended this work by showing age-related alterations in the muscle proteome, including oxidative modifications of myosin and changes in regulatory proteins that may impair force generation and shortening behavior (8). Collectively, these findings support the idea that aging impairs single fiber function, but they also leave several important uncertainties unresolved.

First, age-related reductions in single-fiber power have not been characterized consistently across both Type I and Type II fibers using the same experimental framework. Second, although Type II fiber atrophy is often considered the dominant explanation for reduced power with aging, several studies have reported lower force-related properties even when CSA was not significantly different, indicating that intrinsic contractile quality may be impaired independently of fiber size (5, 6, 8). Third, prior studies have varied substantially in participant characteristics, physical activity status, sex representation, and the specific single-fiber variables reported, making it difficult to determine whether aging primarily impairs force production, shortening velocity, or both (3, 4, 10, 11). Finally, relatively few studies have evaluated both absolute and normalized contractile properties in a way that clearly separates deficits due to reduced fiber size from deficits due to reduced intrinsic quality. As a result, it remains unresolved whether age-related reductions in single-fiber power are primarily force-limited or velocity-limited, whether slow fibers are truly spared, and whether fast-fiber dysfunction can occur in the absence of overt atrophy.

These questions are especially important because the physiological basis of power loss may differ by fiber type. A decline in absolute power could reflect smaller

fiber size, lower force per cross-sectional area, slower shortening velocity, or some combination of these factors. Distinguishing among these possibilities has important mechanistic implications. If aging primarily reduces power through fast-fiber atrophy, then the central explanation would remain one of quantitative muscle loss. If, however, power is reduced despite preserved CSA, this would support the presence of qualitative defects within the contractile apparatus itself. Clarifying this distinction is necessary for a more complete understanding of muscle aging and may help explain why losses in functional performance often exceed losses in muscle mass alone (1, 3, 4).

Accordingly, the purpose of the present study was to determine whether aging alters single-fiber contractile properties in a fiber-type-specific manner in human vastus lateralis muscle. To address this question, we measured CSA, peak isometric force, specific force, maximal shortening velocity (V_{max}), peak power output, and normalized power output in skinned Type I and Type II single fibers isolated from young and older adults. Based on the prevailing literature, we hypothesized that aging would preferentially impair Type II fibers, such that older adults would exhibit smaller Type II fiber CSA and lower Type II force and power, whereas Type I fibers would be comparatively preserved (3, 4, 10). By examining both absolute and normalized mechanical properties, this study was designed to distinguish age-related deficits attributable to fiber size from those attributable to impaired intrinsic contractile quality.

METHODS

Ethical Approval

Participants were recruited from the larger EVEROLIMUS Aging Study (EVERLAST). Ten young (5 men, 5 women) and seven older adults (2 men, 5 women) volunteered to participate. All participants provided written informed consent and completed a medical screening before enrollment. Eligible participants were free of overt chronic disease (e.g., cardiovascular disease, diabetes, Alzheimer's) and were not taking immunosuppressive medications. Experimental procedures were approved by the University of Wisconsin-Madison Health Sciences Institutional Review Board (IRB# 2021-1519).

Experimental Overview

Skeletal muscle biopsies were taken from the vastus lateralis (VL) and processed for single fiber mechanical and molecular biology experiments. Isolated single muscle fibers (SMFs) were used to measure cross-sectional area (CSA), absolute peak force (P_0), specific force (SF; peak force normalized to CSA), loaded shortening velocity (V_{max}), peak power (PPO), and normalized power (NPO; peak power normalized to CSA). After mechanical testing, each fiber was typed by their myosin heavy chain (MHC) content using sodium dodecyl sulfate polyacrylamide gel electrophoresis (SDS-PAGE) to assess for Type 1 "slow" and Type 2 "fast" fiber type differences. Comparisons of contractile properties were then completed between young and older adults on a fiber type basis.

Single Fiber Contractile Experiments

Muscle biopsy and tissue processing. Percutaneous muscle biopsies were obtained at the UW Health University Hospital Clinical Research Unit. Muscle biopsies were performed using a 5 mm skeletal muscle biopsy needle with local anesthesia (1% lidocaine) applied at the biopsy site. A portion of the sample (~10–15 mg) was immediately transferred to a petri dish containing cold relaxing solution composed of (in mM): 100 KCl, 1.75 EGTA, 10 imidazole, 4 ATP, and 5 $MgCl_2$. Biopsy samples were first excised of ~1–2 mm of tissue from each end and stored at -80 °C for MHC distribution analyses. Fiber bundles (~20–50 fibers) were carefully dissected longitudinally from the biopsy and tied at both ends to capillary tubes with 6–0 braided silk suture. Bundles were then placed in skinning solution containing 50% relax solution and 50% glycerol (v:v) for 24 hours at 4 °C to permit the skinning process for subsequent mechanical measurements. After 24 hours, bundles were transferred to fresh skinning solution and stored at -20 °C until mechanical experimentation.

Solutions. Relaxing (described above), pre-activating solution (pCa 9.0) and maximally activating solution (pCa 4.5) for skinned fiber preparations were prepared as previously described (10, 12). The pCa 9.0 solution contained (in mM): 7 EGTA, 20 imidazole, 5.42 $MgCl_2$, 79.16 KCl, 0.01633 $CaCl_2$, 14.5 creatine phosphate, and 4.74 ATP. The pCa 4.5 solution contained (in mM): 7 EGTA, 20 imidazole, 5.26 $MgCl_2$, 64 KCl, 7.01 $CaCl_2$, 14.5 creatine phosphate, and 4.81 ATP. The pH of all single fiber solutions was adjusted to 7.0 at 15 °C with aqueous KOH. Final concentrations of metals, ligands, and metal-ligand complexes were calculated using the computer program of Fabiato (13).

Experimental setup. On the day of contractile experiments, a bundle was removed from skinning solution and placed in a petri dish containing cold relaxation solution under a dissecting microscope. For each experiment, an individual fiber (~2.0–4.0 mm) was isolated from the bundle with fine-point forceps and inspected to ensure it was intact. The experimental technique for fiber mounting and contractile measurements was performed as previously described (10, 12, 14, 15). Briefly, fibers were mounted in a 14 mm × 4 mm chamber containing relax solution within the permeabilized fiber apparatus (Model 802D, Aurora Scientific, ON, Canada) and attached between a capacitance-gauge force transducer (Model 403A, sensitivity of 20 $mV \cdot mg^{-1}$ and resonant frequency of 600 Hz; Aurora Scientific) and a DC torque motor (Model 308; Aurora Scientific). Fiber ends were placed into stainless-steel troughs and secured by overlaying a ~0.25–0.5 mm length of 4–0 monofilament nylon suture on each end and then tying the suture into the troughs with two loops of 10–0 monofilament suture. Length changes during contractile measurements were introduced at one end of the preparation driven by voltage commands from a PC via a 16-bit D/A converter.

The apparatus was mounted on an inverted phase-contrast microscope (IX50, Olympus, Tokyo, Japan) equipped with 4× and 10× objectives and a 15× photo eyepiece coupled to a CCD camera (CCD-IRIS, Sony, Tokyo, Japan). Chamber temperature was maintained at 15 °C by a Peltier device. Micromanipulators attached to the force transducer and motor were used to position the fiber in a taut but unstretched position. Fibers were then visualized at 150× magnification, and the length of the preparation was adjusted so that sarcomere length was set to 2.5 μm in relax solution.

Magnification was then returned to 60×, and fiber length (L_0) was recorded as the segment length between the transducer and motor troughs. Velocity measurements were normalized to L_0 and expressed as fiber lengths per second ($fl \cdot s^{-1}$). Digital images of the fiber were captured from top and side views, and fiber diameter was measured at three equally spaced points along the length of the fiber in each view using ImageJ (16). CSA was calculated assuming the fiber had an elliptical shape.

Before the force-velocity experiments, P_0 was measured and the integrity of the fiber mounting was verified by performing a slack-test previously described by Edman (17). Fibers were transferred from relax solution to pCa 9.0 for 60 seconds and then activated by transferring into pCa 4.5 solution. Once force plateaued, the fiber was rapidly slacked by 20% of L_0, producing an immediate decline in tension, followed by gradual redevelopment. The fiber was immediately returned to pCa 9.0 terminating force development and re-lengthened to L_0. P_0 was calculated as the difference between the peak force generated during isometric contraction and the minimum force recorded following the 20% slack. Fibers were accepted for subsequent force-velocity measurements when force rose smoothly, P_0 remained stable during activation, sarcomere length remained constant at 2.5 μm, no evidence of slippage from the troughs was observed, and the fiber remained structurally intact on visual inspection.

Force-velocity and force-power measurements. Force-velocity and power properties of each SMF were assessed as previously described by Trappe et al. (10, 18, 19). All measurements were performed at a sarcomere length of 2.5 μm. Each fiber was activated by transferring it into pCa 4.5 solution, allowed to develop peak isometric force, and then subjected to three predetermined submaximal isotonic loads spanning

~10–90% of P_0 for 200 ms (load combinations varied across activations to sample the full force-velocity relationship). This was followed by a 20% slack and transfer back to pCa 9.0 to terminate activation, after which the fiber was returned to its original length. Each fiber underwent 4–6 activations, yielding 12–18 isotonic contractions in total.

Loaded shortening velocity was determined from the slope of a linear regression fitted to the change in fiber length during the final 100 ms of each force step. The force-velocity relationship was constructed from the corresponding force and velocity values during each activation and fitted using the Hill equation (20). Power was derived from the fitted F-V parameters. Absolute peak power ($\mu N \cdot fl \cdot s^{-1}$) was calculated as the product of force (μN) and shortening velocity (V_{max}; $fl \cdot s^{-1}$) at the load yielding maximum power along the fitted force-velocity curve, whereas normalized power was calculated as the product of specific force ($kN \cdot m^{-2}$) and shortening velocity (V_{max}; $fl \cdot s^{-1}$) at the load yielding maximum normalized power ($W \cdot L^{-1}$) (21–23).

To ensure data quality, the P_0 recorded during each activation was normalized to the highest P_0 obtained for that fiber. Activations in which force declined to < 90% of the fiber-specific maximal P_0 were excluded, along with their associated force steps from further analysis. Construction of the F-V relationship required a minimum of four successful activations per fiber (yielding ≥ 12 isotonic contractions). Fibers with fitted F-V curves yielding $R^2 < 0.98$ were excluded from further analysis (10, 23).

MHC typing of single muscle fibers. MHC composition of isolated single fibers was determined by SDS-PAGE and silver staining. Following the contractile experiments, each fiber was solubilized in Laemmli buffer (2% SDS, 15% glycerol, 5% β-mercaptoethanol, 0.002% bromophenol blue, and 62.5 mM Tris, pH 6.7) at a volume

of 10 µL per mm of fiber length, heated for 5 min at 95 °C, and vortexed before and after heating to ensure fiber solubilization. Samples were loaded onto 1.0 mm thick hand-cast gels comprising a 4% stacking gel (35% glycerol, 4% acrylamide-bisacrylamide (49:1), 70 mM Tris (pH 6.7), 4 mM EDTA (pH 7.0), 0.4% SDS, 0.1% ammonium persulfate (APS), and 0.01% TEMED) and an 8% separating gel (35% glycerol, 8% acrylamide-bisacrylamide (49:1), 200 mM Tris (pH 8.8), 100 mM glycine, 0.4% SDS, 0.1% APS, and 0.01% TEMED). Human skeletal muscle homogenates containing MHC I, IIA, and IIX isoforms were run in parallel as reference standards. Electrophoresis was performed for 15 hours at 4 °C at a constant 250 V. Gels were then silver stained, and fiber MHC isoform content was determined from the migration pattern of the myosin bands referencing the homogenate control (Fig. 3). Fibers classified as hybrids were reanalyzed on a separate gel to rule out cross-contamination. Type II fibers were pooled, therefore hybrid Type IIX/IIA fibers were classified as Type II, and Type II/Type I hybrid fibers were excluded from further analysis (n = 2).

Statistical Analysis

Age-related differences in single muscle fiber size (CSA) and contractile properties (P_0, SF, V_{max}, PPO, and NPO) were tested using a nested ANOVA with age group (young or older) and fiber type (Type I or Type II) treated as fixed factors to account for the nesting of individual fibers within each participant. Because pure Type IIX and hybrid IIX/IIA fibers represented a small proportion of the total sample (< 6%), these fibers were pooled within a single Type II category, consistent with prior methodological precedent (21, 24). Type II/I hybrid fibers were excluded from analysis. Exact fiber numbers are reported for each outcome because fewer fibers met the

predefined quality criteria for force-velocity and power analyses than for force and CSA measurements. Statistical significance was considered at $P < 0.05$. Data are presented as mean ± SD in the text and tables and mean ± SEM in the figures. Statistical analysis was performed using GraphPad Prism, version 11.0.0 (GraphPad Software Inc., Boston, MA, USA).

RESULTS

Participant Characteristics

Participant anthropometrics are presented in Table 1. Height, weight, body mass index (BMI), lean body mass (LBM), thigh lean mass (TLM), and thigh fat mass (TFM) did not differ between groups, although BMI (30.3 ± 5.8 vs 24.9 ± 2.2 $kg \cdot m^{-2}$; $P = 0.052$) and TFM (4.3 ± 2.2 vs 2.6 ± 1.7 kg; $P = 0.076$) tended to be ~22% and ~65% higher in older adults compared to the younger adults. In contrast, older adults exhibited ~63% greater whole body fat percentage (43.3 ± 9.8 vs 26.6 ± 12.0%; $P = 0.008$) and ~57% greater thigh fat percentage (41.4 ± 12.2 vs 26.4 ± 15.0%; $P = 0.045$) compared to the young adults.

Single Fiber Size and Force

Single fiber CSA, peak force, and specific force values are presented in Table 2. Analyses included 84 Type I and 61 Type II fibers from young adults and 66 Type I and 32 Type II fibers from older adults. In Type I fibers, CSA did not differ between young (5462 ± 1408 μm^2) and older adults (4925 ± 1058 μm^2; $P = 0.273$). Similarly, specific force was not significantly different between young (148.5 ± 30.4 $kN \cdot m^{-2}$) and older adults (114.1 ± 45.9 $kN \cdot m^{-2}$; $P = 0.095$), although the mean value was ~23% lower. In contrast, P_0 was significantly lower (~31%) in older adults (0.53 ± 0.17 mN) compared to younger adults (0.77 ± 0.16 mN, $P = 0.006$; Fig. 1). In Type II fibers, CSA also did not differ between younger (5784 ± 2123 μm^2) and older adults (5017 ± 1398 μm^2; $P = 0.367$). P_0 likewise did not differ significantly between groups, although it was lower on average in older adults (0.66 ± 0.23 vs 0.89 ± 0.33 mN; $P = 0.075$). In contrast, specific

force was ~15% lower in older adults (135.3 ± 31.6 $kN \cdot m^{-2}$) compared to the young adults (158.6 ± 26.9 $kN \cdot m^{-2}$; $P = 0.029$; Fig. 2).

Single Fiber Shortening Velocity and Power

Values for V_{max}, peak power, and normalized power are presented in Table 3. Analyses included 77 Type I and 49 Type II fibers from young adults and 59 Type I and 23 Type II fibers from older adults. Fewer fibers met inclusion criteria for force-velocity and power analyses than for force and CSA measurements, reflecting exclusion of fibers that did not satisfy the predefined activation and curve-fitting quality criteria described in Methods. In Type I fibers, V_{max} was not significantly different between the young and older adults (0.46 ± 0.04 vs 0.42 ± 0.05 $fl \cdot s^{-1}$; $P = 0.187$). Similarly, NPO was not significantly different between the young (2.8 ± 0.7 $W \cdot L^{-1}$) and older adults (2.1 ± 0.8 $W \cdot L^{-1}$; $P = 0.118$), although it was 25% lower on average in older adults. PPO was significantly lower (~32%) in older adults (10.2 ± 2.5 vs 15.1 ± 3.9 $\mu N \cdot fl \cdot s^{-1}$; $P = 0.016$; Fig. 1). In Type II fibers, V_{max} likewise did not differ between groups (0.62 ± 0.12 vs 0.59 ± 0.12 $fl \cdot s^{-1}$; $P = 0.278$). PPO was 32% lower in older adults (28.1 ± 11.1 $\mu N \cdot fl \cdot s^{-1}$ vs 41.1 ± 16.4 $\mu N \cdot fl \cdot s^{-1}$; $P = 0.041$; Fig. 2), and NPO was 19% lower (5.8 ± 1.9 vs 7.2 ± 1.2 $W \cdot L^{-1}$; P = 0.007; Fig. 2).

Summary of Fiber-Type-Specific Age Effects

Overall, aging was associated with a comparable reduction in peak power in both Type I and Type II fibers (~32%), along with lower normalized power in Type II fibers of the older adults. The force-related deficit differed by fiber type, with Type I fibers exhibiting lower absolute peak force and Type II fibers exhibiting lower specific force.

Importantly, these age-related impairments in force and power occurred despite no significant reductions in CSA or V_{max} in either fiber type.

DISCUSSION

Principal Findings

The present study examined the effects of aging on single-fiber contractile properties in Type I and Type II fibers from young and older adults. Four principal findings emerged. First, peak power was 32% lower in older adults in both fiber types. Second, maximal shortening velocity was preserved with aging in both Type I and Type II fibers. Third, the force-related deficit was fiber type specific, with older adults exhibiting lower peak force in Type I fibers and lower specific force in Type II fibers. Fourth, contrary to our hypothesis, aging was not associated with a significant reduction in Type II fiber CSA. Collectively, these findings suggest the age-related reductions observed in this cohort were driven primarily by impaired force and power production rather than slower shortening velocity, and that intrinsic impairments in contractile quality may occur in the absence of atrophy.

Force-Related Basis of Age-Related Power Loss

A central finding was the consistent reduction in peak power across fiber types. Peak power was approximately one-third lower in older adults in both Type I and Type II fibers, indicating that aging impairs the work capacity of both types of single fibers. This observation is physiologically meaningful because muscle power declines earlier and more precipitously than muscle strength with advancing age and is a strong predictor of physical limitations and mortality in older adults (1, 2). Importantly, single fiber contractile properties such as cross-bridge kinetics and isometric tension in Type II fibers have been shown to correlate with whole-muscle power output in older adults (7), suggesting that deficits within the myofilament may scale upward and contribute to the

broader whole muscle power deficits associated with functional decline. At the single fiber level, the present findings are broadly consistent with prior human studies reporting age-related reductions in fast fiber power of approximately 20–50% in older adults (10, 21, 24, 25). However, the present data extend this literature by demonstrating a comparable relative power deficit in Type I fibers, a result less consistently reported and one that contrasts with the prevailing view that slow fiber power is largely preserved with aging or may even be greater in older adults (3, 10, 21, 23–26). Despite a similar overall reduction in peak power across fiber types, the physiological basis of this deficit appeared to diverge.

The preserved V_{max} in both Type I and Type II fibers is notable because it indicates that the age-related reduction in power was not driven by slower shortening velocity. Rather, the power deficit was more closely attributable to reduced force production, specifically lower specific force in Type II fibers and lower peak force in Type I fibers. This pattern is broadly consistent with prior single fiber work suggesting that shortening velocity is less sensitive to aging than force and power related properties when examined at the single fiber level and positions the present findings within a framework of force limited rather than velocity limited contractile decline.

Fiber-Type-Specific Pattern of Contractile Dysfunction

Although peak power was reduced in both fiber types, the underlying pattern differed. In Type I fibers, older adults exhibited lower peak force and lower peak power despite no significant difference in CSA, SF, V_{max}, or NPO. Notably, although neither CSA nor SF differed significantly on its own, both were directionally lower in the older adults. Because absolute force reflects both fiber size and force relative to fiber area,

the lower Type I P_0 likely reflects the combined contribution of these two downward trends rather than an isolated deficit in either variable alone. In this respect, the present findings differ from the commonly held view that Type I fibers are relatively resistant to age-related contractile impairment (3) and are not fully aligned with earlier studies in which age-related differences in Type I function were minimal or influenced by sex and training status (10). In Trappe et al., (2003) lower MHC I peak power was observed in young women relative to the other three groups, and no significant age-related difference in Type I peak power was identified between young and older participants of the same sex. The present finding of lower Type I P_0 and PPO in older adults therefore supports the interpretation that slow fibers were not fully protected from age-related decline as previously reported. Longitudinal data in which older adults were followed over ~9 years reported preserved Type I fiber size and even a tendency toward maintained or increased force over time in older adults (27), suggesting that the extent of Type I dysfunction may vary across cohorts and study designs. The cellular basis for the lower Type I force and power observed here cannot be determined from the present mechanical data, although prior studies have suggested that alterations in myofibrillar protein content may contribute to age-related reductions in force generation. Consistent with this theory, D'Antona et al., (2003) reported that myosin concentration per fiber decreased significantly with aging in both Type I and II human fibers and was linearly correlated with specific force, suggesting that age-related alterations in myofilament protein content may contribute to reduced force generation even when overt atrophy is not evident (6). Because normalized power was not significantly different between groups, the lower Type I peak power appears to have been driven primarily by lower

absolute force production rather than slower shortening velocity. The present data indicate that Type I fibers were not fully protected from age-related decline. This finding was not consistent with our hypothesis that Type I fibers would be preserved with aging and differs from the prevailing view that slow fibers are relatively resistant to age-related contractile impairment.

Our findings in the Type II fibers point more directly to an age-related impairment in intrinsic contractile function. Older adults exhibited lower specific force, lower peak power, and lower normalized power in Type II fibers, despite preserved CSA and Vmax. This pattern indicates that the power deficit in older Type II fibers was more closely related to lower force production than to slower shortening velocity or smaller CSA. This interpretation is consistent with prior data showing that aging can reduce force-related properties of fast fibers independent of fiber atrophy (5). The present data do not identify the molecular basis of this deficit, although prior studies have implicated reduced myosin content, altered cross-bridge kinetics, modifications of contractile or regulatory proteins (e.g., phosphorylation, carbonylation, glycation), and changes in the structural organization of the actomyosin lattice as potential contributors to age-related dysfunction (4, 6–9, 12, 28, 29). Accordingly, the present results support the interpretation that Type II fiber dysfunction extended beyond fiber size alone.

Taken together, these findings indicate that age-related deficits were not confined to fast fibers. Although aging is often described as selectively impairing Type II fibers, older adults in the present study also exhibited lower Type I peak force and peak power. Thus, slow fibers in the vastus lateralis were not fully protected from age-related decline. At the same time, the pattern remained fiber-type specific: Type I deficits were

most evident in absolute function, whereas Type II deficits extended to normalized measures. This distinction suggests broader aging-related effects across fiber types, with more pronounced impairment of intrinsic contractile function in fast fibers.

Type II Dysfunction in the Absence of Overt Atrophy

The absence of a significant reduction in Type II CSA was contrary to our original hypothesis and differs from much of the existing literature supporting selective fast-fiber atrophy with aging (3). Multiple studies have reported reduced Type II fiber size in older adults, all of which support the broader view that fast fiber atrophy contributes to age-related dysfunction (21, 24, 25, 30, 31). This discrepancy is important because reductions in Type II force and power are often interpreted as secondary to smaller fiber size. In the present study, however, Type II normalized power was lower in older adults despite no significant difference in CSA. This suggests that the Type II fiber impairment in this cohort reflects reduced intrinsic quality rather than atrophy alone.

Several factors may explain why the present findings differ somewhat from the dominant pattern reported previously. Methodological differences across studies, including fiber handling, storage, testing conditions, and approaches used to estimate CSA and calculate specific force, may also contribute to the variability in the literature. Finally, it remains possible that Type II fibers in older adults are more fragile and prone to mechanical failure during dissection and experimentation, making them less likely to be successfully mounted and analyzed. In fact, Type II fibers exhibit a higher failure rate during experimentation (32), with this effect being more pronounced in older adults (10, 11, 32). As a result, the most atrophied and functionally compromised fibers may be

underrepresented in analyses, potentially obscuring the true extent of age-related atrophy and may contribute to the inconsistencies observed in some studies.

Body Composition

Older adults also exhibited higher whole-body and thigh fat percentages, indicating less favorable body composition despite no significant difference in lean mass. Although the present study was not designed to determine whether these group differences directly contributed to the observed single fiber impairments, their coexistence with reduced peak power is consistent with the view that age-related muscle dysfunction reflects both compositional and intrinsic contractile changes. Prior studies suggest that greater adiposity and lipid accumulation may adversely affect muscle quality and contractile function with aging, in some cases in a fiber type specific manner (33–35). However, whether the differences in adiposity observed in the present study were associated with the lower specific force and normalized power seen in older adults cannot be determined from this study alone.

Limitations

Several limitations should be acknowledged. The cross-sectional design precludes causal inference and cannot exclude cohort effects, including differences in habitual physical activity and nutrition. This is particularly relevant because habitual physical activity level independently influences single fiber MHC content, contractile velocity, and cross-bridge kinetics in older adults (6, 36, 37), and lifelong exercise training can meaningfully attenuate the trajectory of the age-related dysfunction of single fibers (10, 11, 25). Second, sex was not balanced across groups, and sex-specific differences in age-related impairments within the myofilament may have

influenced the present findings, including the greater age-related slowing of cross-bridge kinetics reported in older women (7), and sex-specific patterns of Type I and II contractile decline (10, 38). Despite these limitations, the consistent reduction in peak power across both fiber types, together with lower Type I peak force and lower Type II specific force, supports the physiological relevance of the observed age-related differences.

Conclusion

In conclusion, aging was associated with contractile impairments in both Type I and Type II single muscle fibers. Contrary to our hypotheses, Type I fibers were not fully protected from age-related decline, and the pattern of dysfunction was fiber type specific. Type I fibers exhibited reductions in absolute peak force and power, whereas Type II fibers showed lower specific force, peak power, and normalized power, indicating a more pronounced impairment in intrinsic function. Neither V_{max} nor CSA differed significantly between groups in either fiber type. Collectively, these findings suggest that age-related reductions in single-fiber contractile function were more apparent in force and power than in shortening velocity, and, in Type II fibers, were not fully explained by differences in fiber size. These cellular-level deficits provide the basis for evaluating the extent to which single fiber dysfunction parallels whole muscle dysfunction in Chapter 3 and for identifying potential molecular correlates in Chapter 4.

TABLES AND FIGURES

Table 1. Anthropometrics of young and older adults

Variable	Units	Young Adults *N* = 10 (5 M:5 W)	Older Adults *N* = 7 (2 M:5 W)	*P* value
Age	years	28.3 ± 1.8	61.3 ± 2.9	**<0.001**
Height	cm	173.6 ± 4.2	169.2 ± 8.6	0.176
Weight	kg	75.0 ± 6.9	86.4 ± 16.9	0.132
Body mass index	$kg \cdot m^{-2}$	24.9 ± 2.2	30.3 ± 5.8	0.052
Lean body mass	kg	52.47 ± 8.1	46.09 ± 7.1	0.114
Body fat	%	26.6 ± 12.0	43.3 ± 9.8	**0.008**
Thigh lean mass	kg	6.7 ± 1.1	5.7 ± 1.1	0.097
Thigh fat mass	kg	2.6 ± 1.7	4.3 ± 2.2	0.076
Thigh fat	%	26.4 ± 15.0	41.4 ± 12.2	**0.045**

Body fat percentage, total lean mass, thigh lean mass, thigh fat mass, and thigh fat percentage were measured by dual-energy X-ray absorptiometry. *N* denotes the number of participants; lowercase *n* denotes number of single muscle fibers. Significant age differences are indicated in bold when $P < 0.05$. Data are presented as the mean ± SD.

Table 2. Fiber size (CSA) and peak force (P_0, SF)

	Units	Young Adults *N* = 9–10 (5M:4–5W)	Older Adults *N* = 6–7 (2M:4–5W)	Difference	*P* value
Slow MHC I	*n*	84	66		
CSA	μm^2	5462 ± 1408	4925 ± 1058	↔	0.273
P_0	mN	0.77 ± 0.16	0.53 ± 0.17	↓ 31%	**0.006**
Specific force	$kN \cdot m^{-2}$	148.5 ± 30.4	114.1 ± 45.9	↔	0.095
Fast MHC II	*n*	61	32		
CSA	μm^2	5784 ± 2123	5017 ± 1398	↔	0.367
P_0	mN	0.89 ± 0.33	0.66 ± 0.23	↔	0.075
Specific force	$kN \cdot m^{-2}$	158.6 ± 26.9	135.3 ± 31.6	↓ 15%	**0.029**

Fiber diameter was measured from digital images obtained from top and side views while the fiber was relaxed and mounted in the experimental apparatus. Cross-sectional area (CSA) was calculated from the mean of the two diameters assuming an elliptical fiber shape. P_0 was defined as the peak isometric force produced during experimentation. Specific force was calculated by normalizing P_0 to CSA. Significant age differences are indicated in bold when $P < 0.05$. Data are presented as the mean ± SD.

Table 3. Fiber maximal shortening velocity (V_{max}) and peak power (PPO, NPO)

	Units	Young Adults *N* = 9–10 (5M:4–5W)	Older Adults *N* = 6–7 (2M:4–5W)	Difference	*P* value
Slow MHC I	*n*	77	59	↔	0.661
V_{max}	fl·s^{-1}	0.46 ± 0.04	0.42 ± 0.05	↔	0.187
Peak power	μN·fl·s^{-1}	15.1 ± 3.9	10.2 ± 2.5	↓ 32%	**0.016**
Normalized power	W·L^{-1}	2.8 ± 0.7	2.1 ± 0.8	↔	0.118
Fast MHC II	n	49	23		
V_{max}	fl·s^{-1}	0.62 ± 0.12	0.59 ± 0.12		0.278
Peak power	μN·fl·s^{-1}	41.1 ± 16.4	28.1 ± 11.1	↓ 32%	**0.041**
Normalized power	W·L^{-1}	7.2 ± 1.2	5.8 ± 1.9	↓ 19%	**0.007**

Absolute power (μN·fl·s^{-1}) and normalized peak power (W·L^{-1}) were calculated from the fitted parameters of the force-velocity curves. Maximal shortening velocity (V_{max}) was derived from the Hill equation fit to the force-velocity relationship. Significant age differences are indicated in bold when $P < 0.05$. Data are presented as the mean ± SD

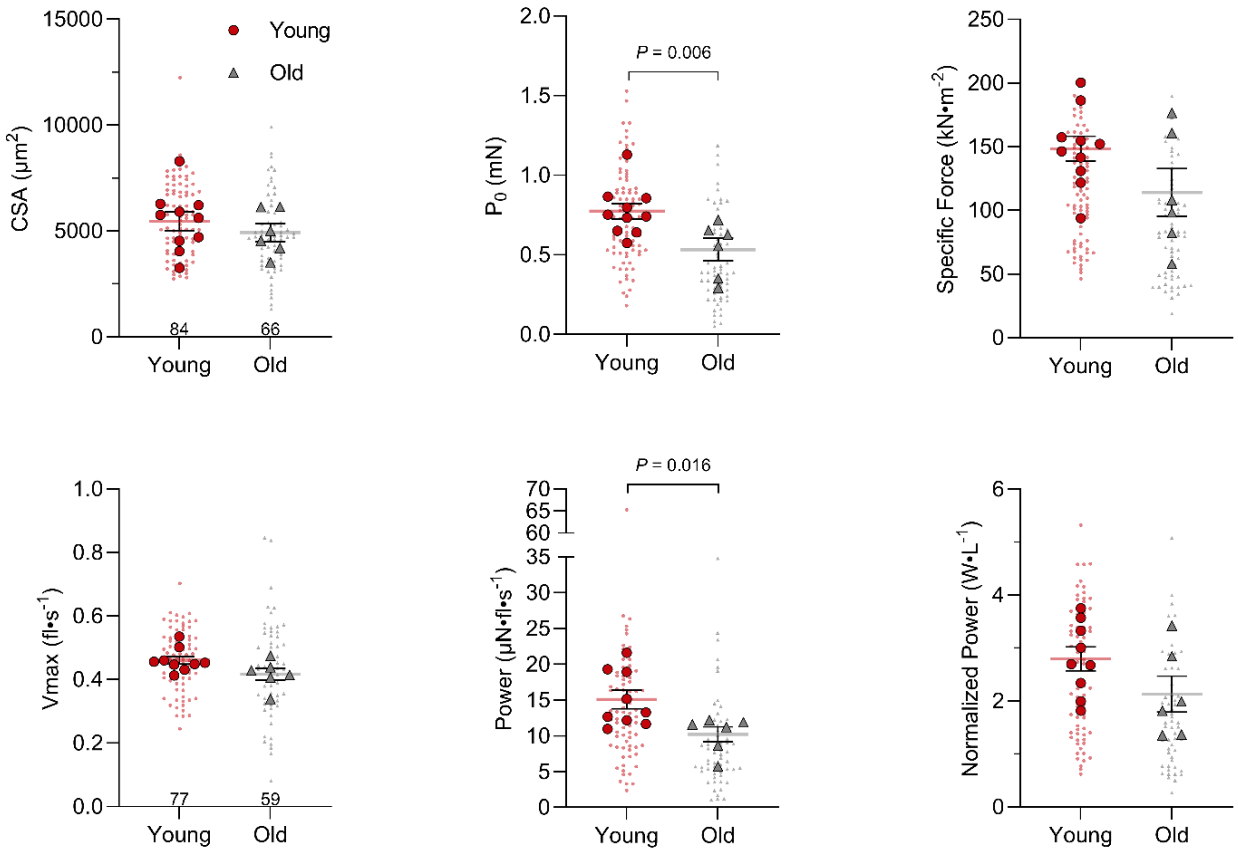

Figure 1. Age-related differences in Type I single muscle fiber properties. Cross-sectional area (CSA), peak force (P_0), specific force (SF; P_0 normalized to CSA), maximal shortening velocity (V_{max}), peak power (PPO) and normalized peak power (NPO; PPO normalized to CSA) were compared between young and older adults. The number of fibers (*n*) is shown on the x-axis for CSA and V_{max} and applies to all variables within the corresponding row. Red and gray horizontal bars indicate group means ± SEM for young and older adults, respectively. Large red circles represent young subject means, and large gray triangles represent older subject means. Small symbols denote individual fibers. Age-related differences were tested using nested ANOVA. Exact *P* values are shown for significant comparisons.

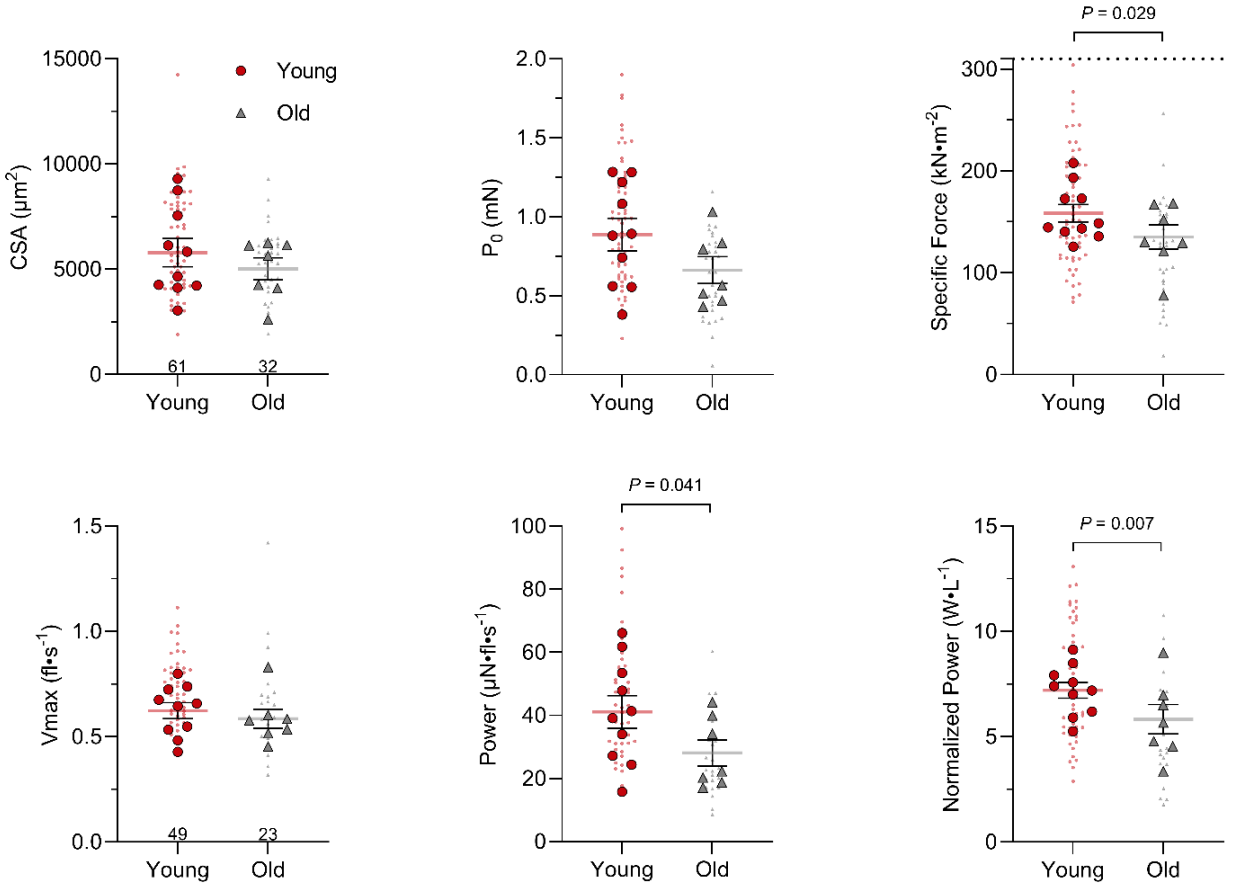

Figure 2. Age-related differences in Type II single muscle fiber properties. Cross-sectional area (CSA), peak force (P_0), specific force (SF; P_0 normalized to CSA), maximal shortening velocity (V_{max}), peak power (PPO), and normalized peak power (NPO; PPO normalized to CSA) were compared between young and older adults. The number of fibers (*n*) is shown on the x-axis for CSA and V_{max} and applies to all variables within the corresponding row. Red and gray horizontal bars indicate group means ± SEM for young and older adults, respectively. Large red circles represent young subject means, and large gray triangles represent older subject means. Small symbols denote individual fibers. Age-related differences were tested using nested ANOVA. Exact *P* values are shown for significant comparisons.

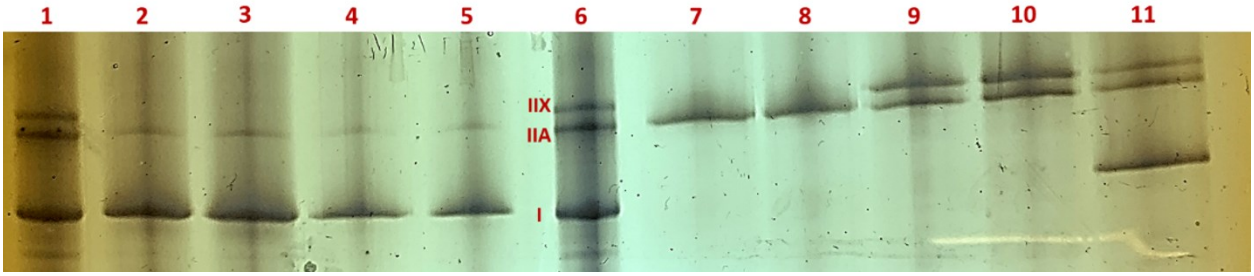

Figure 3. Representative SDS-PAGE gel of human skeletal muscle homogenates and isolated single muscle fibers used for fiber type classification. Lanes 1, 6, and 11 contain human skeletal muscle homogenate standards showing the migration pattern of MHC I, MHC IIA, and MHC IIX isoforms. Lanes 2–5 and 7–10 contain representative single muscle fiber samples. Bands were identified by comparison with the homogenate standards. Lanes 9 and 10 show fibers with a hybrid MHC IIX/IIA pattern; these fibers were run again on a separate gel to confirm hybridization and exclude cross-contamination.

REFERENCES

1. **Reid KF**, **Fielding RA**. Skeletal Muscle Power: A Critical Determinant of Physical Functioning in Older Adults. *Exercise and Sport Sciences Reviews* 40: 4–12, 2012. doi: 10.1097/JES.0b013e31823b5f13.

2. **Byrne C**, **Faure C**, **Keene DJ**, **Lamb SE**. Ageing, Muscle Power and Physical Function: A Systematic Review and Implications for Pragmatic Training Interventions. *Sports Med* 46: 1311–1332, 2016. doi: 10.1007/s40279-016-0489-x.

3. **Grosicki GJ**, **Zepeda CS**, **Sundberg CW**. Single muscle fibre contractile function with ageing. *The Journal of Physiology* 600: 5005–5026, 2022. doi: 10.1113/JP282298.

4. **Lim J-Y**, **Frontera WR**. Single skeletal muscle fiber mechanical properties: a muscle quality biomarker of human aging. *Eur J Appl Physiol* 122: 1383–1395, 2022. doi: 10.1007/s00421-022-04924-4.

5. **Frontera WR**, **Suh D**, **Krivickas LS**, **Hughes VA**, **Goldstein R**, **Roubenoff R**. Skeletal muscle fiber quality in older men and women. *Am J Physiol Cell Physiol* 279: C611-618, 2000. doi: 10.1152/ajpcell.2000.279.3.C611.

6. **D'Antona G**, **Pellegrino MA**, **Adami R**, **Rossi R**, **Carlizzi CN**, **Canepari M**, **Saltin B**, **Bottinelli R**. The effect of ageing and immobilization on structure and function of human skeletal muscle fibres. *The Journal of Physiology* 552: 499–511, 2003. doi: https://doi.org/10.1111/j.1469-7793.2003.00499.x.

7. **Miller MS**, **Bedrin NG**, **Callahan DM**, **Previs MJ**, **Jennings ME**, **Ades PA**, **Maughan DW**, **Palmer BM**, **Toth MJ**. Age-related slowing of myosin actin cross-bridge kinetics is sex specific and predicts decrements in whole skeletal muscle performance in humans. *Journal of Applied Physiology* 115: 1004–1014, 2013. doi: 10.1152/japplphysiol.00563.2013.

8. **Brocca L**, **McPhee JS**, **Longa E**, **Canepari M**, **Seynnes O**, **De Vito G**, **Pellegrino MA**, **Narici M**, **Bottinelli R**. Structure and function of human muscle fibres and muscle proteome in physically active older men. *The Journal of Physiology* 595: 4823–4844, 2017. doi: 10.1113/JP274148.

9. **Day NJ**, **Kelly SS**, **Lui L-Y**, **Mansfield TA**, **Gaffrey MJ**, **Trejo JB**, **Sagendorf TJ**, **Attah IK**, **Moore RJ**, **Douglas CM**, **Newman AB**, **Kritchevsky SB**, **Kramer PA**, **Marcinek DJ**, **Coen PM**, **Goodpaster BH**, **Hepple RT**, **Cawthon PM**, **Petyuk VA**, **Esser KA**, **Qian W-J**, **Cummings SR**. Signatures of cysteine oxidation on muscle structural and contractile proteins are associated with physical performance and muscle function in older adults: Study of Muscle, Mobility and Aging (SOMMA). *Aging Cell* 23: e14094, 2024. doi: 10.1111/acel.14094.

10. **Trappe S**, **Gallagher P**, **Harber M**, **Carrithers J**, **Fluckey J**, **Trappe T**. Single Muscle Fibre Contractile Properties in Young and Old Men and Women. *The Journal of Physiology* 552: 47–58, 2003. doi: 10.1113/jphysiol.2003.044966.

11. **Grosicki GJ**, **Gries KJ**, **Minchev K**, **Raue U**, **Chambers TL**, **Begue G**, **Finch H**, **Graham B**, **Trappe TA**, **Trappe S**. Single muscle fibre contractile characteristics with lifelong endurance exercise. *The Journal of Physiology* 599: 3549–3565, 2021. doi: 10.1113/JP281666.

12. **Gregorich ZR**, **Peng Y**, **Cai W**, **Jin Y**, **Wei L**, **Chen AJ**, **McKiernan SH**, **Aiken JM**, **Moss RL**, **Diffee GM**, **Ge Y**. Top-Down Targeted Proteomics Reveals Decrease in Myosin Regulatory Light-Chain Phosphorylation That Contributes to Sarcopenic Muscle Dysfunction. *J Proteome Res* 15: 2706–2716, 2016. doi: 10.1021/acs.jproteome.6b00244.

13. **Fabiato A**. Computer programs for calculating total from specified free or free from specified total ionic concentrations in aqueous solutions containing multiple metals and ligands. In: *Methods in Enzymology*. Elsevier, p. 378–417.

14. **Melby JA**, **Brown KA**, **Gregorich ZR**, **Roberts DS**, **Chapman EA**, **Ehlers LE**, **Gao Z**, **Larson EJ**, **Jin Y**, **Lopez JR**, **Hartung J**, **Zhu Y**, **McIlwain SJ**, **Wang D**, **Guo W**, **Diffee GM**, **Ge Y**. High sensitivity top–down proteomics captures single muscle cell heterogeneity in large proteoforms. *Proceedings of the National Academy of Sciences* 120: e2222081120, 2023. doi: 10.1073/pnas.2222081120.

15. **Moss RL**. Sarcomere length-tension relations of frog skinned muscle fibres during calcium activation at short lengths. *J Physiol* 292: 177–192, 1979. doi: 10.1113/jphysiol.1979.sp012845.

16. **Schneider CA**, **Rasband WS**, **Eliceiri KW**. NIH Image to ImageJ: 25 years of image analysis. *Nat Methods* 9: 671–675, 2012. doi: 10.1038/nmeth.2089.

17. **Edman KA**. The velocity of unloaded shortening and its relation to sarcomere length and isometric force in vertebrate muscle fibres. *The Journal of Physiology* 291: 143–159, 1979. doi: 10.1113/jphysiol.1979.sp012804.

18. **Trappe S**, **Godard M**, **Gallagher P**, **Carroll C**, **Rowden G**, **Porter D**. Resistance training improves single muscle fiber contractile function in older women. *American Journal of Physiology-Cell Physiology* 281: C398–C406, 2001. doi: 10.1152/ajpcell.2001.281.2.C398.

19. **Trappe S**, **Williamson D**, **Godard M**, **Porter D**, **Rowden G**, **Costill D**. Effect of resistance training on single muscle fiber contractile function in older men. *Journal of Applied Physiology* 89: 143–152, 2000. doi: 10.1152/jappl.2000.89.1.143.

20. **Hill AV**. The heat of shortening and the dynamic constants of muscle. *Proc R Soc Lond B* 126: 136–195, 1938. doi: 10.1098/rspb.1938.0050.

21. **Sundberg CW**, **Teigen LE**, **Hunter SK**, **Fitts RH**. Cumulative effects of H+ and Pi on force and power of skeletal muscle fibres from young and older adults. *The Journal of Physiology* 603: 187–209, 2025. doi: 10.1113/JP286938.

22. **Widrick JJ**, **Trappe SW**, **Costill DL**, **Fitts RH**. Force-velocity and force-power properties of single muscle fibers from elite master runners and sedentary men. *Am J Physiol* 271: C676-683, 1996. doi: 10.1152/ajpcell.1996.271.2.C676.

23. **Harber MP**, **Konopka AR**, **Undem MK**, **Hinkley JM**, **Minchev K**, **Kaminsky LA**, **Trappe TA**, **Trappe S**. Aerobic exercise training induces skeletal muscle hypertrophy and age-dependent adaptations in myofiber function in young and older men. *Journal of Applied Physiology* 113: 1495–1504, 2012. doi: 10.1152/japplphysiol.00786.2012.

24. **Sundberg CW**, **Hunter SK**, **Trappe SW**, **Smith CS**, **Fitts RH**. Effects of elevated H+ and Pi on the contractile mechanics of skeletal muscle fibres from young and old men: implications for muscle fatigue in humans. *The Journal of Physiology* 596: 3993–4015, 2018. doi: 10.1113/JP276018.

25. **Gries KJ**, **Minchev K**, **Raue U**, **Grosicki GJ**, **Begue G**, **Finch WH**, **Graham B**, **Trappe TA**, **Trappe S**. Single-muscle fiber contractile properties in lifelong aerobic exercising women. *Journal of Applied Physiology* 127: 1710–1719, 2019. doi: 10.1152/japplphysiol.00459.2019.

26. **Raue U**, **Slivka D**, **Minchev K**, **Trappe S**. Improvements in whole muscle and myocellular function are limited with high-intensity resistance training in octogenarian women. *Journal of Applied Physiology* 106: 1611–1617, 2009. doi: 10.1152/japplphysiol.91587.2008.

27. **Frontera WR**, **Reid KF**, **Phillips EM**, **Krivickas LS**, **Hughes VA**, **Roubenoff R**, **Fielding RA**. Muscle fiber size and function in elderly humans: a longitudinal study. *J Appl Physiol (1985)* 105: 637–642, 2008. doi: 10.1152/japplphysiol.90332.2008.

28. **Lowe DA**, **Thomas DD**, **Thompson LV**. Force generation, but not myosin ATPase activity, declines with age in rat muscle fibers. *American Journal of Physiology-Cell Physiology* 283: C187–C192, 2002. doi: 10.1152/ajpcell.00008.2002.

29. **Noonan AM**, **Mazara N**, **Zwambag DP**, **Weersink E**, **Power GA**, **Brown SHM**. Age-related changes in human single muscle fibre passive elastic properties are sarcomere length dependent. *Experimental Gerontology* 137: 110968, 2020. doi: 10.1016/j.exger.2020.110968.

30. **Korhonen MT**, **Cristea A**, **Alén M**, **Häkkinen K**, **Sipilä S**, **Mero A**, **Viitasalo JT**, **Larsson L**, **Suominen H**. Aging, muscle fiber type, and contractile function in sprint-trained athletes. *Journal of Applied Physiology* 101: 906–917, 2006. doi: 10.1152/japplphysiol.00299.2006.

31. **McPhee JS**, **Cameron J**, **Maden-Wilkinson T**, **Piasecki M**, **Yap MH**, **Jones DA**, **Degens H**. The Contributions of Fiber Atrophy, Fiber Loss, In Situ Specific Force, and Voluntary Activation to Weakness in Sarcopenia. *J Gerontol A Biol Sci Med Sci* 73: 1287–1294, 2018. doi: 10.1093/gerona/gly040.

32. **Yu F**, **Hedström M**, **Cristea A**, **Dalén N**, **Larsson L**. Effects of ageing and gender on contractile properties in human skeletal muscle and single fibres. *Acta Physiologica* 190: 229–241, 2007. doi: 10.1111/j.1748-1716.2007.01699.x.

33. **Straight CR**, **Voigt TB**, **Jala AV**, **Chase JD**, **Ringham OR**, **Ades PA**, **Toth MJ**, **Miller MS**. Quadriceps Lipid Content Has Sex-Specific Associations With Whole-Muscle, Cellular, and Molecular Contractile Function in Older Adults. *J Gerontol A Biol Sci Med Sci* 74: 1879–1886, 2019. doi: 10.1093/gerona/gly235.

34. **Carter CS**, **Justice JN**, **Thompson L**. Lipotoxicity, aging, and muscle contractility: does fiber type matter? *GeroScience* 41: 297–308, 2019. doi: 10.1007/s11357-019-00077-z.

35. **Gueugneau M**, **Coudy-Gandilhon C**, **Théron L**, **Meunier B**, **Barboiron C**, **Combaret L**, **Taillandier D**, **Polge C**, **Attaix D**, **Picard B**, **Verney J**, **Roche F**, **Féasson L**, **Barthélémy J-C**, **Béchet D**. Skeletal Muscle Lipid Content and Oxidative Activity in Relation to Muscle Fiber Type in Aging and Metabolic Syndrome. *J Gerontol A Biol Sci Med Sci* 70: 566–576, 2015. doi: 10.1093/gerona/glu086.

36. **D'Antona G**, **Pellegrino MA**, **Carlizzi CN**, **Bottinelli R**. Deterioration of contractile properties of muscle fibres in elderly subjects is modulated by the level of physical activity. *Eur J Appl Physiol* 100: 603–611, 2007. doi: 10.1007/s00421-007-0402-2.

37. **Miller MS**, **Callahan DM**, **Toth MJ**. Skeletal muscle myofilament adaptations to aging, disease, and disuse and their effects on whole muscle performance in older adult humans [Online]. *Frontiers in Physiology* 5, 2014. https://www.frontiersin.org/articles/10.3389/fphys.2014.00369 [10 Aug. 2022].

38. **Krivickas LS**, **Suh D**, **Wilkins J**, **Hughes VA**, **Roubenoff R**, **Frontera WR**. Age- and Gender-Related Differences in Maximum Shortening Velocity of Skeletal Muscle Fibers. *American Journal of Physical Medicine & Rehabilitation* 80: 447, 2001.

CHAPTER III

Integration of Whole Muscle Function and Single Fiber Contractile Properties in Human Aging

INTRODUCTION

Natural aging is accompanied by progressive declines in skeletal muscle mass, strength, and power that collectively impair physical function and increase the risk of adverse health outcomes. Beginning around the fourth decade of life, skeletal muscle mass declines at a rate of ~0.5–1% per year, whereas muscle strength tends to decline between ~1–3% per year, and muscle power declines earlier and occurs more precipitously at ~3–4% per year (1–8). These progressive losses in muscle quantity and function accelerate with increasing age, leading to functional impairments, including mobility limitations, fall-related injuries, and increased hospitalization (9, 10). Additionally, declines in muscle mass are frequently associated with comorbidities such as metabolic disease, neurodegenerative disease, and cardiovascular disease, further compounding the burden of age-related muscle dysfunction and increasing all-cause mortality (10–12).

At the whole-muscle level, cross-sectional and longitudinal studies consistently report age-related declines in peak torque, shortening velocity, and power output of the knee extensors (1, 2, 6, 13–18). Age-related deficits in isokinetic peak torque range from 8–47% across angular velocities, with greater impairments at higher contraction speeds, while reductions in isometric peak torque range from 18–89% depending on joint angle and testing conditions (13, 17, 19–28). Whole muscle shortening velocity is also diminished, with older adults approximately 20% slower during repetitive contractions and 25–42% lower power output, particularly at higher velocities (14, 16, 17, 29, 30). Muscle power deficits of 20–60% have been reported even when normalized to thigh lean mass (1, 2, 4, 6, 8, 13, 15, 16, 18, 32–34), suggesting that

intrinsic alterations within skeletal muscle, such as changes in fiber type composition, contractile protein expression, and impaired single muscle fiber (SMF) contractile mechanics, contribute to functional decline beyond what is explained by atrophy alone (1, 2, 4, 8, 13–18, 20, 21, 23, 33, 34). Importantly, age-related changes in thigh tissue composition extend beyond atrophy: reductions in lean mass are accompanied by increased intermuscular and intramuscular adipose tissue, which contribute independently to deficits in strength and power and are not fully captured by lean-mass normalization (4, 31). These compositional changes are thought to impair force transmission and alter the fibers mechanical and biochemical environment, making thigh composition an important covariate when linking single fiber properties to whole muscle function (4, 31).

At the cellular level, the chemically skinned single muscle fiber preparation permits direct assessment of the contractile apparatus independent of neural drive, excitation-contraction coupling, and perfusion-related influences. Using this approach, studies have demonstrated that aging does not uniformly affect all fiber types. Type I (slow-twitch) fibers are generally better preserved, whereas Type II (fast-twitch) fibers exhibit more consistent age-related reductions in size, force, and power (15, 16, 18, 35–49). Much of the evidence in Type II fibers points towards a parallel decline in absolute peak force and power that are primarily attributable to the reduced fiber size (15, 16, 18, 35, 36, 43, 44, 46, 50–53). However, the evidence for intrinsic contractile dysfunction in the Type II fibers is more complex; many published studies report age-related reductions in specific force, shortening velocity, or both in Type II fibers, while others report preservation or even enhancement of normalized properties in older adults (15,

16, 21, 36, 38, 39, 44, 46, 52–57). These inconsistencies suggest that aging may involve both quantitative (atrophy) and qualitative (intrinsic contractile) alterations, particularly within fast-twitch fibers.

Despite advances in characterizing age-related changes at the single fiber level, the extent to which these cellular properties are associated with whole muscle function remains unclear. A commonly cited observation in the literature is an apparent dissociation between single fiber properties and whole-muscle contractile function. Size-normalized intrinsic fiber function, particularly in slow fibers, is largely preserved with age, and age-related deficits in fast fiber force and power are smaller in magnitude than the concurrent declines in whole-muscle strength and power (15, 16, 22, 52, 58). However, relatively few studies have directly examined relationships between single fiber mechanics and whole muscle function within the same individuals (21–23, 32, 59, 60), and even fewer have examined fibers obtained from the same muscle assessed during in vivo functional testing (21–23, 32, 59–61). Existing studies are further limited by incomplete characterization of contractile properties and inconsistent treatment of fiber type-specific effects (52, 62, 63).

Together these limitations have made it difficult to determine whether associations between single fiber properties and whole muscle function reflect meaningful cellular contributions or simply parallel, age-related changes occurring at multiple biological scales. An integrative approach that examines both levels within the same individuals is therefore necessary to clarify the extent to which cellular contractile properties are associated with whole muscle performance.

To address these gaps, the present study integrated whole muscle and single fiber assessments obtained from the vastus lateralis within the same individuals, while preserving fiber type-specific resolution. Analyses were structured across three complementary tiers to rigorously evaluate fiber-to-whole-muscle relationships. First, pooled analyses were used to determine whether associations between single fiber and whole muscle properties exist across all participants. Second, age-adjusted models were used to assess whether these associations persist independent of age group, addressing the possibility that observed relationships reflect shared age-related declines at multiple biological scales. Third, analysis of covariance (ANCOVA) models including an age group × single fiber interaction term was used to test whether the strength of these associations differs with aging. Together, this framework allows for a more comprehensive evaluation of single fiber-to-whole muscle relationships than has been employed in most prior studies (52).

Therefore, the purpose of this study was to determine the extent to which age-related reductions in whole muscle function are accompanied by alterations in single fiber contractile properties, and to identify which cellular variables are most strongly associated with whole muscle function. To address this question, younger and older adults were compared for anthropometric characteristics, regional thigh composition, whole-muscle knee extensor function, and single fiber mechanical properties of the vastus lateralis.

We hypothesized that older adults would exhibit lower whole muscle peak torque, power, and shortening velocity, accompanied by reductions in Type II single fiber size and contractile function, whereas Type I fibers would be comparatively less affected.

We further hypothesized that whole muscle function would be more strongly associated with Type II than Type I single fiber properties. Given that thigh composition shapes the tissue-level context in which fibers generate force, we also hypothesized that greater thigh lean mass would be positively associated with single fiber and whole muscle function. Finally, we hypothesized that the strength of the associations between single fiber properties and whole muscle function would differ between younger and older adults, reflecting age-related changes in how cellular properties translate to whole-muscle function.

METHODS

Participants and Ethical Approval

Participants were recruited from the larger EVEROLIMUS Aging Study (EVERLAST). Two overlapping analytic cohorts were examined: a full cohort comprising participants who completed anthropometric, dual-energy x-ray absorptiometry (DXA), and whole muscle function testing, with sample size varying by outcome measure (N = 49–60), and an integrated cohort comprising participants who also yielded sufficient biopsy tissue and valid single muscle fiber mechanical data (N = 14–17) and corresponds to the cohort described in Chapter 2. The integrated cohort included 10 younger adults (5 men, 5 women) and 7 older adults (2 men, 5 women). All participants provided written informed consent and completed a medical screening before enrollment. Eligible participants were free of overt chronic disease (e.g. cardiovascular disease, diabetes, Alzheimer's disease) and were not taking immunosuppressive medications. Experimental procedures were approved by the University of Wisconsin–Madison Health Sciences Institutional Review Board (IRB# 2021-1519). All measurements were obtained before any intervention.

Experimental Overview

An isokinetic dynamometer, configured for isotonic contractions, was used to measure peak torque, whole-muscle maximum shortening velocity (WM-V_{max}), and power output of the knee extensors. This isotonic approach permitted direct comparison of whole muscle force and power with single fiber absolute force and power properties, which are also obtained under isotonic loading conditions within the same participants. DXA was used to assess whole-body and regional thigh composition. Vastus lateralis

biopsies were obtained for single muscle fiber mechanical experiments and myosin heavy chain (MHC) analyses. Isolated single fibers were used to determine cross-sectional area (CSA), peak isometric force (P_0), specific force (SF), maximum shortening velocity (V_{max}), peak power output (PPO), and normalized power output (NPO), and were subsequently typed by SDS-PAGE according to MHC isoform content. Whole muscle and single fiber variables were compared between younger and older adults, and participant-level single fiber variables were related to whole muscle outcomes. Analyses involving single fiber variables were performed in the integrated cohort, whereas anthropometric, body composition, and whole muscle analyses were performed in the full cohort when data were available. The specific sample size for each analysis is reported in the corresponding figure legend and table.

Anthropometry and Body Composition

Height and weight were measured using a calibrated stadiometer and digital scale (mBCA 514; SECA Corp., Chino, CA, USA). Whole-body composition, thigh fat mass, and thigh lean mass (TLM) were assessed by DXA (Lunar iDXA; GE Healthcare, Madison, WI, USA). TLM was quantified for the upper thigh of the non-dominant leg using manufacturer-provided software (enCORE, version 18; GE Healthcare). The region of interest was delineated superiorly by a diagonal line intersecting the midline of the femoral neck and inferiorly by the tibiofemoral joint. DXA measurements obtained using these anatomical landmarks have been shown to correlate strongly with magnetic resonance imaging (15, 64). TLM was used to normalize whole muscle torque and power to assess function relative to regional muscle mass. Type II TLM was estimated

as the product of thigh lean mass and the proportion of Type II fibers derived from homogenate-based fiber type distribution (18).

Whole Muscle Function Testing

All whole muscle function assessments were conducted across two separate laboratory visits at the University of Wisconsin-Madison Human Exercise Research Core Facility. Participants were instructed to abstain from exercise for at least 48 hours prior to each testing session.

Setup and positioning. Immediately prior to testing, participants completed a five-minute self-paced low-intensity warm-up on either a stationary cycle ergometer (Excalibur 925909; Lode, Groningen, The Netherlands) or a motorized treadmill (Trackmaster TMX425CP; Full Vision, Newton, KS, USA). Knee extensor one-repetition maximum (1RM; peak torque), peak power output, and peak velocity were then measured on the non-dominant leg using a Humac NORM isokinetic dynamometer (502140; CSMi, Stoughton, MA, USA). Participants were seated with the hip angle fixed at 85°, and the test leg was secured at mid-thigh with a stabilization strap to minimize extraneous movement. The contralateral leg was positioned behind the limb stabilizer, with the stabilizer contacting the lower leg proximal to the ankle. The knee joint axis of rotation was aligned with the dynamometer's rotational axis by adjusting the seat, dynamometer, and input arm position. These settings were recorded during Visit 1 and replicated during Visit 2 to ensure anatomical consistency. Once positioned, the input arm was secured to the participant's shin a few centimeters proximal to the malleoli. Range of motion (ROM) was standardized from full knee extension (0°, anatomical

zero) to 100° of flexion, with the flexed position serving as the starting point for all repetitions.

Visit 1: 1RM (peak torque) testing and familiarization. Following setup, participants completed a standardized warm-up consisting of three sets of isotonic knee extensions (8, 4, and 2 repetitions) at progressively increasing resistance. Single repetition isotonic leg extensions were then performed with incremental load increases of approximately 5–20%, separated by 90 seconds of rest, until 1RM was determined. Testing continued until the participant either failed to complete consecutive repetitions or voluntarily terminated the session. After a failed attempt, the load was reduced by 5–20% or set to a midpoint between the last successful and failed attempts. Because objective criteria for successful isotonic 1RM testing using isokinetic dynamometry are limited (65), repetition validity was based on prior literature, normative knee joint angles during activities of daily living, and NSCA guidelines (66). A repetition was considered valid only if it achieved a minimum ROM of 70° within the standardized 100° range (0° = full extension; 100° = starting flexion position). Testing was terminated when the participant voluntarily ended the session, when repeated attempts failed to meet the ROM threshold, or when ROM fell below 50° despite load adjustments. No upper limit was imposed on the number of attempts, but the protocol was designed to identify a valid 1RM within approximately 3–7 sets while minimizing fatigue accumulation to preserve the integrity of PPO measurements during Visit 2. The repetition yielding the highest peak torque was recorded as the 1RM. Participants were then familiarized with the PPO testing protocol.

Visit 2: peak power output testing. Participants repeated the same aerobic warm-up and were positioned identically to Visit 1 using their individualized dynamometer settings. A power-specific warm-up was then performed, consisting of three sets of 3, 2, and 1 repetitions at 50%, 75%, and 90% of the target PPO load (70% of 1RM), respectively. PPO was assessed by performing three sets of three isotonic leg extensions at 70% of the previously determined 1RM, with 90 seconds of rest between sets. The repetition yielding the highest peak power was used for analysis, along with its associated peak velocity.

Muscle Biopsy and Single Muscle Fiber Mechanics

Muscle biopsy. Percutaneous muscle biopsies were obtained at the UW Health University Hospital Clinical Research Unit. Muscle biopsies were performed using a 5 mm skeletal muscle biopsy needle with local anesthesia (1% lidocaine) applied at the biopsy site. A portion of the sample (~10–15 mg) was immediately transferred to a petri dish containing cold relaxing solution composed of (in mM): 100 KCl, 1.75 EGTA, 10 imidazole, 4 ATP, and 5 $MgCl_2$. Biopsy samples were first excised of ~1–2 mm of tissue from each end and stored at -80 °C for MHC distribution analyses. Fiber bundles (~20–50 fibers) were carefully dissected longitudinally from the biopsy and tied at both ends to capillary tubes with 6–0 braided silk suture. Bundles were then placed in skinning solution containing 50% relax solution and 50% glycerol (v:v) for 24 hours at 4 °C to permit the skinning process for subsequent mechanical measurements. After 24 hours, bundles were transferred to fresh skinning solution and stored at -20 °C until mechanical experimentation.

Solutions. Relaxing (described above), pre-activating solution (pCa 9.0) and maximally activating solution (pCa 4.5) for skinned fiber preparations were prepared as previously described (16, 67). The pCa 9.0 solution contained (in mM): 7 EGTA, 20 imidazole, 5.42 $MgCl_2$, 79.16 KCl, 0.01633 $CaCl_2$, 14.5 creatine phosphate, and 4.74 ATP. The pCa 4.5 solution contained (in mM): 7 EGTA, 20 imidazole, 5.26 $MgCl_2$, 64 KCl, 7.01 $CaCl_2$, 14.5 creatine phosphate, and 4.81 ATP. The pH of all single fiber solutions was adjusted to 7.0 at 15 °C with aqueous KOH. Final concentrations of metals, ligands, and metal-ligand complexes were calculated using the computer program of Fabiato (68).

Experimental setup. On the day of contractile experiments, a bundle was removed from skinning solution and placed in a petri dish containing cold relaxation solution under a dissecting microscope. For each experiment, an individual fiber (~2.0–4.0 mm) was isolated from the bundle with fine-point forceps and inspected to ensure it was intact. The experimental technique for fiber mounting and contractile measurements was performed as previously described (16, 67, 69, 70). Briefly, fibers were mounted in a 14 mm × 4 mm chamber containing relax solution within the permeabilized fiber apparatus (Model 802D, Aurora Scientific, ON, Canada) and attached between a capacitance-gauge force transducer (Model 403A, sensitivity of 20 $mV \cdot mg^{-1}$ and resonant frequency of 600 Hz; Aurora Scientific) and a DC torque motor (Model 308; Aurora Scientific). Fiber ends were placed into stainless-steel troughs and secured by overlaying a ~0.25–0.5 mm length of 4–0 monofilament nylon suture on each end and then tying the suture into the troughs with two loops of 10–0 monofilament suture. Length changes during contractile measurements were introduced

at one end of the preparation driven by voltage commands from a PC via a 16-bit D/A converter.

The apparatus was mounted on an inverted phase-contrast microscope (IX50, Olympus, Tokyo, Japan) equipped with 4× and 10× objectives and a 15× photo eyepiece coupled to a CCD camera (CCD-IRIS, Sony, Tokyo, Japan). Chamber temperature was maintained at 15 °C by a Peltier device. Micromanipulators attached to the force transducer and motor were used to position the fiber in a taut but unstretched position. Fibers were then visualized at 150× magnification, and the length of the preparation was adjusted so that sarcomere length was set to 2.5 μm in relax solution. Magnification was then returned to 60×, and fiber length (L_0) was recorded as the segment length between the transducer and motor troughs. Velocity measurements were normalized to L_0 and expressed as fiber lengths per second ($fl \cdot s^{-1}$). Digital images of the fiber were captured from top and side views, and fiber diameter was measured at three equally spaced points along the length of the fiber in each view using ImageJ (77). CSA was calculated assuming an elliptical cross-section.

Before the force-velocity experiments, P_0 was measured and the integrity of the fiber mounting was verified by performing a slack test previously described by Edman (71). Fibers were transferred from relax solution to pCa 9.0 for 60 seconds and then activated by transferring into pCa 4.5 solution. Once force plateaued, the fiber was rapidly slacked by 20% of L_0, producing an immediate decline in tension, followed by gradual redevelopment. The fiber was immediately returned to pCa 9.0, terminating force development and re-lengthened to L_0. P_0 was calculated as the difference between the peak force generated during isometric contraction and the minimum force

recorded following the 20% slack. Fibers were accepted for subsequent force-velocity measurements when force rose smoothly, P_0 remained stable during activation, sarcomere length remained constant at 2.5 μm, no evidence of slippage from the troughs was observed, and the fiber remained structurally intact on visual inspection.

Force-velocity and force-power measurements. Force-velocity and power properties of each SMF were assessed as previously described by Trappe et al. (16, 72, 73). All measurements were performed at a sarcomere length of 2.5 μm. Each fiber was activated by transferring it into pCa 4.5 solution, allowed to develop peak isometric force, and then subjected to three predetermined submaximal isotonic loads spanning ~10–90% of P_0 for 200 ms (load combinations varied across activations to sample the full force-velocity relationship). This was followed by a 20% slack and transfer back to pCa 9.0 to terminate activation, after which the fiber was returned to its original length. Each fiber underwent 4–6 activations, yielding 12–18 isotonic contractions in total.

Loaded shortening velocity was determined from the slope of a linear regression fitted to the change in fiber length during the final 100 ms of each force step. The force-velocity relationship was constructed from the corresponding force and velocity values during each activation and fitted using the Hill equation (74). Power was derived from the fitted F-V parameters. Absolute peak power ($\mu N \cdot fl \cdot s^{-1}$) was calculated as the product of force (μN) and shortening velocity (V_{max}; $fl \cdot s^{-1}$) at the load yielding maximum power along the fitted force-velocity curve, whereas normalized power was calculated as the product of specific force ($kN \cdot m^{-2}$) and shortening velocity (V_{max}; $fl \cdot s^{-1}$) at the load yielding maximum normalized power ($W \cdot L^{-1}$) (15, 75, 76).

To ensure data quality, the P_0 recorded during each activation was normalized to the highest P_0 obtained for that fiber. Activations in which force declined to < 90% of the fiber-specific maximal P_0 were excluded, along with their associated force steps from further analysis. Construction of the F-V relationship required a minimum of four successful activations per fiber (yielding ≥ 12 isotonic contractions). Fibers with fitted F-V curves yielding R^2 < 0.98 were excluded from further analysis (16, 76).

MHC Isoform Identification and Fiber Type Distribution

MHC typing of single muscle fibers. MHC composition of isolated single fibers was determined by SDS-PAGE and silver staining. Following the contractile experiments, each fiber was solubilized in Laemmli buffer (2% SDS, 15% glycerol, 5% β-mercaptoethanol, 0.002% bromophenol blue, and 62.5 mM Tris, pH 6.7) at a volume of 10 µL per mm of fiber length, heated for 5 min at 95 °C, and vortexed before and after heating to ensure fiber solubilization. Samples were loaded onto 1.0 mm thick hand-cast gels comprising a 4% stacking gel (35% glycerol, 4% acrylamide-bisacrylamide (49:1), 70 mM Tris (pH 6.7), 4 mM EDTA (pH 7.0), 0.4% SDS, 0.1% ammonium persulfate (APS), and 0.01% TEMED) and an 8% separating gel (35% glycerol, 8% acrylamide-bisacrylamide (49:1), 200 mM Tris (pH 8.8), 100 mM glycine, 0.4% SDS, 0.1% APS, and 0.01% TEMED). Human skeletal muscle homogenates containing MHC I, IIA, and IIX isoforms were run in parallel as reference standards. Electrophoresis was performed for 15 hours at 4 °C at a constant 250 V. Gels were then silver stained, and fiber MHC isoform content was determined from the migration pattern of the myosin bands referencing the homogenate control. Fibers classified as hybrids were reanalyzed on a separate gel to rule out cross-contamination. Type IIX/IIA fibers were classified as Type

II; Type I/Type II hybrids were excluded from further analysis (*n* = 2 hybrid fibers total across all participants).

MHC distribution. Total Type I and Type II fiber type distribution was determined from bulk homogenate of the vastus lateralis biopsy. A portion of the biopsy sample was weighed and transferred to a microcentrifuge tube containing ~100 mM potassium phosphate buffer (KPi; 18 mM K_2HPO_4, 81 mM KH_2PO_4) at a ratio of 10 µL buffer per mg of wet-weight tissue. Tissue was manually homogenized using a 0.5 mL Kimble Pellet Pestle (DWK Life Sciences, Millville, NJ, USA), and the homogenate was vortexed and centrifuged. The supernatant was transferred to a new microcentrifuge tube, combined with an equivalent volume of 2× Laemmli buffer, vortexed, and heated for 5 min at 95 °C. Homogenates that did not immediately undergo electrophoresis were stored at -80 °C until analysis. Homogenates were run using the same SDS-PAGE protocol described above for single fiber MHC isoform identification.

Staining linearity was validated using a reference VL homogenate run across a range of loading volumes prior to analysis of study samples. Densitometric quantification of the reference homogenate yielded consistent Type II (~60%, summed across Type IIA and Type IIX bands) and Type I (~40%) distributions across the tested loading range, confirming that band intensities fell within the linear response range of the silver stain. This reference homogenate was subsequently included on every study gel to serve as an empirical endpoint control during staining development: the silver stain reaction was terminated as soon as the reference bands reached a pre-defined moderate staining intensity, before saturation could develop. This approach ensured that all study samples were stained to a level that permitted reliable densitometric

quantification while remaining below the silver stain saturation threshold. It also controlled for gel-to-gel variation in staining development time. Type I and Type II band intensities were quantified by densitometry using ImageJ (77). Fiber type distribution was expressed as the percentage of each fiber type relative to the total MHC signal.

Statistical analysis

Age-group differences in anthropometric, body composition, whole muscle, and MHC distribution variables were evaluated in the full (N = 49–60) and integrated cohorts (N = 14–17) using two-tailed independent t-tests. Welch's correction or Mann–Whitney tests were used when assumptions of normality or equal variance were violated. Age-related differences in single muscle fiber properties were tested using a nested ANOVA with age group (younger or older) and fiber type (Type I or Type II) as fixed factors and individual fibers nested within each participant (N = 17). Because Type IIX and hybrid IIX/IIA fibers were underrepresented, these fibers were pooled into a single Type II category, consistent with prior studies in this literature (15, 18).

For analyses relating single fiber properties to whole muscle outcomes, the unit of analysis was the participant. Subject-level means were calculated separately for Type I and Type II fibers for each single fiber variable and regressed against participant-level whole muscle outcomes. The primary analyses were organized into three analytic tiers, including pooled unadjusted correlations and simple linear regressions, age-adjusted multiple linear regressions with age group included as a covariate, and ANCOVA models including an age group × single fiber property interaction term to test whether regression slopes differed by age group. Collectively, these analyses test whether SMF-

to-WM associations exist, whether they are independent of age, and whether age modifies the strength of the association.

To assess the robustness of the strongest age-adjusted findings, leave-one-out cross-validation (LOOCV) sensitivity analyses were performed for the three age-adjusted models with the highest R^2 values, all predicting WM-PPO (Type II CSA, Type II PPO, and Type II P_0, each with age group as a covariate), and for the significant ANCOVA interactions (Type II CSA × age group and Type II P_0 × age group predicting WM-PPO). Each of the 17 participants was iteratively removed, models were re-estimated on the remaining sample, and the R^2, regression coefficients, and P values were compared with the full-model estimates. Stability of these parameters across iterations was used to assess whether any single participant disproportionately influenced the primary findings.

Statistical analyses were performed using GraphPad Prism, version 11.0.0 (GraphPad Software Inc., Boston, MA, USA). Statistical significance was accepted at $P < 0.05$. Because analyses were hypothesis-driven and pre-specified, no adjustment for multiple comparisons was applied. Findings were interpreted on the basis of effect size and consistency across analytic approaches rather than nominal P values alone. Data are presented as the mean ± SD in the text and tables and the mean ± SEM in the figures.

RESULTS

Participant Characteristics, Whole Muscle Function, and Fiber Type Distribution

Participant characteristics and knee extensor function for the full cohort are presented in Table 1. Body weight (84.2 ± 19.5 vs 73.3 ± 7.4 kg; $P = 0.003$), body mass index (29.9 ± 6.4 vs 24.3 ± 2.1 kg·m^{-2}; $P < 0.001$), body fat (39.6 ± 9.7 vs 25.2 ± 9.9%; $P < 0.001$), thigh fat mass (3.9 ± 2.4 vs 2.3 ± 1.4 kg; $P = 0.004$), and thigh fat percentage (37.1 ± 12.6 vs 25.1 ± 12.4%; $P = 0.002$) were significantly greater in the older adults compared to young. Lean body mass and thigh lean mass did not differ between groups. Knee extensor function values were significantly lower in all functional measurements (peak torque, normalized peak torque, absolute power, normalized power, and WM-V_{max}) for the older adults compared to young.

Participant characteristics and knee extensor function for the integrated cohort are presented in Table 2. Height, weight, BMI, lean body mass (LBM), TLM, and thigh fat mass (TFM) did not differ between groups, although BMI (30.3 ± 5.8 vs 24.9 ± 2.2 kg·m^{-2}; $P = 0.052$) and TFM (4.3 ± 2.2 vs 2.6 ± 1.7 kg; $P = 0.076$) tended to be ~22% and ~65% higher in older adults compared to the young. Older adults exhibited 16.7 percentage points greater relative body fat (43.3 ± 9.8 vs 26.6 ± 12.0%; $P = 0.008$) and 15 percentage points greater relative thigh fat (41.4 ± 12.2 vs 26.4 ± 15.0%; $P = 0.045$). Knee extensor function showed significant age-related deficits, peak torque (PT) was ~41% lower, WM-PPO was ~61% lower, WM-NPO was ~54% lower, and WM-V_{max} was ~30% lower in the older adults (Table 2; Fig. 1).

Fiber type distribution did not differ significantly between younger and older adults in either cohort. In the full cohort ($N = 49$: 12 young, 37 older), Type II fiber

percentage was 54.9 ± 9.8% in young and 53.0 ± 12.8% in older adults (P = 0.615). In the integrated cohort (N = 14: 8 younger, 6 older), Type II percentage was 59.8 ± 7.3% in young and 52.6 ± 10.0% in older adults (P = 0.144). Type II thigh lean mass also did not differ between groups in the integrated cohort (3.89 ± 0.82 vs 2.94 ± 1.05 kg; P = 0.072).

Age-Related Differences in Single Muscle Fiber Contractile Properties

Single fiber size and force. Significant single fiber properties are presented in Table 2. Analyses included 84 Type I and 61 Type II fibers from young adults and 66 Type I and 32 Type II fibers from older adults. In Type I fibers (Fig. 2), CSA did not differ between young (5462 ± 1408 μm^2) and older adults (4925 ± 1058 μm^2; P = 0.273). Similarly, specific force was not significantly different between younger (148.5 ± 30.4 $kN \cdot m^{-2}$) and older adults (114.1 ± 45.9 $kN \cdot m^{-2}$; P = 0.095), although the mean value was ~23% lower. In contrast, P_0 was significantly lower (~31%) in older adults (0.53 ± 0.17 mN) compared to young adults (0.77 ± 0.16 mN; P = 0.006; Fig. 2). In Type II fibers, CSA also did not differ between older (5017 ± 1398 μm^2) and younger adults (5784 ± 2123 μm^2; P = 0.367). P_0 showed only a nonsignificant tendency to be lower in older adults (0.66 ± 0.23 vs 0.89 ± 0.33 mN; P = 0.075). In contrast, specific force was ~15% lower in older adults (135.3 ± 31.6 $kN \cdot m^{-2}$) compared to the younger adults (158.6 ± 26.9 $kN \cdot m^{-2}$; P = 0.029; Fig. 3).

Single fiber force-velocity and power. Significant single fiber contractile properties are presented in Table 2; Fig. 2-3. Analyses included 77 Type I and 49 Type II fibers from young adults and 59 Type I and 23 Type II fibers from older adults. In Type I fibers, V_{max} was not significantly different between the young and older adults (0.46 ± 0.04 vs

0.42 ± 0.05 fl·s^{-1}; *P* = 0.187). Similarly, NPO was not significantly different between the young (2.8 ± 0.7 W·L^{-1}) and old adults (2.1 ± 0.8 W·L^{-1}; *P* = 0.118), although it was 25% lower on average in older adults. PPO was significantly lower (~32%) in older adults (10.2 ± 2.5 vs 15.1 ± 3.9 μN·fl·s^{-1}; *P* = 0.016; Fig. 2). In Type II fibers, V_{max} likewise did not differ between groups (young 0.62 ± 0.12 vs older 0.59 ± 0.12 fl·s^{-1}; *P* = 0.278). PPO was 32% lower in older adults (28.1 ± 11.1 μN·fl·s^{-1} vs 41.1 ± 16.4 μN·fl·s^{-1}; *P* = 0.041; Fig. 3), and NPO was 19% lower in older adults (5.8 ± 1.9 vs 7.2 ± 1.2 W·L^{-1}; *P* = 0.007; Fig. 3).

Overall, aging was associated with a comparable reduction in peak power in both Type I and Type II fibers (~32%), along with lower normalized power in Type II fibers of the older adults. The force-related deficit differed by fiber type, with Type I fibers exhibiting lower absolute peak force and Type II fibers exhibiting lower specific force. Importantly, these age-related impairments in force and power occurred despite no significant reductions in CSA or V_{max} in either fiber type.

Associations Between Single Fiber Mechanics and Whole Muscle Function

Pooled unadjusted associations. Unless otherwise stated, analyses involving single fiber variables were performed at the participant level in the integrated cohort using subject-mean Type I or Type II values regressed against participant-level whole muscle outcomes. Sample size varied across analyses according to data availability.

Type I P_0 was significantly associated with WM-PPO (R^2 = 0.340; *P* = 0.018), WM-NPO (R^2 = 0.317; *P* = 0.023), and WM-V_{max} (R^2 = 0.312; *P* = 0.024) (Table 3). Type I CSA was associated with WM-PPO (R^2 = 0.290; *P* = 0.032), and Type I PPO was associated with WM-PPO (R^2 = 0.270; *P* = 0.047; Table 3). Type I P_0 approached

significance for peak torque (R^2 = 0.244; P = 0.052). No Type I fiber variable was significantly associated with normalized peak torque. Type I SF, V_{max}, and NPO showed no significant associations with any whole muscle outcome (all P > 0.05).

In contrast, Type II fiber properties showed numerous and substantially stronger associations with whole muscle function (Table 3). Whole muscle peak power was the outcome most strongly predicted by Type II fiber properties. Type II PPO was the single strongest cellular predictor of WM-PPO (R^2 = 0.643; P < 0.001; slope = 13.04 W per $\mu N \cdot fl \cdot s^{-1}$), indicating that for every 10 $\mu N \cdot fl \cdot s^{-1}$ increase in Type II fiber peak power, whole muscle power increased by approximately 130 W. Type II P_0 was similarly strongly associated with WM-PPO (R^2 = 0.586; P < 0.001; slope = 637.8 W per mN). Type II CSA was also associated with WM-PPO (R^2 = 0.498; P = 0.002; slope = 0.096 W per μm^2) (Fig. 4).

Type II PPO also showed strong associations with peak torque (R^2 = 0.504; P = 0.001; slope = 1.79 Nm per $\mu N \cdot fl \cdot s^{-1}$), WM-$V_{max}$ (R^2 = 0.488; P = 0.002), and normalized peak torque (R^2 = 0.376; P = 0.009). Type II P_0 was associated with WM-NPO (R^2 = 0.467; P = 0.002), peak torque (R^2 = 0.445; P = 0.003), and WM-V_{max} (R^2 = 0.340; P = 0.014). Type II NPO was associated with normalized peak torque (R^2 = 0.322; P = 0.018). Type II CSA was associated with normalized peak torque (R^2 = 0.340; P = 0.014), WM-V_{max} (R^2 = 0.303; P = 0.022), and peak torque (R^2 = 0.286; P = 0.027). Type II SF was only significantly associated with normalized peak torque (R^2 = 0.298; P = 0.024). Type II V_{max} was not significantly associated with any whole muscle outcome (all P > 0.07). To contextualize the magnitude difference between fiber types, the three strongest Type II associations (Type II PPO vs WM-PPO, R^2 = 0.643; Type II P_0 vs WM-

PPO, R^2 = 0.586; Type II PPO vs PT, R^2 = 0.504) were approximately 1.5- to 2-fold stronger than the strongest Type I association (Type I P_0 vs WM-PPO, R^2 = 0.340), consistent with the a priori hypothesis that whole muscle function would be more strongly associated with Type II than Type I fiber properties.

Age-adjusted associations. When age group was included as a covariate in multiple regression models, the results diverged by fiber type and by whether absolute or normalized fiber properties were examined (Table 4).

Despite the significant pooled associations noted above, Type I fiber variables were largely non-significant predictors of whole muscle outcomes after adjusting for age. The single exception was Type I CSA, which remained a significant predictor of WM-PPO (P = 0.028; R^2 = 0.662; Table 4). For all other Type I models, the age group covariate was significant (P = 0.001–0.047) while the SMF variable was not (all P > 0.20), and model R^2 values (0.38–0.67) were driven almost entirely by the age variable. Thus, after age adjustment, pooled Type I associations were largely no longer significant.

The absolute Type II fiber properties (PPO, P_0, CSA) remained significant independent predictors of whole muscle function after age adjustment, with the strongest effects again converging on WM-PPO as the outcome (Table 4). Type II CSA was the strongest age-adjusted predictor of WM-PPO (R^2 = 0.849; SMF P < 0.001; age P < 0.001). Type II PPO also remained highly significant for WM-PPO (R^2 = 0.827; SMF P < 0.001; age P = 0.002) and for peak torque (P = 0.009) and WM-NPO (P = 0.007). Type II P_0 remained significant for WM-PPO (R^2 = 0.811; SMF P < 0.001; age P = 0.001), peak torque (P = 0.013), and WM-NPO (P = 0.005). Type II CSA also remained

significant for WM-V_{max} (P = 0.013), WM-NPO (P = 0.009), and peak torque (P = 0.029). In each of these models, the age covariate was also significant, indicating that both age and the Type II absolute fiber property contributed independently to the prediction of whole muscle function.

In contrast, Type II SF, V_{max}, and NPO were not significant predictors of any whole muscle outcome after age adjustment (all $P > 0.05$ for the SMF β coefficient). In these models, age was the only significant predictor. Therefore, after age adjustment, only the absolute Type II properties (CSA, P_0, and PPO) retained significant associations with whole muscle outcomes, whereas Type II SF, NPO, and V_{max} did not.

Age Modification of the Single Fiber-to-Whole Muscle Relationship. ANCOVA models including an age group × single fiber property interaction term were used to test whether regression slopes relating single fiber variables to whole muscle outcomes differed between younger and older adults (Table 5). Most comparisons were not statistically significant, indicating that aging largely shifts the intercept of the SMF-to-WM relationship (i.e., both groups decline together) without substantially altering the slope. The two significant interactions observed were for Type II fiber P_0 and CSA vs WM-PPO.

Two comparisons reached significance for Type II fibers, both involving WM-PPO as the outcome: Type II P_0 versus WM-PPO (F = 5.08; P = 0.042) and Type II CSA versus WM-PPO (F = 5.90; P = 0.030; Fig. 6). In young adults, each 1 mN increase in Type II P_0 was associated with a 594 W increase in WM-PPO, whereas in older adults the same increase was associated with only a 110 W increase, a roughly 5-fold attenuation. Similarly, each 1000 μm² increase in Type II CSA was associated with a 95

W increase in WM-PPO in young adults compared to only a 22 W increase in older adults. All other Type II comparisons were non-significant (P = 0.07–0.97), and all Type II SF, V_{max}, and NPO comparisons were non-significant (P > 0.43). All Type I comparisons were likewise non-significant.

Muscle Quantity, Fiber Type Composition, and Confirmatory Analyses

Thigh lean mass was positively associated with WM-PPO (R^2 = 0.555; P < 0.001; slope = 165.9 W per kg), peak torque (R^2 = 0.492, P = 0.002; slope = 24.3 Nm per kg), WM-V_{max} (R^2 = 0.309, P = 0.020), and WM-NPO (R^2 = 0.307, P = 0.021). TLM was also positively associated with Type II CSA (R^2 = 0.654, P < 0.001), Type II PPO (R^2 = 0.565; P < 0.001; slope = 10.4 μN·fl·s^{-1} per kg), Type II P_0 (R^2 = 0.483, P = 0.002), Type I CSA (R^2 = 0.374; P = 0.012), and Type II V_{max} (R^2 = 0.312, P = 0.020). TLM was not significantly associated with any Type I force or power variable, nor with Type II SF or NPO.

In pooled analyses of the integrated cohort (N = 14), Type II fiber percentage was significantly correlated with peak torque (r = 0.570; P = 0.033) but not with any other whole muscle outcome (WM-PPO; P = 0.112, normalized peak torque; P = 0.099, WM-NPO; P = 0.174, WM-V_{max}; P = 0.598). Type II thigh lean mass was associated with peak torque (r = 0.677; P = 0.008), WM-PPO (r = 0.705; P = 0.005), WM-NPO (r = 0.571; P = 0.033), and TLM (r = 0.857; P < 0.001). However, TLM alone was a stronger predictor of WM-PPO than Type II TLM (r = 0.745 vs 0.705; Fig. 5).

To assess the generalizability of the anthropometric associations observed in the integrated cohort, the same analyses were performed in the full cohort of participants who completed whole muscle testing and DXA (N = 48–60). The full cohort findings

were consistent with and confirmatory of the subset results. TLM was strongly associated with WM-PPO (r = 0.741; R^2 = 0.549; P < 0.001; N = 59), peak torque (r = 0.729; R^2 = 0.531; P < 0.001; N = 60), WM-V_{max} (r = 0.517; R^2 = 0.267; P < 0.001; N = 59), WM-NPO (r = 0.485; R^2 = 0.236; P < 0.001; N = 59), and normalized peak torque (r = 0.261; R^2 = 0.068; P = 0.044; N = 60). The direction and relative magnitude of these associations were consistent with the subset, with TLM vs WM-PPO showing similar effect sizes in both samples (subset r = 0.745; full cohort r = 0.741).

In the full cohort, Type II fiber percentage was not significantly associated with any whole muscle outcome (all P > 0.12; N = 48–49), confirming the subset finding. Type II thigh lean mass was associated with WM-PPO (r = 0.647; P < 0.001; N = 48), peak torque (r = 0.608; P < 0.001; N = 49), WM-V_{max} (r = 0.465; P < 0.001; N = 48), and WM-NPO (r = 0.447; P = 0.001; N = 48). As in the subset, TLM alone was a stronger predictor of WM-PPO than Type II TLM (full cohort r = 0.741 vs 0.647), further confirming that the Type II TLM associations were driven primarily by the TLM component rather than by fiber type composition.

Sensitivity Analyses

To evaluate the robustness of the primary findings to individual observations, LOOCV analyses were performed for the three strongest age-adjusted multiple linear regression models predicting WM-PPO (Type II CSA, Type II PPO, and Type II P_0, each with age group as a covariate) and for the two significant ANCOVA interactions (Type II CSA × age group and Type II P_0 × age group predicting WM-PPO). Each of the 17 participants was iteratively removed, models were re-estimated on the remaining 16

participants, and the resulting R^2 values, regression coefficients, and *P* values were compared with the full-model estimates.

The three age-adjusted models were robust across all 17 iterations. For the Type II CSA + age model, R^2 remained stable (range 0.817–0.868; mean 0.850; full-model R^2 = 0.849), the regression coefficient for Type II CSA remained within a narrow range (0.073–0.088 W per μm^2; full-model β = 0.079), and both the SMF and age effects remained highly significant in every iteration (all $P < 0.001$). The Type II PPO + age model showed similar stability (R^2 range 0.789–0.881; β range 9.02–10.37 W per $\mu N \cdot fl \cdot s^{-1}$; all P ≤ 0.001 for SMF, all P ≤ 0.007 for age). The Type II P_0 + age model was likewise stable (R^2 range 0.780–0.873; β range 436–549 W per mN; all $P \leq 0.0024$ for SMF, all P ≤ 0.006 for age). These results indicate that the age-adjusted associations between absolute Type II fiber properties and WM-PPO are not driven by any single participant.

For the ANCOVA the Type II P_0 × age group interaction was robust to leave-one-out removal: the slope difference between younger and older adults remained statistically significant in all 17 iterations (*P* range 0.001–0.050; mean 0.024; full-model $P = 0.042$), with the older-adult slope consistently 4- to 8-fold smaller than the younger-adult slope. The Type II CSA × age group interaction was robust in 14 of 17 iterations ($P < 0.05$) but lost significance when any of three specific older adults were removed (P = 0.058, 0.065, and 0.162), although the direction and magnitude of the slope difference were preserved across all iterations (older-adult slope always 3- to 6-fold smaller than younger-adult slope). This pattern indicates that the Type II CSA interaction, while

directionally consistent across participants, is more sensitive to the small older-adult sample than the Type II P_0 interaction.

DISCUSSION

Principal Findings

This study integrated single muscle fiber contractile mechanics with whole muscle knee extensor function and regional body composition in younger and older adults to determine the extent to which cellular contractile properties explain whole muscle function and whether these relationships differ with aging. The principal findings were that: (1) Type II single fiber properties showed stronger and more numerous associations with whole muscle function than Type I properties; (2) after adjustment for age group, only the absolute Type II properties (CSA, P_0, and PPO) retained independent associations with whole muscle outcomes, whereas most Type I and normalized Type II associations did not; (3) thigh lean mass was positively associated with both whole muscle performance and Type II fiber properties (a pattern that was confirmed in the full cohort; $N = 59$), whereas fiber type distribution contributed little additional explanatory value; and (4) aging generally preserved the single fiber-to-whole muscle relationship, with the notable exception that the relationships of Type II P_0 and CSA with whole muscle peak power were attenuated in older adults. Together, these findings indicate that Type II fiber force, size, and power are the dominant cellular correlates of whole muscle function in this cohort and that whole muscle peak power is the functional outcome most tightly linked to Type II fiber mechanics.

Type II Fiber Properties are the Dominant Cellular Correlates of Whole Muscle Function

The most striking finding from the pooled analyses was the clear dominance of Type II fiber properties as cellular predictors of whole muscle function. Although Type I P_0 showed significant associations with WM-PPO ($R^2 = 0.340$), WM-NPO, and WM-

V_{max}, the corresponding Type II associations were substantially stronger: Type II PPO explained nearly twice as much variance in WM-PPO (R^2 = 0.643) as the strongest Type I predictor (Type I P_0; R^2 = 0.340). In total, 17 of 30 Type II pairings reached significance in pooled unadjusted analyses, compared to only 5 of 30 for Type I. This fiber type asymmetry is consistent with the molecular level findings of Miller et al. (2013), who reported that correlations between single fiber function and whole muscle isokinetic power were apparent only in Type IIA fibers and not in MHC I fibers (22). This observation was attributed to the fact that Type IIA fibers produce approximately three times the power output of MHC I fibers and therefore disproportionately determine dynamic whole muscle performance. The present data extend this finding by demonstrating that the Type II dominance is evident not only at the molecular level using sinusoidal analysis but also at the level of standard contractile properties (P_0, PPO, CSA) measured in the same individuals who completed whole muscle testing.

The three strongest SMF-to-WM associations all involved WM-PPO as the outcome (Type II PPO R^2 = 0.643; Type II P_0 R^2 = 0.586; Type II CSA R^2 = 0.498), establishing whole muscle power as the functional outcome most tightly coupled to Type II fiber mechanics. The slope of the Type II PPO-to-WM-PPO regression provides a quantitative estimate of this coupling: for every 10 $\mu N \cdot fl \cdot s^{-1}$ increase in Type II fiber peak power, whole muscle peak power increased by approximately 130 W. Jeon et al. (2018) similarly reported that single fiber P_0 exerted a larger influence on isokinetic power than V_0 in young men (78), and the present data reinforce this conclusion across a broader age range and a mixed-sex cohort. Type II V_{max} was not associated with any whole muscle outcome despite Type II PPO and P_0 showing strong associations, further

reinforcing the idea that the cellular basis of the SMF-to-WM link is force-driven rather than velocity-driven. Notably, although whole-muscle peak power is itself a force-velocity product, the cellular predictors of this whole-muscle outcome were specifically force-related rather than velocity-related. This is consistent with the present age group comparisons showing that V_{max} was preserved in both fiber types. Together, these observations suggest that it is the force and power components of Type II fiber function, rather than shortening velocity, that scale upward to influence whole muscle performance.

Age-Adjustment Distinguishes Shared Age-Related Decline from Independent Cellular Contributions

The age-adjusted analyses were critical for distinguishing ecological correlations, where both variables decline with aging but are not causally linked, from genuine cellular contributions to whole muscle function. This distinction was cleanest for Type I fibers: all five significant pooled Type I associations were fully accounted for by age, with the single exception of Type I CSA vs WM-PPO ($P = 0.028$). This means the pooled Type I associations were driven entirely by the shared age-related decline in both Type I fiber properties and whole muscle function, not by a direct cellular-to-whole-muscle mechanistic link.

For Type II fibers, the age-adjusted results split cleanly between absolute and normalized properties. Type II PPO, P_0, and CSA remained significant independent predictors of WM function after age adjustment, with the strongest effects again converging on WM-PPO. The age-adjusted model combining Type II CSA and age group explained 85% of the variance in WM-PPO (model $R^2 = 0.849$; CSA $P < 0.001$;

age $P < 0.001$). The models for Type II PPO and P_0 were similarly strong (model R^2 = 0.827 and 0.811, respectively). All three findings were robust to LOOCV, indicating that the relationships are not driven by individual high-leverage observations. This means that these absolute Type II fiber properties contribute independently to whole muscle power beyond what age alone explains. In contrast, Type II SF, NPO, and V_{max} were not significant after age adjustment, indicating that these intrinsic measures and velocity add no independent information once the shared age-related decline is accounted for.

Frontera et al. (2000) were the first to examine the relationship between whole muscle specific force and single fiber specific force in the same cohort of young men, older men, and older women, reporting a weak but significant pooled correlation (r = 0.37; P = 0.042) that they described as complex and nonlinear (21). However, because their analysis did not adjust for age, it remained unclear whether the observed association reflected shared age-related decline or a genuine cellular contribution to whole muscle function. The present age-adjusted analysis resolves this ambiguity: for absolute Type II properties, the association persists after removing the age confound, providing evidence for a genuine cellular-to-whole-muscle mechanistic link. For Type I fibers and normalized Type II properties, the pooled association reflects shared age-related decline rather than an independent cellular-to-whole-muscle relationship.

This dissociation has implications for interpreting the broader literature, as studies that report pooled correlations between single fiber properties and whole muscle function across age ranges without adjusting for age, such as the cross-sectional analyses of Wang et al. (2019), may be partly capturing shared age-related decline rather than a purely cellular-to-whole-muscle relationship (60). The retention of

significance for absolute Type II properties after age adjustment provides the strongest evidence to date for a genuine cellular contribution to whole muscle function and not solely an artifact of shared aging.

Muscle Quantity, Rather than Fiber Type Composition, Explains Additional Variance in Whole Muscle Function

Thigh lean mass was significantly associated with both whole muscle function (WM-PPO, R^2 = 0.555; peak torque, R^2 = 0.492 in the integrated cohort) and Type II fiber properties (Type II CSA, R^2 = 0.654; Type II PPO, R^2 = 0.565), positioning TLM as a shared structural correlate. Individuals with more thigh lean mass had both more powerful Type II fibers and greater whole muscle performance. Wang et al. (2019) similarly reported that thigh muscle volume correlated positively with both Type I and Type II fiber force at baseline in older overweight and obese adults (60). In the present study, TLM correlations were selective for Type II fiber properties, with no significant associations with Type I force or power variables. This selectivity further supports the interpretation that the functional link between regional muscle size and dynamic whole muscle output operates primarily through fast fiber contributions.

These findings were confirmed in the full cohort, where TLM showed nearly identical associations with WM-PPO (full cohort R^2 = 0.549 vs subset cohort R^2 = 0.555) and peak torque (full cohort R^2 = 0.531 vs subset cohort R^2 = 0.492). The consistency between the subset (N = 17) and full cohort (N = 59) demonstrates that the smaller subset used for the single fiber analyses is representative of the broader sample, strengthening confidence in the SMF-to-WM findings that could only be tested in the subset.

Type II fiber percentage did not differ between age groups in either the full cohort (P = 0.615; N = 49) or the subset (P = 0.144; N =14), consistent with the view that age-related muscle dysfunction in this cohort cannot be attributed primarily to a fiber type shift. Type II thigh lean mass was associated with WM-PPO (R^2 = 0.419; P < 0.001) and peak torque (R^2 = 0.370; P < 0.001) in the full cohort and showed a trend toward being lower in older adults in the subset cohort (P = 0.072). However, because Type II percentage itself carried no independent predictive value and Type II TLM was strongly correlated with total TLM (R^2 = 0.624; P < 0.001), these associations were driven by the TLM component rather than by fiber type composition. Accordingly, Type II TLM was a weaker predictor of WM-PPO than TLM alone (full cohort R^2 = 0.549 vs 0.419), indicating that multiplying by a non-predictive fiber type percentage added noise rather than information. This contrasts with the findings of Sundberg et al. (2018), who observed a selective 48% reduction in MHC II lean mass with preserved MHC I lean mass in men aged 73–89 years, making the MHC II TLM metric genuinely informative in that cohort because the fiber-type-specific mass loss was the distinguishing feature. The absence of a comparable compositional shift in the present cohort suggests that the selective fast fiber mass loss that drives the predictive value of Type II TLM may emerge later in the aging process than the ages studied here (~61 years), or that it may be more pronounced in men than in the mixed-sex sample studied presently. Regardless, the present data indicate that in this cohort, it is the absolute quantity of muscle tissue rather than its fiber type composition that primarily determines whole muscle performance.

The Single Fiber-to-Whole Muscle Relationship is Largely Preserved, with Selective Attenuation for Whole Muscle Power

ANCOVA revealed that aging generally does not change how strongly single fiber properties predict whole muscle function. Most comparisons were not significant, indicating that aging shifts the intercept of the regression (i.e., older adults start from a lower baseline) but preserves the fundamental scaling relationship between cellular and whole muscle mechanics. This is an important null result, as it suggests that the mechanistic coupling between single fiber contractile output and whole muscle performance is age-invariant, even though the absolute level of both declines with aging. Frontera et al. (2008) longitudinally demonstrated that whole muscle strength declined over ~9 years in older adults despite preservation of single fiber contractile function (80). They noted a dissociation between changes in muscle size and the mechanisms driving strength loss. The present ANCOVA results suggest that this dissociation is not due to a breakdown in the fundamental scaling between cellular and whole muscle mechanics, but rather to a downward shift in the absolute level of both, and that the coupling itself is preserved.

Two targeted exceptions emerged, both involving WM-PPO as the outcome. Type II P_0 versus WM-PPO ($P = 0.042$) and Type II CSA versus WM-PPO ($P = 0.030$). In young adults, each 1 mN increase in Type II P_0 was associated with a 594 W increase in WM-PPO, whereas in older adults the same increase was associated with only a 110 W increase, which is roughly a 5-fold attenuation. Similarly, each 1000 μm^2 increase in Type II CSA was associated with a 95 W increase in WM-PPO in young adults compared to only a 22 W increase in older adults. LOOCV confirmed that the

Type II P_0 × age interaction was robust, with the slope difference remaining significant across all 17 iterations (*P* range 0.001–0.050). The Type II CSA × age interaction was directionally consistent across all iterations (older-adult slope always 3- to 6-fold smaller) but reached significance in 14 of 17 iterations, indicating somewhat greater sensitivity to individual observations in the older subgroup. Both significant interactions involving WM-PPO as the outcome are consistent with the broader pattern emerging from this study: whole muscle power is the functional outcome most tightly coupled to Type II fiber mechanics, and it is also the outcome where aging most specifically disrupts that coupling. Miller et al. (2013) reported a complementary finding at the molecular level. Age-related slowing of myosin-actin cross-bridge kinetics in MHC IIA fibers correlated with reduced whole muscle isokinetic power, with the effect driven primarily by women (22). Their observation that molecular-level dysfunction was more pronounced for dynamic than isometric performance aligns with the present finding that the coupling attenuation was specific to whole muscle power rather than peak torque.

This attenuation could reflect age-related changes in factors that mediate the translation of cellular force into whole muscle power, such as tendon compliance, lateral force transmission, neuromuscular activation efficiency, muscle architecture, or intramuscular adipose infiltration. The fact that the coupling was preserved for peak torque and V_{max} but attenuated for power specifically suggests that the translation bottleneck is not in force transmission per se, but rather in the rate-dependent processes that determine how efficiently force is converted into velocity-dependent power output at the whole-muscle level.

Integration with Chapters 2 and 4

These findings provide the mechanistic bridge between the cellular observations of Chapter 2 and the molecular observations of Chapter 4. Chapter 2 established that aging impairs Type II fiber function intrinsically, older fibers produced less force (specific force) and power (normalized power) per unit area without significant CSA reduction. The present chapter demonstrates the whole-muscle consequence of these intrinsic deficits: although absolute Type II properties (P_0, CSA, PPO) remained the strongest cellular predictors of whole-muscle peak power after age adjustment, the slope of these relationships was attenuated in older adults. Specifically, a given absolute Type II P_0 or CSA value translated into less whole-muscle peak power in older adults than in younger adults, by a factor of roughly 4- to 8-fold for P_0 and 3- to 6-fold for CSA. This slope attenuation is biologically consistent with the intrinsic Type II dysfunction identified in Chapter 2, even when older fibers reach a given absolute force or attain a given size, the underlying contractile machinery is compromised, so the translation into whole-muscle output is less efficient. Chapter 4 then completes the chain by identifying sarcomeric proteoform changes that correlate with single fiber mechanics within the same fibers. Together, the three chapters identify correlated changes spanning sarcomeric proteoforms, single fiber mechanics, and whole muscle function, establishing a multi-scale framework for age-related contractile dysfunction in human skeletal muscle.

Limitations

A few limitations should be noted. First, the present study was conducted in a human single-fiber physiology cohort of a size that is typical for studies of this

experimental complexity, but the smaller number of older adults nevertheless limits precision for subgroup-specific regression and interaction analyses. To address this, LOOCV was performed on the primary age-adjusted models and ANCOVA interactions and confirmed that the three age-adjusted models predicting WM-PPO and the Type II P_0 × age interaction were robust across all 17 iterations, while the Type II CSA × age interaction was directionally consistent across all iterations and significant in 14 of 17. Second, the older group included a higher proportion of women (71% vs 50%) and the cohort sizes when stratified by both age and sex (5 young men, 5 young women, 2 older men, 5 older women) preclude formal analysis of sex effects. Sex-specific patterns in single fiber contractile properties and whole muscle function have been reported in the aging literature, with some groups showing differential preservation of Type II fiber size and force in older women compared with older men (16, 22). Although sex was not included as a covariate in the present analyses, the older men subgroup (N = 2) would render any sex × age interaction uninterpretable and any sex main effect would be partially confounded with the age imbalance. Sex therefore represents an important variable that future studies with balanced recruitment should explicitly examine. Third, the biopsy sampled only a small region of the vastus lateralis and may not fully represent the whole muscle.

In summary, Type II single fiber force, power, and size were the principal cellular correlates of whole muscle knee extensor function, whereas Type I associations were weaker and were largely accounted for by shared age-related decline. Whole muscle peak power was the functional outcome most tightly coupled with Type II fiber mechanics and the specific outcome where aging modified the cellular-to-whole-muscle

scaling relationship. Absolute Type II properties (PPO, P_0, CSA) retained independent predictive value after adjusting for age, demonstrating a genuine cellular contribution to whole muscle function that exceeds shared age-related decline. Thigh lean mass emerged as a shared structural correlate of both cellular and whole muscle function. Together, these findings support a model in which age-related whole muscle dysfunction is driven by force-limited power deficits in Type II fibers that are compounded by changes in regional muscle quantity, rather than by impaired shortening velocity.

TABLES AND FIGURES

Table 1. Full cohort anthropometrics and knee extensor function for young and old adults

		Young Adults	Old Adults	*P* value
Variable	Units	*N* = 15 (7 M:8 W)	*N* = 44 (19 M:25 W)	
Anthropometrics				
Age	years	28.5 ± 3.0	64.5 ± 5.6	**<0.001**
Height	cm	173.9 ± 5.5	167.7 ± 10.1	**0.005**
Weight	kg	73.3 ± 7.4	84.2 ± 19.5	**0.003**
Body mass index	$kg \cdot m^{-2}$	24.3 ± 2.1	29.9 ± 6.4	**<0.001**
Total lean mass	kg	52.3 ± 7.4	47.9 ± 10.5	0.137
Body fat	%	25.2 ± 9.9	39.6 ± 9.7	**<0.001**
Thigh lean mass	kg	6.7 ± 1.0	6.1 ± 1.4	0.131
Thigh fat mass	kg	2.3 ± 1.4	3.9 ± 2.4	**0.004**
Thigh fat	%	25.1 ± 12.4	37.1 ± 12.6	**0.002**
Knee extensor function				
Peak torque	Nm	127.0 ± 31.9	89.7 ± 34.6	**<0.001**
Normalized peak torque	$Nm \cdot kg^{-1}$	19.0 ± 3.8	14.6 ± 3.6	**<0.001**
Absolute Power	W	581.0 ± 201.4	313.8 ± 152.4	**<0.001**
Normalized Power	$W \cdot kg^{-1}$	85.6 ± 22.0	50.0 ± 15.8	**<0.001**
V_{max}	$deg \cdot s^{-1}$	344.0 ± 70.1	265.7 ± 60.3	**<0.001**

Body fat percentage, total lean mass, thigh lean mass, thigh fat mass, and thigh fat percentage were measured via dual X-ray absorptiometry. Peak torque was the highest output recorded from the one-repetition max testing session. Peak power output was the highest output recorded during the maximal power testing session. Normalized peak torque and power values were calculated with the thigh lean mass. *N* is representative of whole muscle and subject sample size (compared to single muscle fibers presented by *n)*. Significant differences are indicated in bold when $P < 0.05$. Data are presented as the mean ± SD.

Table 2. Integrated cohort anthropometrics, knee extensor function, fiber type distribution, and key single fiber mechanical properties

		Young Adults	Old Adults	*P* value
Variable	Units	N = 10 (5 M:5 W)	N = 7 (2 M:5 W)	
Anthropometrics				
Age	years	28.3 ± 1.8	61.3 ± 2.9	**<0.001**
Height	cm	173.6 ± 4.2	169.2 ± 8.6	0.176
Weight	kg	75.0 ± 6.9	86.4 ± 16.9	0.132
Body mass index	$kg \cdot m^{-2}$	24.9 ± 2.2	30.3 ± 5.8	0.052
Lean body mass	kg	52.47 ± 8.1	46.09 ± 7.1	0.114
Body fat	%	26.6 ± 12.0	43.3 ± 9.8	**0.008**
Thigh lean mass	kg	6.7 ± 1.1	5.7 ± 1.1	0.097
Thigh fat mass	kg	2.6 ± 1.7	4.3 ± 2.2	0.076
Thigh fat	%	26.4 ± 15.0	41.4 ± 12.2	**0.045**
Knee extensor function				
Peak torque	Nm	126.1 ± 36.8	73.6 ± 14.5	**0.001**
Normalized peak torque	$Nm \cdot kg^{-1}$	18.9 ± 4.1	13.0 ± 2.3	**0.004**
WM-Peak Power	W	595.9 ± 226.4	233.4 ± 56.5	**<0.001**
WM-NPO	$W \cdot kg^{-1}$	87.7 ± 25.3	40.7 ± 5.7	**<0.001**
WM-V_{max}	$deg \cdot s^{-1}$	349.8 ± 76.2	246.3 ± 31.2	**0.002**
Fiber type distribution				
Type II	%	59.8 ± 7.3	52.6 ± 10.0	0.144
Type II thigh lean mass	kg	3.89 ± 0.82	2.94 ± 1.05	0.072
Key SMF age differences				
Type I P_0	mN	0.77 ± 0.16	0.53 ± 0.17	**0.006**
Type I PPO	$\mu N \cdot fl \cdot s^{-1}$	15.1 ± 3.9	10.2 ± 2.5	**0.016**
Type II SF	$kN \cdot m^{-2}$	158.6 ± 26.9	135.3 ± 31.6	**0.029**
Type II PPO	$\mu N \cdot fl \cdot s^{-1}$	41.1 ± 16.4	28.1 ± 11.1	**0.041**
Type II NPO	$W \cdot L^{-1}$	7.2 ± 1.2	5.8 ± 1.9	**0.007**

Data are presented as the mean ± SD. The integrated cohort included the participants who completed SMF contractile experiments and corresponds to the cohort examined in Chapter 2. Whole muscle variables were measured by isokinetic dynamometry. Body composition was measured by DXA. Fiber type distribution was determined from muscle homogenate SDS-PAGE. The single fiber block includes only the age-related variables central to the main text.

Table 3. Pooled unadjusted regressions between single fiber mechanics and whole muscle function in the integrated cohort

Whole muscle outcome	Type I predictor	R^2	*P* value	Type II predictor	R^2	*P* value
WM-PPO	Type I P_0	0.340	**0.018**	Type II PPO	0.643	**<0.001**
WM-PPO	Type I CSA	0.290	**0.032**	Type II P_0	0.586	**<0.001**
WM-PPO	Type I PPO	0.270	**0.047**	Type II CSA	0.498	**0.002**
Peak torque	Type I P_0	0.244	0.052	Type II PPO	0.504	**0.001**
Peak torque	—	—	—	Type II P_0	0.445	**0.003**
Normalized torque	—	—	—	Type II PPO	0.376	**0.009**
Normalized torque	—	—	—	Type II NPO	0.322	**0.018**
Normalized torque	—	—	—	Type II SF	0.298	**0.024**
WM-NPO	Type I P_0	0.317	**0.023**	Type II P_0	0.467	**0.002**
WM-V_{max}	Type I P_0	0.312	**0.024**	Type II PPO	0.488	**0.002**
WM-V_{max}	—	—	—	Type II P_0	0.340	**0.014**
WM-V_{max}	—	—	—	Type II CSA	0.303	**0.022**
Normalized peak torque	—	—	—	Type II CSA	0.340	**0.014**

Pooled unadjusted regressions were performed in the integrated cohort at the participant level using subject-mean Type I or Type II single fiber values regressed against participant-level whole muscle outcomes. Only the strongest and/or statistically significant associations central to the main text are shown here. Integrated cohort (*N* = 14–17; 10 young, 7 older)

Table 4. Age-adjusted multiple linear regression models in which single fiber properties remained associated with whole muscle outcomes

SMF variable	WM outcome	*N*	Model R^2	P_{SMF}	P_{Age}	β_{SMF}	β_{Age}
Type II CSA	WM-PPO	17	0.849	<0.001	<0.001	0.08	-301.85
Type II PPO	WM-PPO	17	0.827	<0.001	0.002	9.79	-234.70
Type II P_0	WM-PPO	17	0.811	<0.001	0.001	477.20	-254.98
Type II P_0	WM-NPO	17	0.782	0.004	<0.001	46.08	-36.59
Type II PPO	WM-NPO	17	0.769	0.007	0.001	0.89	-35.41
Type II CSA	WM-NPO	17	0.760	0.009	<0.001	0.01	-41.82
Type II PPO	Peak Torque	17	0.675	0.009	0.017	1.30	-35.45
Type I CSA	WM-PPO	16	0.662	0.028	0.002	0.08	-317.30
Type II P_0	Peak Torque	17	0.656	0.013	0.011	62.28	-38.41
Type II CSA	WM-V_{max}	17	0.638	0.013	0.004	0.02	-88.07
Type II CSA	Peak Torque	17	0.618	0.029	0.004	0.01	-45.75

Multiple linear regression models with age group (young vs. older) and the single fiber variable as simultaneous predictors of each whole muscle outcome. Only models in which the single fiber variable retained statistical significance ($P < 0.05$) after age-adjustment are shown. β_{SMF}, unstandardized regression coefficient for the single fiber predictor; β_{Age}, unstandardized regression coefficient for the age group indicator. Integrated cohort (N = 14–17; 10 young, 7 older).

Table 5. ANCOVA: regression models testing whether the single fiber-to-whole muscle relationship differs between young and older adults.

Model	Term	β	SE	95% CI	*F*	*P* value
Type II CSA vs WM-PPO				*R^2 = 0.896*		*n = 17*
	Age group	75.90	162.06	[-274.21, 426.02]	0.22	0.647
	Type II CSA	**0.10**	0.01	[0.06, 0.13]	45.06	**<0.001**
	Age × CSA	**-0.07**	0.03	[-0.14, -0.01]	5.90	**0.030**
	Within-group slopes: Young = 0.10, Old = 0.02					
Type II P_0 vs WM-PPO				*R^2 = 0.864*		*n = 17*
	Age group	91.95	163.38	[-261.01, 444.91]	0.32	0.583
	Type II P_0	**594.02**	105.43	[366.25, 821.79]	31.74	**<0.001**
	Age × P_0	**-483.72**	214.55	[-947.23, -20.22]	5.08	**0.042**
	Within-group slopes: Young = 594.02, Old = 110.29					
Type II P_0 vs WM-NPO				*R^2 = 0.834*		*n = 17*
	Age group	5.09	21.98	[-42.39, 52.58]	0.05	0.820
	Type II P_0	**60.12**	14.18	[29.47, 90.76]	17.96	**<0.001**
	Age × P_0	-58.13	28.87	[-120.49, 4.23]	4.05	0.065
	Within-group slopes: Young = 60.12, Old = 1.99					
Type II PPO vs WM-PPO				*R^2 = 0.868*		*n = 17*
	Age group	31.46	144.39	[-280.47, 343.39]	0.05	0.831
	Type II PPO	**11.77**	2.06	[7.32, 16.23]	32.54	**<0.001**
	Age × PPO	-8.54	4.28	[-17.79, 0.70]	3.99	0.067
	Within-group slopes: Young = 11.77, Old = 3.23					
Type II CSA vs WM-NPO				*R^2 = 0.810*		*n = 17*
	Age group	5.33	26.62	[-52.17, 62.83]	0.04	0.844
	Type II CSA	**0.01**	0.00	[0.00, 0.01]	14.08	**0.002**
	Age × CSA	-0.01	0.00	[-0.02, 0.00]	3.41	0.088
	Within-group slopes: Young = 0.01, Old = -0.00					

ANCOVA models with age group, single fiber property, and their interaction (age group × single fiber property) as predictors. Only models with interaction $P < 0.10$ are shown; all remaining Type II and Type I comparisons were non-significant ($P = 0.10–0.97$). β, unstandardized regression coefficient; SE, standard error; CI, confidence interval; F, F statistic. The interaction β represents the difference in regression slopes between older and young adults (negative values indicate a shallower slope in older adults). Within-group slopes are unstandardized simple regression coefficients estimated separately within each age group. Bold values indicate statistical significance.

Table 6. Associations between anthropometric variables and whole muscle function in the SMF+WM subset and full cohort.

	Integrated Cohort			Full Cohort		
	N	R^2	*P* value	*N*	R^2	*P* value
TLM (kg)						
Peak Torque	17	**0.493****	**0.002**	60	**0.531*****	**<0.001**
WM-NPT	17	0.080	0.271	60	**0.068***	**0.044**
WM-PPO	17	**0.555*****	**<0.001**	59	**0.549*****	**<0.001**
WM-NPO	17	**0.307***	**0.021**	59	**0.235*****	**<0.001**
WM-V_{max}	17	**0.309***	**0.020**	59	**0.267*****	**<0.001**
Type II TLM (kg)						
Peak Torque	14	**0.458****	**0.008**	49	**0.370*****	**<0.001**
WM-NPT	14	0.124	0.217	49	0.046	0.140
WM-PPO	14	**0.497****	**0.005**	48	**0.419*****	**<0.001**
WM-NPO	14	**0.326***	**0.033**	48	**0.200****	**0.001**
WM-V_{max}	14	0.272	0.055	48	**0.216*****	**<0.001**
Type II fiber (%)						
Peak Torque	14	**0.325***	**0.033**	49	0.036	0.188
WM-NPT	14	0.211	0.099	49	0.010	0.493
WM-PPO	14	0.197	0.112	48	0.051	0.124
WM-NPO	14	0.148	0.174	48	0.032	0.221
WM-V_{max}	14	0.024	0.598	48	0.016	0.398

Associations between anthropometric variables and whole muscle function in the integrated cohort and full cohort. Coefficients of determination (R^2) from pooled unadjusted simple linear regressions. TLM, thigh lean mass; Type II TLM, thigh lean mass × Type II fiber percentage from bulk homogenate; Type II fiber (%), percentage of Type II MHC from bulk homogenate; WM-PPO, whole muscle peak power output; WM-NPO, normalized whole muscle peak power output; WM-NPT, normalized peak torque; WM-V_{max}, whole muscle peak shortening velocity. Integrated cohort: N = 14–17 (10 young, 7 older); full cohort: N = 48–60 (15 young, 44 older). N varies due to availability of fiber type distribution data. Bold values indicate statistical significance (*P < 0.05, **P < 0.01, ***P < 0.001).

Figures

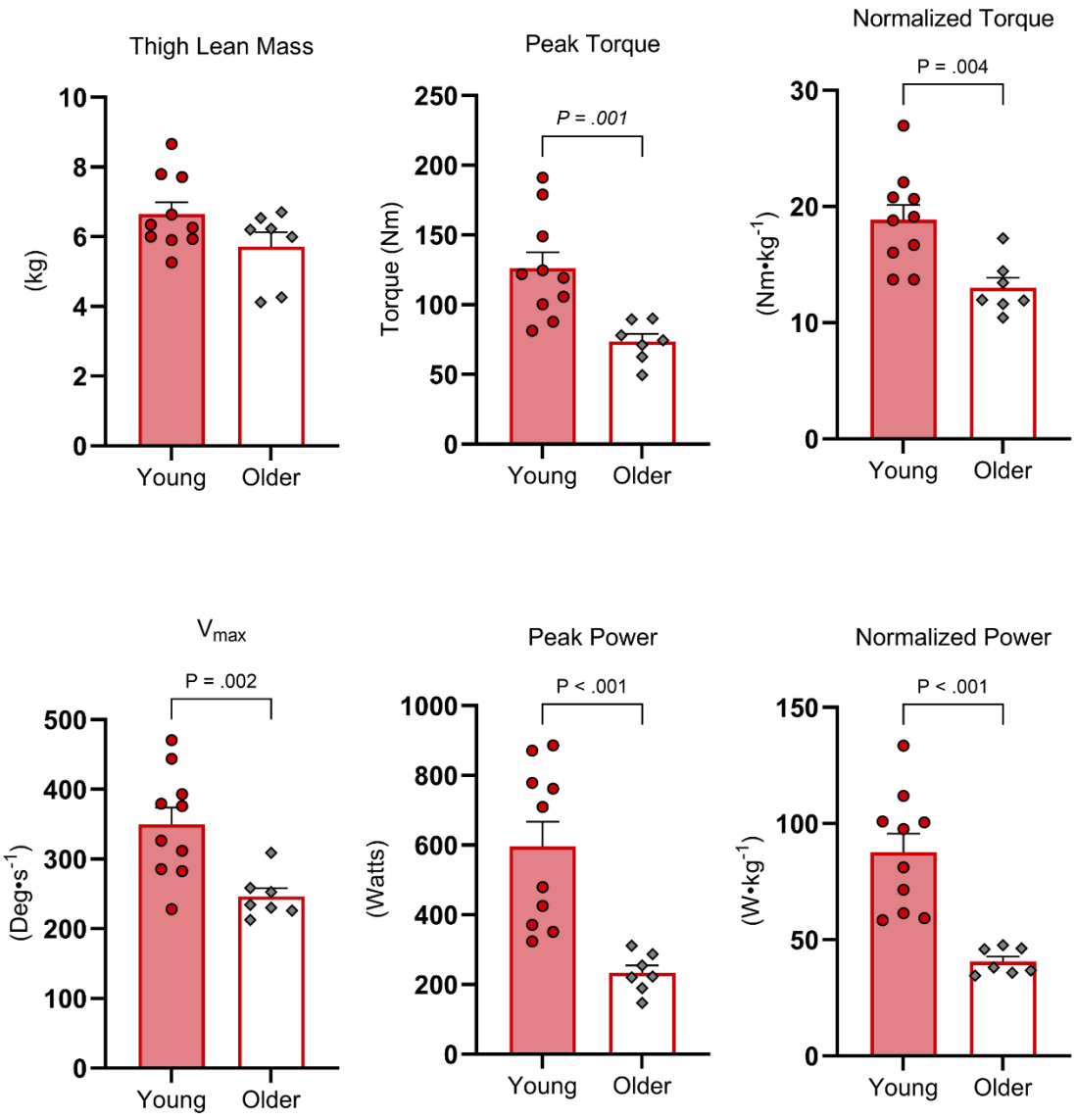

Figure 1. Thigh lean mass (TLM), peak torque, normalized peak torque, whole muscle maximum shortening velocity (WM-V_{max}), whole muscle peak power output (WM-PPO), and normalized power output (WM-NPO) in younger (N = 10; red circles) and older (N = 7; gray diamonds) adults. Data are presented as mean ± SEM with individual data points. P values are shown for significant comparisons (P < 0.05)

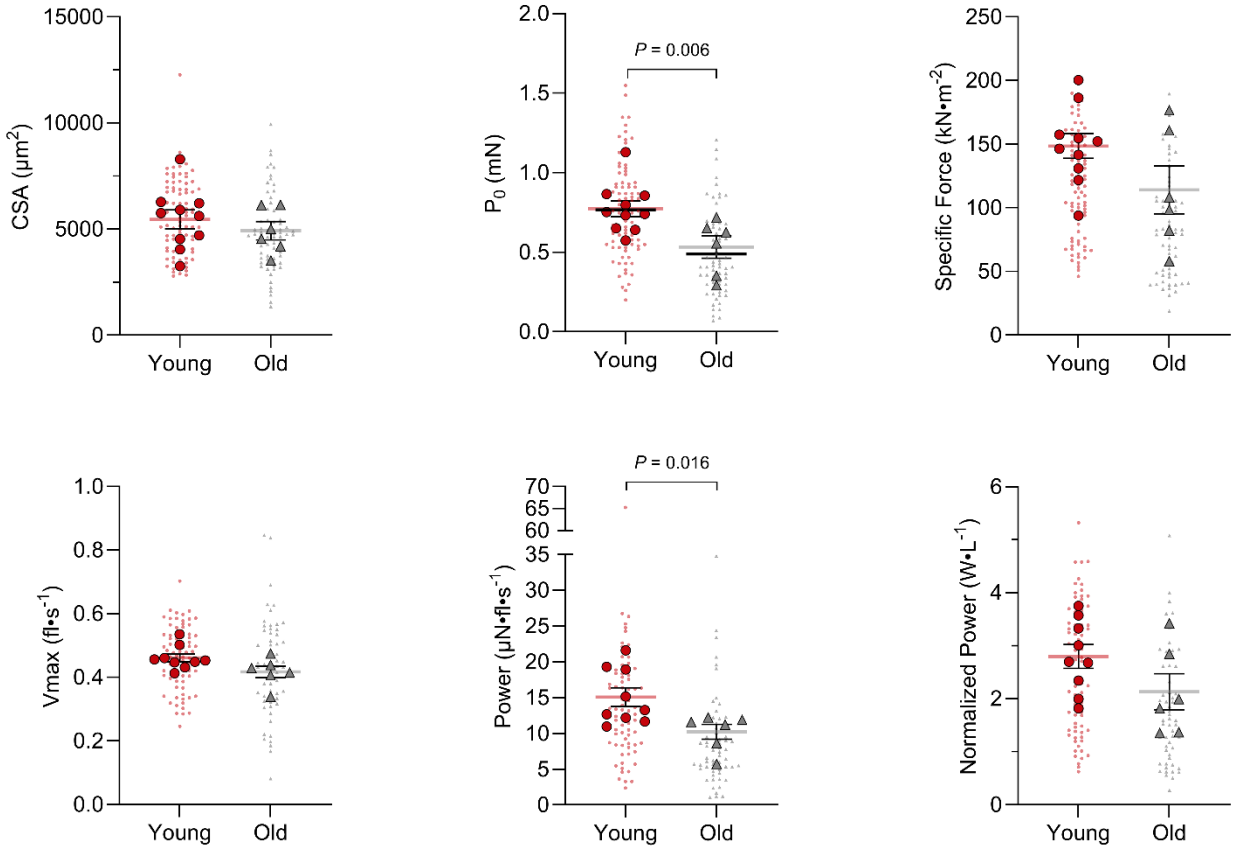

Figure 2. Type I single muscle fiber contractile properties in younger and older adults. Cross-sectional area (CSA), peak isometric force (P_0), specific force (SF), maximum shortening velocity (V_{max}), peak power output (PPO), and normalized power output (NPO) of Type I fibers. Large symbols represent subject-level means; small symbols represent individual fibers. Horizontal bars indicate group means ± SEM. Younger adults: *N* = 10 subjects, *n* = 84 fibers (red); older adults: *N* = 7 subjects, *n* = 66 fibers (gray). *P* values are shown for significant comparisons ($P < 0.05$).

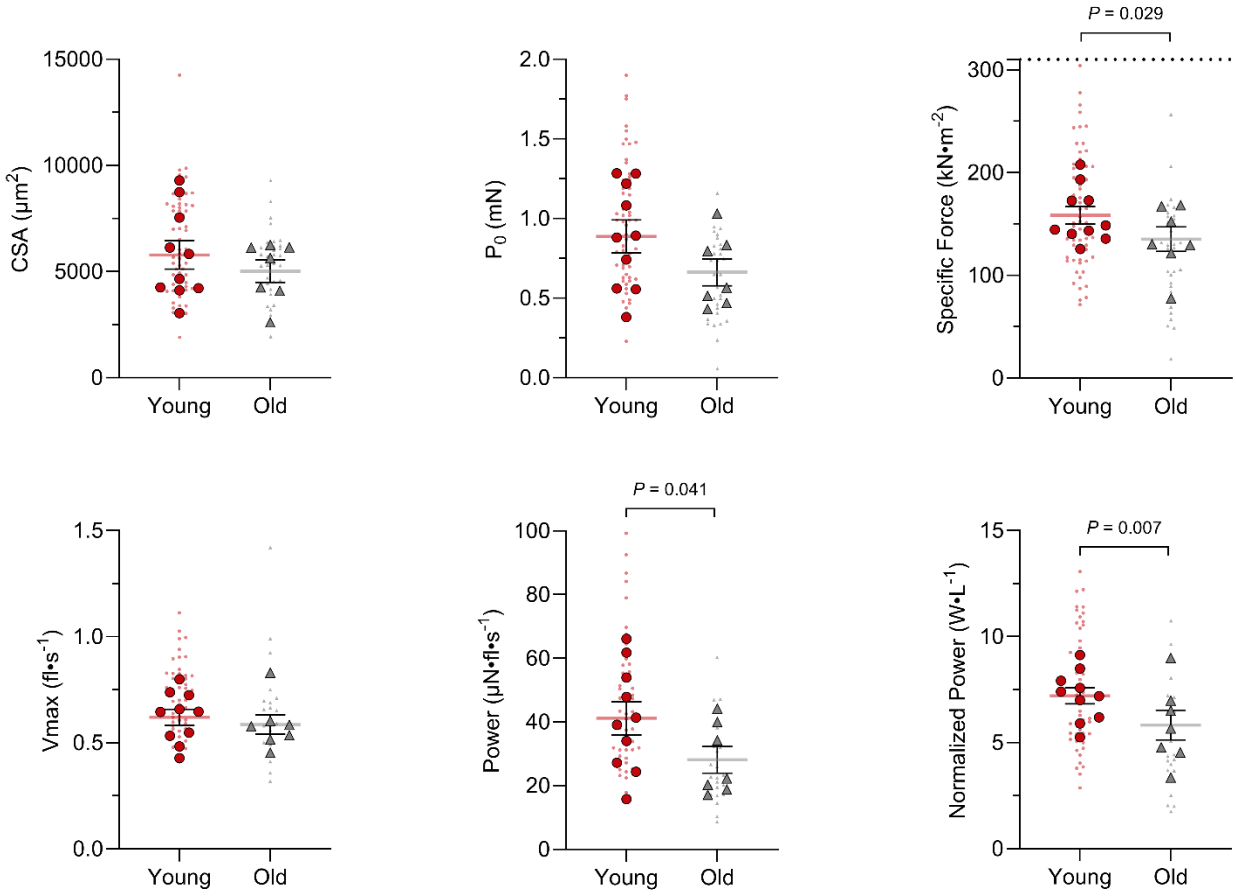

Figure 3. Type II single muscle fiber contractile properties in younger and older adults. Cross-sectional area (CSA), peak isometric force (P_0), specific force (SF), maximum shortening velocity (V_{max}), peak power output (PPO), and normalized power output (NPO) of Type II fibers. Large symbols represent subject-level means; small symbols represent individual fibers. Horizontal bars indicate group means ± SEM. Younger adults: *N* = 10 subjects, *n* = 61 fibers (red); older adults: *N* = 7 subjects, n = 32 fibers (gray). *P* values are shown for significant comparisons (*P* < 0.05).

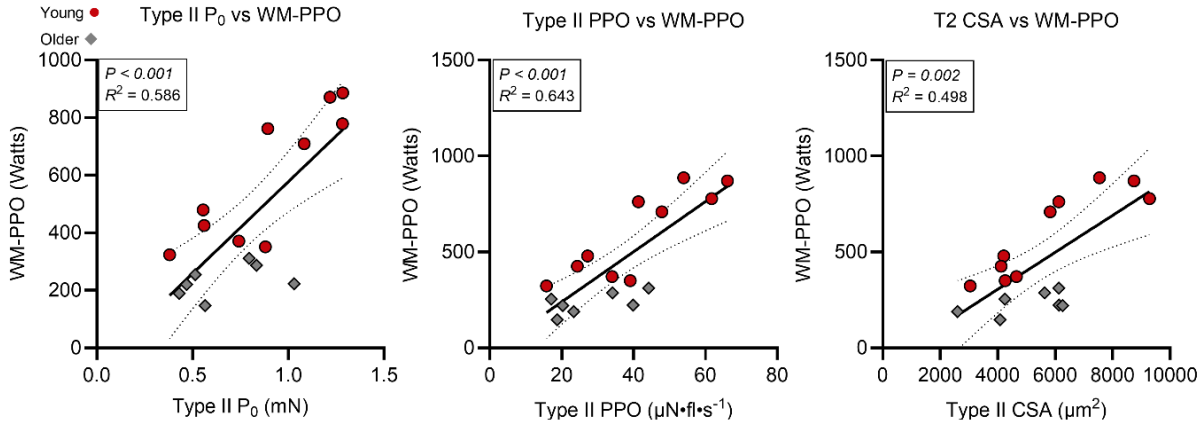

Figure 4. Pooled unadjusted regressions between the three strongest Type II single fiber predictors and whole muscle peak power output (WM-PPO). Left: Type II P_0 vs WM-PPO (R^2 = 0.586; P < 0.001). Center: Type II PPO vs WM-PPO (R^2 = 0.643; P < 0.001). Right: Type II CSA vs WM-PPO (R^2 = 0.498; P = 0.002). Solid lines represent linear regression fits; dashed lines represent 95% confidence intervals. Younger adults (red circles); older adults (gray diamonds). Integrated cohort (N = 17).

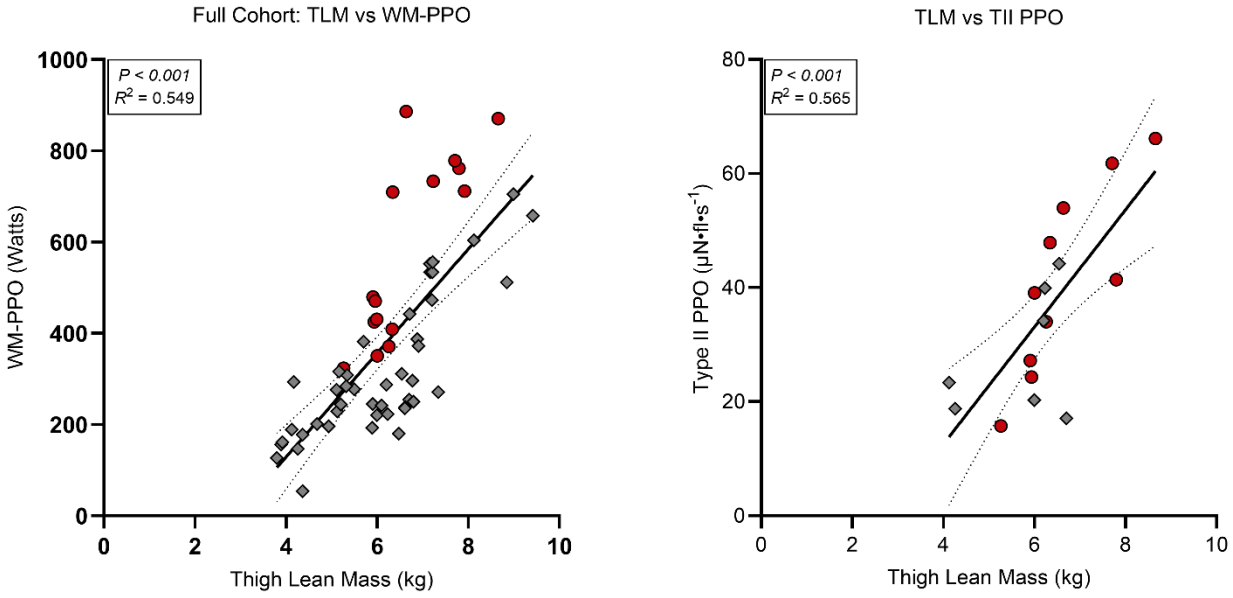

Figure 5. Thigh lean mass as a shared structural correlate of whole muscle and single fiber function. Left: TLM vs WM-PPO in the full cohort (R^2 = 0.549; P < 0.001; N = 59). Right: TLM vs Type II PPO in the integrated cohort (R^2 = 0.565; P < 0.001; N = 17). Solid lines represent linear regression fits; dashed lines represent 95% confidence intervals. Younger adults (red circles); older adults (gray diamonds).

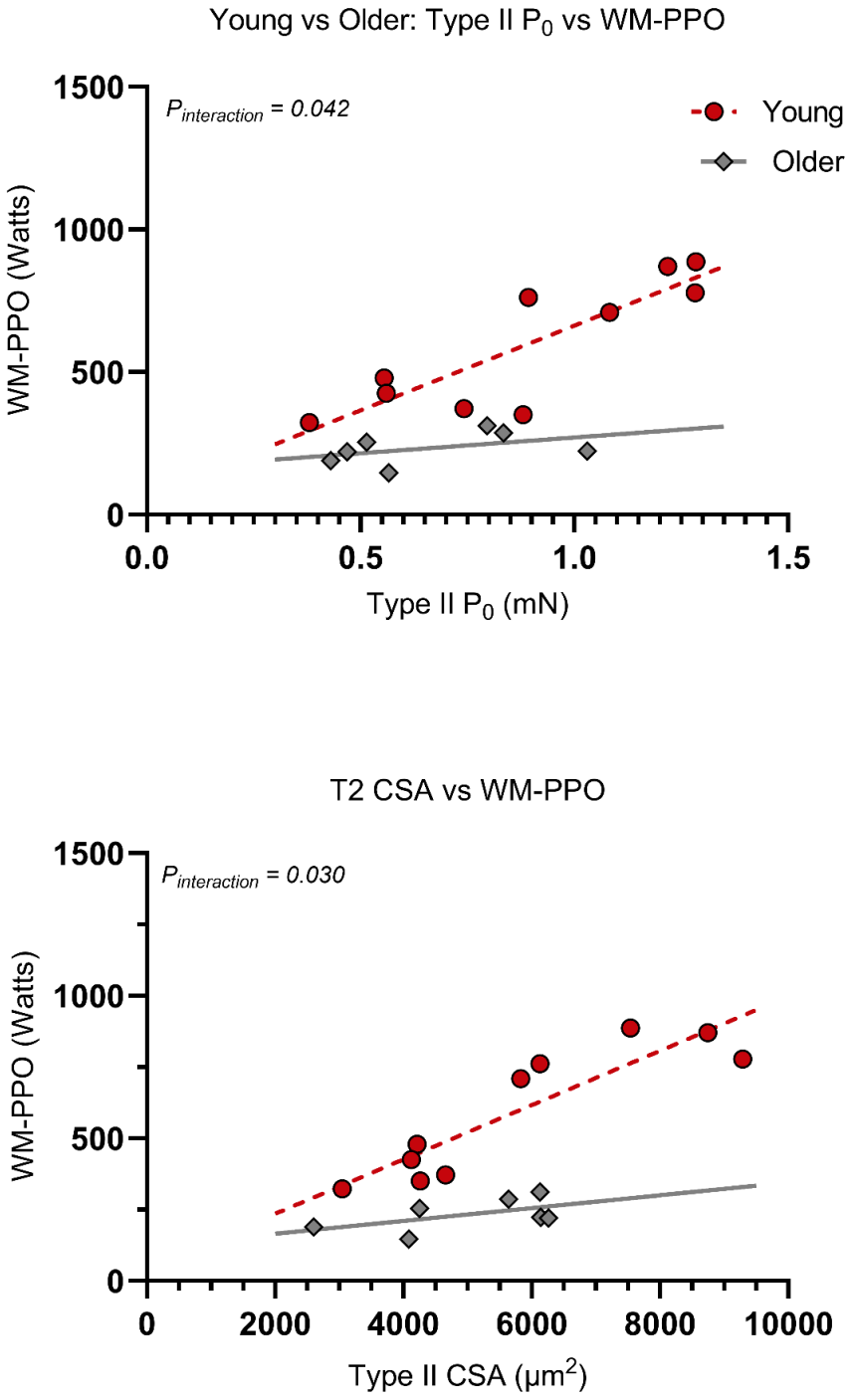

Figure 6. ANCOVA interaction plots showing age-modified regression slopes between Type II single fiber properties and whole muscle peak power output (WM-PPO). Separate regression lines are shown for younger (red) and older (gray) adults to illustrate the attenuation of the single fiber-to-whole muscle relationship with aging. The interaction term tests whether the regression slope differs significantly between age groups. Integrated cohort (*N* = 17; 10 younger, 7 older).

REFERENCES

1. **Kennis E**, **Verschueren S**, **Van Roie E**, **Thomis M**, **Lefevre J**, **Delecluse C**. Longitudinal impact of aging on muscle quality in middle-aged men. *AGE* 36: 9689, 2014. doi: 10.1007/s11357-014-9689-1.

2. **Reid KF**, **Fielding RA**. Skeletal Muscle Power: A Critical Determinant of Physical Functioning in Older Adults. *Exercise and Sport Sciences Reviews* 40: 4–12, 2012. doi: 10.1097/JES.0b013e31823b5f13.

3. **Skelton DA**, **Greig CA**, **Davies JM**, **Young A**. Strength, power and related functional ability of healthy people aged 65-89 years. *Age Ageing* 23: 371–377, 1994. doi: 10.1093/ageing/23.5.371.

4. **Goodpaster BH**, **Park SW**, **Harris TB**, **Kritchevsky SB**, **Nevitt M**, **Schwartz AV**, **Simonsick EM**, **Tylavsky FA**, **Visser M**, **Newman AB**. The loss of skeletal muscle strength, mass, and quality in older adults: the health, aging and body composition study. *J Gerontol A Biol Sci Med Sci* 61: 1059–1064, 2006. doi: 10.1093/gerona/61.10.1059.

5. **Metter EJ**, **Conwit R**, **Tobin J**, **Fozard JL**. Age-Associated Loss of Power and Strength in the Upper Extremities in Women and Men. *The Journals of Gerontology: Series A* 52A: B267–B276, 1997. doi: 10.1093/gerona/52A.5.B267.

6. **Alcazar J**, **Rodriguez-Lopez C**, **Delecluse C**, **Thomis M**, **Van Roie E**. Ten-year longitudinal changes in muscle power, force, and velocity in young, middle-aged, and older adults. *Journal of Cachexia, Sarcopenia and Muscle* 14: 1019–1032, 2023. doi: 10.1002/jcsm.13184.

7. **Delmonico MJ**, **Harris TB**, **Visser M**, **Park SW**, **Conroy MB**, **Velasquez-Mieyer P**, **Boudreau R**, **Manini TM**, **Nevitt M**, **Newman AB**, **Goodpaster BH**, **Health, Aging, and Body**. Longitudinal study of muscle strength, quality, and adipose tissue infiltration. *Am J Clin Nutr* 90: 1579–1585, 2009. doi: 10.3945/ajcn.2009.28047.

8. **Reid KF**, **Pasha E**, **Doros G**, **Clark DJ**, **Patten C**, **Phillips EM**, **Frontera WR**, **Fielding RA**. Longitudinal decline of lower extremity muscle power in healthy and mobility-limited older adults: influence of muscle mass, strength, composition, neuromuscular activation and single fiber contractile properties. *Eur J Appl Physiol* 114: 29–39, 2014. doi: 10.1007/s00421-013-2728-2.

9. **Xu J**, **Wan CS**, **Ktoris K**, **Reijnierse EM**, **Maier AB**. Sarcopenia Is Associated with Mortality in Adults: A Systematic Review and Meta-Analysis. *Gerontology* 68: 361–376, 2021. doi: 10.1159/000517099.

10. **Koon-Yee Lee G**, **Chun-Ming Au P**, **Hoi-Yee Li G**, **Chan M**, **Li H-L**, **Man-Yung Cheung B**, **Chi-Kei Wong I**, **Ho-Fun Lee V**, **Mok J**, **Hon-Kei Yip B**, **King-Yip**

Cheng K, **Wu C-H**, **Cheung C-L**. Sarcopenia and mortality in different clinical conditions: A meta-analysis. *Osteoporosis and Sarcopenia* 7: S19–S27, 2021. doi: 10.1016/j.afos.2021.02.001.

11. **Pacifico J**, **Reijnierse EM**, **Lim WK**, **Maier AB**. The Association between Sarcopenia as a Comorbid Disease and Incidence of Institutionalisation and Mortality in Geriatric Rehabilitation Inpatients: REStORing health of acutely unwell adulTs (RESORT). *Gerontology* 68: 498–508, 2022. doi: 10.1159/000517461.

12. **Pacifico J**, **Geerlings MAJ**, **Reijnierse EM**, **Phassouliotis C**, **Lim WK**, **Maier AB**. Prevalence of sarcopenia as a comorbid disease: A systematic review and meta-analysis. *Exp Gerontol* 131: 110801, 2020. doi: 10.1016/j.exger.2019.110801.

13. **Petrella JK**, **Kim J**, **Tuggle SC**, **Hall SR**, **Bamman MM**. Age differences in knee extension power, contractile velocity, and fatigability. *Journal of Applied Physiology* 98: 211–220, 2005. doi: 10.1152/japplphysiol.00294.2004.

14. **Dalton BH**, **Power GA**, **Vandervoort AA**, **Rice CL**. The age-related slowing of voluntary shortening velocity exacerbates power loss during repeated fast knee extensions. *Exp Gerontol* 47: 85–92, 2012. doi: 10.1016/j.exger.2011.10.010.

15. **Sundberg CW**, **Teigen LE**, **Hunter SK**, **Fitts RH**. Cumulative effects of H+ and Pi on force and power of skeletal muscle fibres from young and older adults. *The Journal of Physiology* 603: 187–209, 2025. doi: 10.1113/JP286938.

16. **Trappe S**, **Gallagher P**, **Harber M**, **Carrithers J**, **Fluckey J**, **Trappe T**. Single Muscle Fibre Contractile Properties in Young and Old Men and Women. *The Journal of Physiology* 552: 47–58, 2003. doi: 10.1113/jphysiol.2003.044966.

17. **Lanza IR**, **Towse TF**, **Caldwell GE**, **Wigmore DM**, **Kent-Braun JA**. Effects of age on human muscle torque, velocity, and power in two muscle groups. *J Appl Physiol (1985)* 95: 2361–2369, 2003. doi: 10.1152/japplphysiol.00724.2002.

18. **Sundberg CW**, **Hunter SK**, **Trappe SW**, **Smith CS**, **Fitts RH**. Effects of elevated H+ and Pi on the contractile mechanics of skeletal muscle fibres from young and old men: implications for muscle fatigue in humans. *The Journal of Physiology* 596: 3993–4015, 2018. doi: 10.1113/JP276018.

19. **Keller K**, **Engelhardt M**. Strength and muscle mass loss with aging process. Age and strength loss. *Muscles Ligaments Tendons J* 3: 346–350, 2014.

20. **Gür H**, **Gransberg L**, **vanDyke D**, **Knutsson E**, **Larsson L**. Relationship between in vivo muscle force at different speeds of isokinetic movements and myosin isoform expression in men and women. *Eur J Appl Physiol* 88: 487–496, 2003. doi: 10.1007/s00421-002-0760-8.

21. **Frontera WR**, **Suh D**, **Krivickas LS**, **Hughes VA**, **Goldstein R**, **Roubenoff R**. Skeletal muscle fiber quality in older men and women. *Am J Physiol Cell Physiol* 279: C611-618, 2000. doi: 10.1152/ajpcell.2000.279.3.C611.

22. **Miller MS**, **Bedrin NG**, **Callahan DM**, **Previs MJ**, **Jennings ME**, **Ades PA**, **Maughan DW**, **Palmer BM**, **Toth MJ**. Age-related slowing of myosin actin cross-bridge kinetics is sex specific and predicts decrements in whole skeletal muscle performance in humans. *Journal of Applied Physiology* 115: 1004–1014, 2013. doi: 10.1152/japplphysiol.00563.2013.

23. **Straight CR**, **Ades PA**, **Toth MJ**, **Miller MS**. Age-related reduction in single muscle fiber calcium sensitivity is associated with decreased muscle power in men and women. *Exp Gerontol* 102: 84–92, 2018. doi: 10.1016/j.exger.2017.12.007.

24. **Baron R**. Normative data for muscle strength in relation to age, knee angle and velocity. *Wien Med Wochenschr* 145: 600–606, 1995.

25. **Sundberg CW**, **Prost RW**, **Fitts RH**, **Hunter SK**. Bioenergetic basis for the increased fatigability with ageing. *J Physiol* 597: 4943–4957, 2019. doi: 10.1113/JP277803.

26. **Wrucke DJ**, **Kuplic A**, **Adam MD**, **Hunter SK**, **Sundberg CW**. Neural and muscular contributions to the age-related differences in peak power of the knee extensors in men and women. *J Appl Physiol (1985)* 137: 1021–1040, 2024. doi: 10.1152/japplphysiol.00773.2023.

27. **Delgadillo JD**, **Sundberg CW**, **Kwon M**, **Hunter SK**. Fatigability of the knee extensor muscles during high-load fast and low-load slow resistance exercise in young and older adults. *Exp Gerontol* 154: 111546, 2021. doi: 10.1016/j.exger.2021.111546.

28. **Thompson BJ**, **Whitson M**, **Sobolewski EJ**, **Stock MS**. The Influence of Age, Joint Angle, and Muscle Group on Strength Production Characteristics at the Knee Joint. *J Gerontol A Biol Sci Med Sci* 73: 603–607, 2018. doi: 10.1093/gerona/glx156.

29. **Ng AV**, **Kent-Braun JA**. Slowed muscle contractile properties are not associated with a decreased EMG/force relationship in older humans. *J Gerontol A Biol Sci Med Sci* 54: B452-458, 1999. doi: 10.1093/gerona/54.10.b452.

30. **Raj IS**, **Bird SR**, **Shield AJ**. Aging and the force-velocity relationship of muscles. *Exp Gerontol* 45: 81–90, 2010. doi: 10.1016/j.exger.2009.10.013.

31. **Straight CR**, **Voigt TB**, **Jala AV**, **Chase JD**, **Ringham OR**, **Ades PA**, **Toth MJ**, **Miller MS**. Quadriceps Lipid Content Has Sex-Specific Associations With Whole-Muscle, Cellular, and Molecular Contractile Function in Older Adults. *J Gerontol A Biol Sci Med Sci* 74: 1879–1886, 2019. doi: 10.1093/gerona/gly235.

32. **Reid KF**, **Doros G**, **Clark DJ**, **Patten C**, **Carabello RJ**, **Cloutier GJ**, **Phillips EM**, **Krivickas LS**, **Frontera WR**, **Fielding RA**. Muscle power failure in mobility-limited older adults: preserved single fiber function despite lower whole muscle size, quality and rate of neuromuscular activation. *Eur J Appl Physiol* 112: 2289–2301, 2012. doi: 10.1007/s00421-011-2200-0.

33. **Hicks GE**, **Shardell M**, **Alley DE**, **Miller RR**, **Bandinelli S**, **Guralnik J**, **Lauretani F**, **Simonsick EM**, **Ferrucci L**. Absolute strength and loss of strength as predictors of mobility decline in older adults: the InCHIANTI study. *J Gerontol A Biol Sci Med Sci* 67: 66–73, 2012. doi: 10.1093/gerona/glr055.

34. **Freitas SR**, **Cruz-Montecinos C**, **Ratel S**, **Pinto RS**. Powerpenia Should be Considered a Biomarker of Healthy Aging. *Sports Med Open* 10: 27, 2024. doi: 10.1186/s40798-024-00689-6.

35. **Teigen LE**, **Sundberg CW**, **Kelly LJ**, **Hunter SK**, **Fitts RH**. Ca2+ dependency of limb muscle fiber contractile mechanics in young and older adults. *Am J Physiol Cell Physiol* 318: C1238–C1251, 2020. doi: 10.1152/ajpcell.00575.2019.

36. **Larsson L**, **Li X**, **Frontera WR**. Effects of aging on shortening velocity and myosin isoform composition in single human skeletal muscle cells. *American Journal of Physiology-Cell Physiology* 272: C638–C649, 1997. doi: 10.1152/ajpcell.1997.272.2.C638.

37. **Frontera WR**, **Hughes VA**, **Krivickas LS**, **Kim S-K**, **Foldvari M**, **Roubenoff R**. Strength training in older women: Early and late changes in whole muscle and single cells. *Muscle & Nerve* 28: 601–608, 2003. doi: 10.1002/mus.10480.

38. **Ochala J**, **Frontera WR**, **Dorer DJ**, **Hoecke JV**, **Krivickas LS**. Single Skeletal Muscle Fiber Elastic and Contractile Characteristics in Young and Older Men. *The Journals of Gerontology: Series A* 62: 375–381, 2007. doi: 10.1093/gerona/62.4.375.

39. **Yu F**, **Hedström M**, **Cristea A**, **Dalén N**, **Larsson L**. Effects of ageing and gender on contractile properties in human skeletal muscle and single fibres. *Acta Physiologica* 190: 229–241, 2007. doi: 10.1111/j.1748-1716.2007.01699.x.

40. **Raue U**, **Slivka D**, **Minchev K**, **Trappe S**. Improvements in whole muscle and myocellular function are limited with high-intensity resistance training in octogenarian women. *Journal of Applied Physiology* 106: 1611–1617, 2009. doi: 10.1152/japplphysiol.91587.2008.

41. **Hvid LG**, **Ørtenblad N**, **Aagaard P**, **Kjaer M**, **Suetta C**. Effects of ageing on single muscle fibre contractile function following short-term immobilisation. *The Journal of Physiology* 589: 4745–4757, 2011. doi: 10.1113/jphysiol.2011.215434.

42. **Jee H**, **Lim J-Y**. Discrepancies between Skinned Single Muscle Fibres and Whole Thigh Muscle Function Characteristics in Young and Elderly Human Subjects. *Biomed Res Int* 2016: 6206959, 2016. doi: 10.1155/2016/6206959.

43. **Mazara N**, **Zwambag DP**, **Noonan AM**, **Weersink E**, **Brown SHM**, **Power GA**. Rate of force development is Ca2+-dependent and influenced by Ca2+-sensitivity in human single muscle fibres from older adults. *Experimental Gerontology* 150: 111348, 2021. doi: 10.1016/j.exger.2021.111348.

44. **Grosicki GJ**, **Gries KJ**, **Minchev K**, **Raue U**, **Chambers TL**, **Begue G**, **Finch H**, **Graham B**, **Trappe TA**, **Trappe S**. Single muscle fibre contractile characteristics with lifelong endurance exercise. *The Journal of Physiology* 599: 3549–3565, 2021. doi: 10.1113/JP281666.

45. **Venturelli M**, **Saggin P**, **Muti E**, **Naro F**, **Cancellara L**, **Toniolo L**, **Tarperi C**, **Calabria E**, **Richardson RS**, **Reggiani C**, **Schena F**. In vivo and in vitro evidence that intrinsic upper- and lower-limb skeletal muscle function is unaffected by ageing and disuse in oldest-old humans. *Acta Physiol (Oxf)* 215: 58–71, 2015. doi: 10.1111/apha.12524.

46. **Gries KJ**, **Minchev K**, **Raue U**, **Grosicki GJ**, **Begue G**, **Finch WH**, **Graham B**, **Trappe TA**, **Trappe S**. Single-muscle fiber contractile properties in lifelong aerobic exercising women. *Journal of Applied Physiology* 127: 1710–1719, 2019. doi: 10.1152/japplphysiol.00459.2019.

47. **Lim J-Y**, **Choi SJ**, **Widrick JJ**, **Phillips EM**, **Frontera WR**. Passive force and viscoelastic properties of single fibers in human aging muscles. *Eur J Appl Physiol* 119: 2339–2348, 2019. doi: 10.1007/s00421-019-04221-7.

48. **Callahan DM**, **Bedrin NG**, **Subramanian M**, **Berking J**, **Ades PA**, **Toth MJ**, **Miller MS**. Age-related structural alterations in human skeletal muscle fibers and mitochondria are sex specific: relationship to single-fiber function. *Journal of Applied Physiology* 116: 1582–1592, 2014. doi: 10.1152/japplphysiol.01362.2013.

49. **Murgia M**, **Toniolo L**, **Nagaraj N**, **Ciciliot S**, **Vindigni V**, **Schiaffino S**, **Reggiani C**, **Mann M**. Single Muscle Fiber Proteomics Reveals Fiber-Type-Specific Features of Human Muscle Aging. *Cell Reports* 19: 2396–2409, 2017. doi: 10.1016/j.celrep.2017.05.054.

50. **Lexell J**, **Taylor CC**, **Sjöström M**. What is the cause of the ageing atrophy?: Total number, size and proportion of different fiber types studied in whole vastus lateralis muscle from 15- to 83-year-old men. *Journal of the Neurological Sciences* 84: 275–294, 1988. doi: 10.1016/0022-510X(88)90132-3.

51. **Lexell J**, **Taylor CC**. Variability in muscle fibre areas in whole human quadriceps muscle: effects of increasing age. *J Anat* 174: 239–249, 1991.

52. **Grosicki GJ**, **Zepeda CS**, **Sundberg CW**. Single muscle fibre contractile function with ageing. *The Journal of Physiology* 600: 5005–5026, 2022. doi: 10.1113/JP282298.

53. **Brocca L**, **McPhee JS**, **Longa E**, **Canepari M**, **Seynnes O**, **De Vito G**, **Pellegrino MA**, **Narici M**, **Bottinelli R**. Structure and function of human muscle fibres and muscle proteome in physically active older men. *The Journal of Physiology* 595: 4823–4844, 2017. doi: 10.1113/JP274148.

54. **D'Antona G**, **Pellegrino MA**, **Adami R**, **Rossi R**, **Carlizzi CN**, **Canepari M**, **Saltin B**, **Bottinelli R**. The effect of ageing and immobilization on structure and function of human skeletal muscle fibres. *J Physiol* 552: 499–511, 2003. doi: 10.1113/jphysiol.2003.046276.

55. **Korhonen MT**, **Cristea A**, **Alén M**, **Häkkinen K**, **Sipilä S**, **Mero A**, **Viitasalo JT**, **Larsson L**, **Suominen H**. Aging, muscle fiber type, and contractile function in sprint-trained athletes. *Journal of Applied Physiology* 101: 906–917, 2006. doi: 10.1152/japplphysiol.00299.2006.

56. **D'Antona G**, **Pellegrino MA**, **Carlizzi CN**, **Bottinelli R**. Deterioration of contractile properties of muscle fibres in elderly subjects is modulated by the level of physical activity. *Eur J Appl Physiol* 100: 603–611, 2007. doi: 10.1007/s00421-007-0402-2.

57. **Krivickas LS**, **Suh D**, **Wilkins J**, **Hughes VA**, **Roubenoff R**, **Frontera WR**. Age- and Gender-Related Differences in Maximum Shortening Velocity of Skeletal Muscle Fibers. *American Journal of Physical Medicine & Rehabilitation* 80: 447, 2001.

58. **Power GA**, **Minozzo FC**, **Spendiff S**, **Filion M-E**, **Konokhova Y**, **Purves-Smith MF**, **Pion C**, **Aubertin-Leheudre M**, **Morais JA**, **Herzog W**, **Hepple RT**, **Taivassalo T**, **Rassier DE**. Reduction in single muscle fiber rate of force development with aging is not attenuated in world class older masters athletes. *Am J Physiol Cell Physiol* 310: C318-327, 2016. doi: 10.1152/ajpcell.00289.2015.

59. **Jeon Y-N**, **Kim H-J**, **Yang S-Y**, **Lee S-H**, **Kim D-Y**, **Bae J-H**, **Lee H-J**, **Lim J-Y**, **Choi S-J**. Contractile Properties of Single Muscle Fiber and Their Relations to Whole Muscle Strength in Korean Young Male. *Exerc Sci* 27: 23–31, 2018. doi: 10.15857/ksep.2018.27.1.23.

60. **Wang Z-M**, **Leng X**, **Messi ML**, **Choi SJ**, **Marsh AP**, **Nicklas B**, **Delbono O**. Relationship of Physical Function to Single Muscle Fiber Contractility in Older Adults: Effects of Resistance Training With and Without Caloric Restriction. *The Journals of Gerontology: Series A* 74: 412–419, 2019. doi: 10.1093/gerona/gly047.

61. **Jeon Y**, **Choi J**, **Kim HJ**, **Lee H**, **Lim J-Y**, **Choi S-J**, **Jeon Y**, **Choi J**, **Kim HJ**, **Lee H**, **Lim J-Y**, **Choi S-J**. Sex- and fiber-type-related contractile properties in human single muscle fiber. *J Exerc Rehabil* 15: 537–545, 2019. doi: 10.12965/jer.1938336.168.

62. **Kalakoutis M**, **Pollock RD**, **Lazarus NR**, **Atkinson RA**, **George M**, **Berber O**, **Woledge RC**, **Ochala J**, **Harridge SDR**. Revisiting specific force loss in human permeabilized single skeletal muscle fibers obtained from older individuals. *Am J Physiol Cell Physiol* 325: C172–C185, 2023. doi: 10.1152/ajpcell.00525.2022.

63. **Miller MS**, **Callahan DM**, **Toth MJ**. Skeletal muscle myofilament adaptations to aging, disease, and disuse and their effects on whole muscle performance in older adult humans [Online]. *Frontiers in Physiology* 5, 2014. https://www.frontiersin.org/articles/10.3389/fphys.2014.00369 [10 Aug. 2022].

64. **Maden-Wilkinson TM**, **Degens H**, **Jones DA**, **McPhee JS**. Comparison of MRI and DXA to measure muscle size and age-related atrophy in thigh muscles. .

65. **Alcazar J**, **Guadalupe-Grau A**, **García-García FJ**, **Ara I**, **Alegre LM**. Skeletal Muscle Power Measurement in Older People: A Systematic Review of Testing Protocols and Adverse Events. *The Journals of Gerontology: Series A* 73: 914–924, 2018. doi: 10.1093/gerona/glx216.

66. **Hyodo K**, **Masuda T**, **Aizawa J**, **Jinno T**, **Morita S**. Hip, knee, and ankle kinematics during activities of daily living: a cross-sectional study. *Braz J Phys Ther* 21: 159–166, 2017. doi: 10.1016/j.bjpt.2017.03.012.

67. **Gregorich ZR**, **Peng Y**, **Cai W**, **Jin Y**, **Wei L**, **Chen AJ**, **McKiernan SH**, **Aiken JM**, **Moss RL**, **Diffee GM**, **Ge Y**. Top-Down Targeted Proteomics Reveals Decrease in Myosin Regulatory Light-Chain Phosphorylation That Contributes to Sarcopenic Muscle Dysfunction. *J Proteome Res* 15: 2706–2716, 2016. doi: 10.1021/acs.jproteome.6b00244.

68. **Fabiato A**. Computer programs for calculating total from specified free or free from specified total ionic concentrations in aqueous solutions containing multiple metals and ligands. In: *Methods in Enzymology*. Elsevier, p. 378–417.

69. **Moss RL**. Sarcomere length-tension relations of frog skinned muscle fibres during calcium activation at short lengths. *J Physiol* 292: 177–192, 1979. doi: 10.1113/jphysiol.1979.sp012845.

70. **Melby JA**, **Brown KA**, **Gregorich ZR**, **Roberts DS**, **Chapman EA**, **Ehlers LE**, **Gao Z**, **Larson EJ**, **Jin Y**, **Lopez JR**, **Hartung J**, **Zhu Y**, **McIlwain SJ**, **Wang D**, **Guo W**, **Diffee GM**, **Ge Y**. High sensitivity top–down proteomics captures single muscle cell heterogeneity in large proteoforms. *Proceedings of the National Academy of Sciences* 120: e2222081120, 2023. doi: 10.1073/pnas.2222081120.

71. **Edman KA**. The velocity of unloaded shortening and its relation to sarcomere length and isometric force in vertebrate muscle fibres. *The Journal of Physiology* 291: 143–159, 1979. doi: 10.1113/jphysiol.1979.sp012804.

72. **Trappe S**, **Williamson D**, **Godard M**, **Porter D**, **Rowden G**, **Costill D**. Effect of resistance training on single muscle fiber contractile function in older men. *Journal of Applied Physiology* 89: 143–152, 2000. doi: 10.1152/jappl.2000.89.1.143.

73. **Trappe S**, **Godard M**, **Gallagher P**, **Carroll C**, **Rowden G**, **Porter D**. Resistance training improves single muscle fiber contractile function in older women. *American Journal of Physiology-Cell Physiology* 281: C398–C406, 2001. doi: 10.1152/ajpcell.2001.281.2.C398.

74. **Hill AV**. The heat of shortening and the dynamic constants of muscle. *Proc R Soc Lond B* 126: 136–195, 1938. doi: 10.1098/rspb.1938.0050.

75. **Widrick JJ**, **Trappe SW**, **Costill DL**, **Fitts RH**. Force-velocity and force-power properties of single muscle fibers from elite master runners and sedentary men. *Am J Physiol* 271: C676-683, 1996. doi: 10.1152/ajpcell.1996.271.2.C676.

76. **Harber MP**, **Konopka AR**, **Undem MK**, **Hinkley JM**, **Minchev K**, **Kaminsky LA**, **Trappe TA**, **Trappe S**. Aerobic exercise training induces skeletal muscle hypertrophy and age-dependent adaptations in myofiber function in young and older men. *Journal of Applied Physiology* 113: 1495–1504, 2012. doi: 10.1152/japplphysiol.00786.2012.

77. **Schneider CA**, **Rasband WS**, **Eliceiri KW**. NIH Image to ImageJ: 25 years of image analysis. *Nat Methods* 9: 671–675, 2012. doi: 10.1038/nmeth.2089.

78. **Jeon Y-N**, **Kim H-J**, **Yang S-Y**, **Lee S-H**, **Kim D-Y**, **Bae J-H**, **Lee H-J**, **Lim J-Y**, **Choi S-J**. Contractile Properties of Single Muscle Fiber and Their Relations to Whole Muscle Strength in Korean Young Male. *Exerc Sci* 27: 23–31, 2018. doi: 10.15857/ksep.2018.27.1.23.

79. **Lexell J**, **Henriksson-Larsén K**, **Winblad B**, **Sjöström M**. Distribution of different fiber types in human skeletal muscles: effects of aging studied in whole muscle cross sections. *Muscle Nerve* 6: 588–595, 1983. doi: 10.1002/mus.880060809.

80. **Frontera WR**, **Reid KF**, **Phillips EM**, **Krivickas LS**, **Hughes VA**, **Roubenoff R**, **Fielding RA**. Muscle fiber size and function in elderly humans: a longitudinal study. *J Appl Physiol (1985)* 105: 637–642, 2008. doi: 10.1152/japplphysiol.90332.2008.

CHAPTER IV

Integrating contractile mechanics and top-down proteomics in the same human single muscle fibers identifies molecular correlates of contractile function

INTRODUCTION

Sarcopenia, the age-related loss of skeletal muscle mass and function, is a leading cause of disability, loss of independence, and reduced quality of life in older adults (1). While muscle atrophy contributes to functional decline, the disproportionate loss of muscle strength and power compared to mass indicates that intrinsic alterations within the muscle also play a substantial role (2). Scientific work at the single muscle fiber (SMF) level has been important in this regard because it isolates the myofilament from neural activation, whole-muscle architecture & tendon compliance, substrate delivery, and metabolic state. Studies of permeabilized human fibers have shown there is age-related atrophy and reduced force, shortening velocity, and power, although the pattern and magnitude of impairment vary across cohorts and fiber types (3). Despite the biological heterogeneity, several studies have reported deficits exist even in the absence of changes in fiber size, implying that at least part of age-related muscle dysfunction is intrinsic to the muscle cell (4, 5). Indeed, previous studies have reported molecular alterations and the existence of a sarcomeric proteome (6–8).

In older adults, lower fiber force and power are not always fully explained by differences in cross-sectional area alone (5, 9, 10). Even when SMF size is preserved, deficits in shortening velocity or in normalized function can still emerge, consistent with impaired contractile quality. Brocca et al. (2017) reported that in physically active older men, reductions in SMF specific force and unloaded shortening velocity (V_0) occurred alongside proteomic evidence of altered post-translational modifications (PTMs), suggesting that qualitative alterations of the contractile proteome may be more important than simple loss of protein content (5). Likewise, age-related actomyosin

dysfunction and age-specific myosin PTMs have been implicated in human muscle, further supporting the idea that molecular remodeling of the sarcomere may contribute directly to reduced performance (11, 12). The sarcomere, which is the basic contractile unit of skeletal muscle, provides a strong mechanistic framework for these observations. Force, shortening velocity, and power emerge from the coordinated actions of thick and thin filament proteins, their isoforms, and their post-translational modifications. Myosin heavy and light chains influence cross-bridge kinetics and the mechanical profile of contraction, whereas troponin and tropomyosin regulate activation and thin-filament behavior. Classical single-fiber physiology studies (for an in-depth review see Bottinelli et al. 1991, 1996; Schiaffino and Reggiani, 2011; Schiaffino et al. 2025) established that contractile speed and power differ systematically across fibers with different myosin profiles (13–16). However, proteins are not expressed as single immutable molecules, which introduces significant complexity. Each gene can yield multiple proteoforms through PTMs, alternative splicing, or both. Consequently, molecular determinants of fiber function likely reside not only in broad isoform expression patterns, but also in proteoform-level differences that are obscured by bulk analyses.

This heterogeneity of SMFs has presented methodological challenges in characterizing the molecular signatures of aging. Traditional bottom-up proteomics provides broad protein coverage, but digestion into peptides breaks the linkage between splice variants and post-translational modifications present on the same intact protein. In contrast, top-down proteomics analyzes intact proteins directly and is therefore uniquely positioned to define proteoforms, preserve PTMs, and quantify abundance and modification state within the same molecular species (6, 17, 18). These advantages are

particularly relevant in skeletal muscle, where closely related sarcomeric protein isoforms and phosphorylation-dependent proteoforms may influence function in subtle but biologically important ways.

Early integrative studies in rodents established the conceptual basis for this approach. Gregorich et al. (2016) used single fiber mechanics and top-down targeted proteomics in a subset of parallel fiber groups in aging rat fast-twitch muscle and reported that decreased phosphorylation of myosin regulatory light chain could account for age-related reductions in force, Ca^{2+} sensitivity, shortening velocity, and power (7). Wei et al. (2018) broadened that framework by identifying additional age-associated remodeling in both fast and slow twitch rat muscles, including proteoform changes involving tropomyosin, troponin I, and Z-disc associated proteins (19). Together, those studies suggest that age-related muscle dysfunction may reflect specific sarcomeric proteoforms rather than uniform loss of bulk protein (e.g., loss of fibers, myosin content). However, the relevance of those mechanisms to human muscle remained unresolved because human tissue is more heterogeneous, biopsy material is limited, and maintaining molecular integrity after mechanical testing is technically demanding.

Methodological progress in top-down proteomics has now made single-fiber analyses increasingly feasible. Lin et al. (2019) developed a targeted top-down liquid chromatography-mass spectrometry platform for simultaneous quantification of protein expression and modification in sarcomeric proteins, thereby providing an antibody-independent means of measuring abundance and post-translational state within the same workflow (6). Melby et al. (2023) then demonstrated reproducible detection of large proteoforms, including myosin heavy chain isoforms, in individual rodent fibers,

establishing proof of concept for fiber-resolved proteoform heterogeneity (20). Wilson et al. (2026) subsequently adapted this strategy for chemically permeabilized human single muscle fibers and showed that skinned fibers can yield reproducible proteoform resolved measurements after contractile testing, and PTM abundance is substantial both within and between individuals (21). Peptide-centric human single-fiber proteomics studies have likewise shown that aging effects can differ by fiber phenotype (8), and newer higher-throughput single-fiber workflows indicate that substantially larger studies are now technically achievable (22). The distinct contribution of the present approach is that it complements those broader workflows by preserving proteoform resolution and linking molecular data directly to mechanics within the exact same fiber.

At the same time, translation from animal models to human muscle must be approached carefully. Human vastus lateralis contains a broad continuum of pure and hybrid fibers, is shaped by lifelong activity and disease exposures, and exhibits greater inter-individual heterogeneity than relatively homogeneous rodent muscles (8, 15). For example, in contrast to rodent findings implicating regulatory light chain phosphorylation in age-associated slowing (7), Teigen et al. (2020) reported that regulatory light-chain abundance and phosphorylation were not altered by age or sex in human slow and fast fibers (23). Thus, human pairwise studies are needed not only to replicate rodent observations, but also to determine which mechanistic propositions survive translation to human muscle fibers.

The present study was designed within that framework. We integrated comprehensive contractile measurements with top-down proteomics in the exact same skinned human muscle fibers. Because the number of fibers that could successfully

complete both workflows was limited, and because direct MHC isoform typing was not available for these same fibers, we chose to analyze each specimen as an individual fiber and interpreted the molecular data using isoforms and proteoforms associated with faster or slower phenotypes. This distinction is important since human fibers frequently occupy a continuum rather than a perfectly discrete type of boundary, and the absence of direct MHC typing makes overclassification inappropriate. A restrained interpretation better matches the data and allows the molecular-functional relationships to be evaluated on their own terms.

The primary objective of the present study was to employ an integrative approach combining single muscle fiber contractile experiments with top-down MS-based proteomics to define the molecular landscape of the mechanically tested fibers and determine whether the analyzed subset displayed heterogenous combinations of fast and slow associated markers. The second aim was to test whether the resolved isoform and proteoform molecular features were associated with single fiber mechanics. The last objective of the study was to determine whether fibers from older subjects exhibited a distinct mechanical and molecular pattern within this paired-analysis subset. By performing proteomics on the exact same skinned human fibers that completed comprehensive contractile experiments, we directly paired molecular and functional data at the single cell level in both younger and older adults. This represents, to our knowledge, the first study to achieve this level of integration in human muscle.

We hypothesized that molecular features associated with faster-contracting phenotypes would be positively correlated with fiber shortening velocity and power, whereas markers associated with slower phenotypes would show the opposite pattern.

We further hypothesized that age-related alterations in sarcomeric proteoforms, including changes in phosphorylation and modification state of contractile and regulatory proteins, are directly associated with lower force, velocity, and power, and would help explain the observed heterogeneity in contractile performance beyond differences in size alone. Because direct MHC typing was unavailable, we deliberately framed these hypotheses around molecular associations and phenotype linked markers rather than classical fast versus slow fiber types.

MATERIALS AND METHODS

Experimental overview

Participants were recruited from the larger EVEROLIMUS Aging Study (EVERLAST). The paired-analysis subset used here included 15 muscle fibers from ten total adults (4 men, 6 women) between the ages of 27–67 years old. All participants provided written informed consent before enrollment, completed medical screening, and were free of overt chronic disease (e.g., cardiovascular disease, diabetes, Alzheimer's) and were not taking immunosuppressive medications. Experimental procedures were approved by the University of Wisconsin-Madison Health Sciences Institutional Review Board (IRB# 2021-1519).

Skeletal muscle biopsies were obtained from the vastus lateralis (VL) and processed for single fiber mechanical experiments. Isolated single muscle fibers (SMFs) had their CSA and contractile properties measured, including P_0, SF, V_{max}, PPO, and NPO. Fibers that successfully completed mechanical testing and met predefined quality control criteria were stored individually at -80 °C for downstream proteomics. A larger pool of more than 250 mechanically tested fibers was generated in the parent study, of which fifteen were selected for paired contractile-proteomic analysis. Selection was constrained by technical feasibility and was enriched for fibers with successful high-quality contractile data and relatively high absolute power, thereby maximizing the likelihood of obtaining interpretable molecular signal from the same fibers. For this first proof-of-concept human aging analysis, the enrichment strategy ensured that any observed molecular-functional relationships were anchored to fibers with unequivocally interpretable mechanical data. However, it also created an intentionally enriched subset

rather than an unbiased sample of the full fiber population. Accordingly, age-group comparisons in this study are interpreted as descriptive or exploratory, whereas molecular-functional associations are the principal focus. Because direct myosin heavy chain fiber typing was not available for these exact fibers, they were not assigned definitive fast or slow fiber types. Instead, each fiber was analyzed as an individual observation, and proteins such as fsTnI, ssTnI, fsTnC, ssTnC, αTpm, βTpm, MLC1F, MLC2F, MLC3F, MLC1V, and MLC2S were interpreted as molecular markers associated with faster or slower phenotypes.

Muscle Biopsy and Single Muscle Fiber Mechanics

Muscle biopsy. Biopsy samples were cleared of visible adipose and connective tissue. Bundles of 20–50 SMFs were dissected from the sample and placed in a petri dish containing relax solution composed of (in mM): 100 KCl, 1.75 EGTA, 10 imidazole, 4 ATP, and 5 $MgCl_2$ under a dissecting microscope. Fiber bundles were secured to a capillary tube using 6–0 braided silk sutures on each end, then submerged in a skinning solution (50% relax solution and 50% glycerol (v:v)) for 24 hours at 4 °C. After 24 hours, the fiber bundles were placed in fresh skinning solution at -20 °C for storage until the day of contractile measurement.

Solutions. Relaxing (described above), pre-activating solution (pCa 9.0) and maximally activating solution (pCa 4.5) for skinned fiber preparations were prepared as previously described (7, 10). The pCa 9.0 solution contained (in mM): 7 EGTA, 20 imidazole, 5.42 $MgCl_2$, 79.16 KCl, 0.01633 $CaCl_2$, 14.5 creatine phosphate, and 4.74 ATP. The pCa 4.5 solution contained (in mM): 7 EGTA, 20 imidazole, 5.26 $MgCl_2$, 64 KCl, 7.01 $CaCl_2$, 14.5 creatine phosphate, and 4.81 ATP. The pH of all single fiber

solutions was adjusted to 7.0 at 15 °C with aqueous KOH. Final concentrations of metals, ligands, and metal-ligand complexes were calculated using the computer program of Fabiato (24).

Experimental setup. On the day of contractile experiments, a bundle was removed from skinning solution and placed in a petri dish containing cold relaxation solution under a dissecting microscope. For each experiment, an individual fiber (~2.0–4.0 mm) was isolated from the bundle with fine-point forceps and inspected to ensure it was intact. The experimental technique for fiber mounting and contractile measurements was performed as previously described (7, 10, 20, 25). Briefly, fibers were mounted in a 14 mm × 4 mm chamber containing relax solution within the permeabilized fiber apparatus (Model 802D, Aurora Scientific, ON, Canada) and attached between a capacitance-gauge force transducer (Model 403A, sensitivity of 20 $mV \cdot mg^{-1}$ and resonant frequency of 600 Hz; Aurora Scientific) and a DC torque motor (Model 308; Aurora Scientific). Fiber ends were placed into stainless-steel troughs and secured by overlaying a ~0.25–0.5 mm length of 4–0 monofilament nylon suture on each end and then tying the suture into the troughs with two loops of 10–0 monofilament suture. Length changes during contractile measurements were introduced at one end of the preparation driven by voltage commands from a PC via a 16-bit D/A converter.

The apparatus was mounted on an inverted phase-contrast microscope (IX50, Olympus, Tokyo, Japan) equipped with 4× and 10× objectives and a 15× photo eyepiece coupled to a CCD camera (CCD-IRIS, Sony, Tokyo, Japan). Chamber temperature was maintained at 15 °C by a Peltier device. Micromanipulators attached to

the force transducer and motor were used to position the fiber in a taut but unstretched position. Fibers were then visualized at 150× magnification, and the length of the preparation was adjusted so that sarcomere length was set to 2.5 μm in relax solution. Magnification was then returned to 60×, and fiber length (L_0) was recorded as the segment length between the transducer and motor troughs. Velocity measurements were normalized to L_0 and expressed as fiber lengths per second ($fl \cdot s^{-1}$). Digital images of the fiber were captured from top and side views, and fiber diameter was measured at three equally spaced points along the length of the fiber in each view using ImageJ (26). CSA was calculated assuming the fiber assumes the shape of an ellipse.

Before the force-velocity experiments, P_0 was measured and the integrity of the fiber mounting was verified by performing a slack test previously described by Edman (27). Fibers were transferred from relax solution to pCa 9.0 for 60 seconds and then activated by transferring into pCa 4.5 solution. Once force plateaued, the fiber was rapidly slacked by 20% of L_0, producing an immediate decline in tension, followed by gradual redevelopment. The fiber was immediately returned to pCa 9.0, terminating force development and re-lengthened to L_0. P_0 was calculated as the difference between the peak force generated during isometric contraction and the minimum force recorded following the 20% slack. Fibers were accepted for subsequent force-velocity measurements when force rose smoothly, P_0 remained stable during activation, sarcomere length remained constant at 2.5 μm, no evidence of slippage from the troughs was observed, and the fiber remained structurally intact on visual inspection.

Force-velocity and force-power measurements. Force-velocity and power properties of each SMF were measured as previously described (10, 28, 29). All

measurements were performed at a sarcomere length of 2.5 μm. Each fiber was activated by transferring it into pCa 4.5 solution, allowed to develop peak isometric force, and then subjected to three predetermined submaximal isotonic loads spanning ~10–90% of P_0 for 200 ms (load combinations varied across activations to sample the full force-velocity relationship). This was followed by a 20% slack and transfer back to pCa 9.0 to terminate activation, after which the fiber was returned to its original length. Each fiber underwent 4–6 activations, yielding 12–18 isotonic contractions in total.

Loaded shortening velocity was determined from the slope of a linear regression fitted to the change in fiber length during the final 100 ms of each force step. The force-velocity relationship was constructed from the corresponding force and velocity values during each activation and fitted using the Hill equation (30). Power was derived from the fitted F-V parameters. Absolute peak power ($\mu N \cdot fl \cdot s^{-1}$) was calculated as the product of force (μN) and shortening velocity (V_{max}; $fl \cdot s^{-1}$) at the load yielding maximum power along the fitted force-velocity curve, whereas normalized power was calculated as the product of specific force ($kN \cdot m^{-2}$) and shortening velocity (V_{max}; $fl \cdot s^{-1}$) at the load yielding maximum normalized power ($W \cdot L^{-1}$) (31–33).

To ensure data quality, the P_0 recorded during each activation was normalized to the highest P_0 obtained for that fiber. Activations in which force declined to < 90% of the fiber-specific maximal P_0 were excluded, along with their associated force steps from further analysis. Construction of the F-V relationship required a minimum of four successful activations per fiber (yielding ≥ 12 isotonic contractions). Fibers with fitted F-V curves yielding $R^2 < 0.98$ were excluded from further analysis (10, 33).

Top-Down Proteomics

Surfactant-free protein extraction. After completion of mechanical testing, the same individual fibers were transferred to lo-bind microcentrifuge tubes and stored for intact protein analysis. Protein extraction and sample handling were kept in a minimal volume one-pot format to limit adsorptive loss and preserve intact proteoforms, consistent with prior single fiber and targeted top-down proteomics workflows (6, 20). Surfactant-free protein extraction was performed using a workflow by Wilson et al. (2026) (21). On the day of extraction, single muscles fibers were briefly thawed on ice, and all sample handling was performed on ice to minimize protein degradation and artificial oxidation. Any remaining residual relax solution was removed by gently rinsing each fiber with 40 µL of ammonium acetate. Fibers were then briefly centrifuged, and the remaining ammonium was removed, and then fibers were suspended in 20 µL of extraction solution (100% HFIP, 1X HALT protease and phosphatase inhibitor, and 10 mM L-methionine). Once the fiber was visibly dissolved in the solution (~1 min), samples were immediately centrifuged, and the resulting extracts were buffer exchanged into 0.2% formic acid (FA) using a 10kDa molecular weight cutoff spin filter. Extracts were then concentrated to a final volume of ~20 µL. Finally, 10 µL of each extract were used to estimate protein concentrations using a Bradford assay, and the remaining ~10 µL were transferred to HPLC vials for LC-MS analysis.

Liquid chromatography-mass spectrometry analysis of SMF extracts. Extracts were analyzed by reverse-phase liquid chromatography coupled to high-resolution mass spectrometry. Protein separation was carried out on a NanoAcuity Ultra-High Pressure LC system similarly as previously described (20, 34). Approximately 500 ng total protein

was injected for each sample. Elution was performed using a home-packed C4 column (200 mm x 0.250 mm, 2.7 µm, 1000 Å C4 (Halo)) maintained at 50 °C with a flow rate of 5 µL/min. Eluted proteins were electrosprayed into a high-resolution Impact II quadrupole time-of-flight (QTOF) mass spectrometer (Bruker Daltonics, Bremen, Germany).

Proteomic data analysis. LC-MS data was processed and analyzed using DataAnalysis (v4.3, Bruker Daltonics) software (35). The Top 5–7 most abundant charge state ions from the non-deconvoluted spectra were used to produce extracted ion chromatograms (EICs), and relative abundances of isoforms were measured using the ratios of the area under the curve (AUC) of each isoform's EIC. Relative quantification of proteoforms was performed by deconvoluting mass spectra using the Maximum Entropy Deconvolution algorithm and taking the ratio of the highest peak intensity of the proteoform to the summed intensities of all proteoforms of that protein and chromatographic peaks and deconvoluted intact masses were used to assign sarcomeric isoforms and proteoforms. Total phosphorylation of proteins with multiple phosphorylation sites was calculated as the ratio of the sum of the peak intensity of all phosphorylated proteoforms (multiplied by the integer number of phosphorylated sites on that proteoform) to the sum of all proteoform peak intensities of that protein, similarly as reported previously (20, 21, 34, 36, 37).

Isoform and Proteoform Variables

Isoform level variables included fast and slow troponin I (fsTnI, ssTnI), α- and β-tropomyosin (αTpm, βTpm), fast and slow troponin C (fsTnC, ssTnC), and myosin light chain isoforms associated with fast or slow phenotypes (MLC1F, MLC2F, MLC3F,

MLC1V/S, MLC2S). Relative percentages within specific isoform families were also calculated, including %MLC1F, %MLC2F, %MLC3F, %MLC1V, and %MLC2S. Proteoform level variables included αTpm, pαTpm, βTpm, αTpm total phosphorylation, βTpm/total Tpm ratio, MLC2F, pMLC2F, MLC2F total phosphorylation, MLC2S, MLC2S +30 Da, pMLC2S, MLC2S total phosphorylation, and the ratio of MLC2S +30 Da to total MLC2S. Because some slow-associated proteoforms were present in only a small subset of fibers, analyses involving those variables were interpreted cautiously, particularly when effective sample size was reduced by sparse detection.

Statistical Analysis

Descriptive data are presented as mean ± SD unless otherwise indicated. For the primary molecular-functional analyses, Pearson correlations were used to quantify associations between isoform/proteoform variables and SMF mechanics (P_0, specific force, V_{max}, absolute peak power, and normalized peak power). Pearson *r* values were interpreted using conventional effect-size benchmarks (approximately 0.10–0.29 weak, 0.30–0.49 moderate, 0.50–0.69 strong, and ≥0.70 very strong), while also considering biological plausibility and effective sample size. Biological plausibility was judged against established sarcomeric physiology; for example, positive associations of fast-associated light-chain or troponin markers with V_{max} or absolute peak power were considered more mechanistically coherent than associations lacking an obvious contractile rationale (6, 7, 13, 14, 38). Scatterplots were visually inspected to ensure that no single point or overtly nonlinear pattern appeared to dominate the observed relationship. A formal a priori power calculation was not used to set the final paired sample because the number of fibers available for complete mechanical and proteomic

pairing depended on technical success across both workflows. Accordingly, all correlations were treated as exploratory rather than threshold definitive. Because the principal scientific question concerned pairwise molecular-functional relationships within the analyzed fibers, these correlations constitute the core inferential analysis.

Exploratory comparisons between fibers from younger and older subjects were also examined at the fiber level using Welch's two-tailed t-tests. These comparisons should not be interpreted as definitive age-group estimates for the broader cohort because the paired-analysis subset was small, unbalanced, and purposively enriched for technically successful, higher-power fibers. In addition to the within-fiber molecular-functional correlations, a complementary fiber-level comparison was performed to evaluate whether the abundances of selected fast-associated isoforms and proteoforms differed between fibers from younger and older subjects. Welch's two-tailed t-tests were used to compare MLC1F, MLC2F, MLC3F, fsTnC, sa-actin, MLC2F proteoform, pMLC2F proteoform, and MLC2F total phosphorylation between the younger (n = 10) and older (n = 5) fibers in the paired-analysis subset. These comparisons were subject to the same interpretive caveats noted above. This fiber count is consistent with prior published top-down proteomics studies in skeletal muscle (20).

Given the small sample size and multiple exploratory correlations, no adjustment for multiple comparisons was applied. Findings were interpreted as exploratory and hypothesis-generating, with emphasis placed on effect size, biological plausibility, consistency across related molecular markers, and agreement between within-fiber correlations and descriptive age patterns. Statistical analysis was performed using

GraphPad Prism, version 11.0.0 (GraphPad Software Inc., Boston, MA, USA). $P < 0.05$ was considered statistically significant.

RESULTS

Paired Molecular-Functional Analysis

Fifteen fibers from ten participants were available for paired mechanical and proteomic analysis. Ten fibers were from 6 younger subjects (3 men and 3 women), and five fibers were from 4 older subjects (1 man and 3 women). Mean age was 28.1 ± 1.8 years in the younger group and 61.1 ± 3.8 years in the older group (Table 1). Because this subset was selected from a much larger mechanically tested pool, it should be viewed as a technically successful and functionally enriched subset rather than a representative census of all fibers studied in the parent project.

Exploratory Mechanical Profile of the Selected Fibers

Within the paired-analysis subset, fibers from older subjects displayed lower absolute contractile function than fibers from the young adults, but these age contrasts should be interpreted as descriptive rather than definitive. Mean P_0 was 0.78 ± 0.20 mN in older fibers compared with 1.27 ± 0.25 mN in younger fibers. V_{max} was 0.58 ± 0.08 $fl \cdot s^{-1}$ in older fibers and 0.75 ± 0.12 $fl \cdot s^{-1}$ in younger fibers. Absolute peak power was likewise lower in older fibers (34.7 ± 7.6 vs. 54.8 ± 21.9 $\mu N \cdot fl \cdot s^{-1}$). By contrast, specific force and normalized peak power were comparatively similar between groups (157.2 ± 50.2 vs. 179.0 ± 39.5 $kN \cdot m^{-2}$ for specific force; 7.27 ± 3.22 vs. 7.72 ± 3.40 $W \cdot L^{-1}$ for normalized peak power) (Table 1; Fig. 1). These patterns suggest that, in this selected subset, aging-related impairment was expressed more strongly in absolute force, shortening velocity, and absolute power than in size-normalized indices.

Molecular Heterogeneity of the Analyzed Fibers

The paired-analysis fibers were molecularly heterogeneous, but the subset was clearly enriched for markers associated with faster-contracting phenotypes. Twelve fibers displayed dominant fast-associated troponin signatures, defined by high fsTnI and fsTnC with little or no slow troponin signal. Two fibers showed dominant slow-associated troponin signatures, and one fiber exhibited a mixed troponin profile. Light-chain markers revealed additional heterogeneity beyond the troponin pattern alone. For example, some fibers with strong fast-associated troponin signatures still contained detectable slow-associated myosin light-chain proteoforms, whereas one mixed troponin fiber showed appreciable coexistence of fast- and slow-associated light-chain markers. Relative αTpm and βTpm abundance also varied across fibers rather than separating them into perfectly discrete clusters (Figure 2). Collectively, these patterns support the decision to analyze fibers individually and to interpret isoforms and proteoforms as phenotype-linked markers rather than as a substitute for definitive fiber typing.

Molecular Correlates of Contractile Function

Isoform-level relationships. Several isoform-level variables were significantly associated with contractile performance (Table 2; Fig. 3). The strongest isoform relationship observed was between MLC1F and V_{max} (r = 0.747, P = 0.001). MLC2F was also positively associated with V_{max} (r = 0.684, P = 0.005), as was fsTnC (r = 0.655, P = 0.008). Notably, the absolute abundances of these fast-associated isoforms were highly inter-correlated (MLC1F vs MLC2F: r = 0.957; MLC1F vs fsTnC: r = 0.866; MLC2F vs fsTnC: r = 0.929), indicating that they reflect a shared fast-phenotype signal

rather than independent molecular predictors. Each was also significantly correlated with fiber CSA (r = 0.65–0.70), consistent with larger fibers containing more total sarcomeric protein. βTpm was negatively associated with V_{max} (r = -0.592, P = 0.020), whereas MLC3F was positively associated with V_{max} (r = 0.584, P = 0.022).

When analyzed as relative composition within the fast light-chain pool, %MLC1F was negatively associated with V_{max} (r = -0.556, P = 0.031), whereas %MLC2F was positively associated with V_{max} (r = 0.551, P = 0.033). However, because %MLC3F occupied a small and relatively invariant fraction of the MLCF pool (~4%), %MLC1F and %MLC2F were nearly perfectly anti-correlated (r = -0.995) and therefore cannot be interpreted as independent predictors, these associations represent complementary expressions of the same compositional signal.

For P_0, positive associations were observed with MLC1F (r = 0.666, P = 0.007), MLC2F (r = 0.630, P = 0.012), and fsTnC (r = 0.555, P = 0.032). Absolute peak power also tracked multiple fast-associated isoforms. Significant positive relationships were present for MLC1F (r = 0.620, P = 0.014), fsTnI (r = 0.598, P = 0.019), MLC2F (r = 0.582, P = 0.023), %MLC2F (r = 0.584, P = 0.022), and fsTnC (r = 0.569, P = 0.027). Conversely, %MLC1F showed a negative association with absolute peak power (r = -0.581, P = 0.023). No isoform variable was significantly related to specific force. For normalized peak power, only a negative trend with βTpm reached the prespecified exploratory range (r = -0.500, P = 0.058).

Proteoform-level relationships. Proteoform analyses identified several significant associations with fiber mechanics (Table 3; Fig. 3). Absolute peak power showed the strongest overall proteoform relationship with αTpm (r = 0.738, P = 0.002). Absolute

peak power was also positively associated with MLC2F proteoform abundance (r = 0.667, P = 0.007) and with pMLC2F (r = 0.621, P = 0.013). In contrast, the βTpm/total Tpm ratio was negatively associated with absolute peak power (r = -0.532, P = 0.041). P_0 was positively associated with βTpm (r = 0.687, P = 0.005), MLC2F (r = 0.582, P = 0.023), and αTpm (r = 0.575, P = 0.025). Notably, MLC2F total phosphorylation was negatively associated with P_0 (r = -0.553, P = 0.033). V_{max} was positively associated with βTpm (r = 0.667, P = 0.007), MLC2F (r = 0.655, P = 0.008), and αTpm (r = 0.653, P = 0.008), whereas MLC2F total phosphorylation showed a negative trend with V_{max} (r = -0.466, P = 0.080). For normalized peak power, positive and negative trends were observed for pMLC2F (r = 0.490, P = 0.064) and βTpm/total Tpm ratio (r = -0.464, P = 0.081), respectively. As with the isoform analysis, no proteoform variable was significantly associated with specific force.

Direct Comparisons of Isoform and Proteoform Abundance Between Younger and Older Fibers

Direct fiber-level comparisons between younger (n = 10) and older (n = 5) fibers revealed one significant age-related difference and one trend among the eight isoforms and proteoforms tested (Table 4; Fig. 4). Sarcomeric α-actin (sa-actin) abundance was significantly lower in older fibers compared to younger fibers (0.98 vs 2.14 AUC a.u.; P = 0.024), representing a 54% reduction. MLC2F total phosphorylation showed a strong trend toward higher values in older fibers (0.098 vs 0.027; P = 0.088). The remaining comparisons did not reach statistical significance, although the directional patterns were consistent with the lower mechanical performance observed in the older subset: MLC2F (5.98 vs 9.49; P = 0.266), MLC3F (0.55 vs 1.03; P = 0.176), MLC1F (8.92 vs 12.92; P =

0.218), fsTnC (0.54 vs 0.83; $P = 0.267$), MLC2F proteoform (effectively the same comparison as MLC2F isoform) and pMLC2F proteoform (1.04 vs 1.37; $P = 0.551$) were all numerically lower in older fibers, by approximately 24–47%. These directional reductions in fast-associated sarcomeric protein abundance in older fibers are consistent with the within-fiber correlations described above, in which higher fast-associated isoform/proteoform abundance was positively associated with P_0, V_{max}, and absolute peak power. Given the small number of older fibers ($n = 5$), these comparisons should be interpreted as exploratory and hypothesis-generating rather than as definitive age-group estimates.

DISCUSSION

Principal Findings

This study integrated contractile mechanics with top-down proteomics in the exact same human single muscle fibers and, to our knowledge, provides one of the clearest human demonstrations to date that fiber-by-fiber heterogeneity can be related directly to fiber mechanics after functional testing. The major findings were as follows. First, the analyzable fibers were molecularly heterogenous but enriched for markers associated with faster-contracting phenotypes, emphasizing both the technical feasibility of the approach and the importance of restrained interpretation when direct MHC type is unavailable. Additionally, multiple fast-associated isoforms and proteoforms were positively associated with P_0, V_{max}, and absolute peak power, with especially strong relationships involving MLC1F, MLC2F, fsTnC, αTpm, βTpm, and pMLC2F. Furthermore, no molecular variable was associated with specific force, suggesting that the molecular determinants captured here were more closely linked to absolute performance than to a uniform decrement in size-normalized contractile function.

Within-fiber Molecular Correlates of Force, Velocity, and Power

A central strength of the present work is the within-fiber pairing itself. Much of the literature on aging muscle has necessarily inferred mechanisms by aligning bulk proteomics with separate cohorts of mechanically characterized fibers, or by comparing fiber function while measuring proteins at the whole-muscle level. Those designs are informative, but they are vulnerable to sampling mismatch in skeletal muscle as heterogeneous as the human vastus lateralis. By measuring mechanics first and proteoforms second in the same fiber, the present study reduced that ambiguity

substantially. A fiber with higher V_{max} or greater absolute peak power could be asked directly whether it also exhibited more MLC1F, more MLC2F, more αTpm, or greater pMLC2F, or whether the ratio of MLC1F to MLC total potentially slowed V_{max}. That is a conceptually important advancement, even though the sample size remained small.

The mechanical profile of the subset itself is informative. Although these fifteen fibers were not intended to represent the full parent cohort, the older subject fibers nevertheless showed lower P_0, V_{max}, and absolute peak power. Those patterns are directionally consistent with the broader human single-fiber literature showing that aging can impair absolute force and power, particularly in fibers with faster-contracting characteristics (3, 5, 9, 10, 31, 39, 40). At the same time, specific force and normalized peak power were not clearly lower in the selected older fibers. That combination suggests that in this enriched subset, aging-related impairment was not expressed as a universal collapse of size-normalized function. Instead, the dominant signature was lower absolute contractile function, particularly for power which depends jointly on force and shortening velocity. This observation matters because it places the molecular correlations in context, the strongest molecular associations in the present dataset also clustered around P_0, V_{max}, and absolute peak power rather than around specific force.

The isoform results reinforce the importance of myosin light-chain composition in shaping fiber mechanics. Absolute MLC1F abundance was the single strongest isoform correlate of V_{max} and was also positively associated with P_0 and absolute peak power. MLC2F and fsTnC showed similar patterns. Importantly, however, the absolute abundances of these fast-associated isoforms were highly inter-correlated ($r > 0.85$ in most pairings) and each was significantly associated with fiber CSA, indicating that they

represent a coordinated fast-phenotype expression pattern rather than independent molecular determinants. A fiber with more total fast type sarcomeric protein tended to be larger, faster, and more powerful. These patterns are biologically coherent and expected within an analyzed subset already biased toward mechanically successful higher-power fibers, but the individual correlations should not be interpreted as evidence that any single protein independently drives contraction. The positive association between MLC3F and V_{max} is also noteworthy and aligns with prior work implicating relative MLC composition in modulation of shortening velocity (38, 41). In rat fibers, both Bottinelli et al. (1995) and Zhong and Thompson (2007) linked greater relative MLC3F content to faster unloaded shortening (38, 41). Our human data extend that general concept, albeit cautiously, by showing that MLC3F abundance in this paired human fiber dataset was directionally related to higher V_{max} (Table 2).

At first glance, one result may appear paradoxical: absolute MLC1F was positively associated with V_{max} and absolute peak power, whereas the percentage of MLC1F within the fast light-chain pool was negatively associated with both outcomes. In practice, these findings are not contradictory. Absolute abundance and relative composition answer different questions. An individual muscle fiber can contain more total fast light-chain protein overall, which would increase absolute MLC1F together with other fast-associated proteins. At the same time, within the fast light-chain compartment, a lower proportional dominance of MLC1F, and correspondingly greater representation of MLC2F and MLC3F, may characterize the faster and more powerful end of the phenotype continuum. It should be noted that because MLC3F occupied a small and relatively invariant fraction of the pool (~4%), %MLC1F and % MLC2F were

nearly perfectly anti-correlated (r = -0.995) and cannot be interpreted as independent predictors. The relevant compositional signal is therefore the proportional balance within the MLCF pool, not the behavior of any single percentage in isolation. Prior work has shown that the relative content of ELC isoforms (MLC3F vs MLC1F) modulates shortening velocity specifically at zero load, with diminishing influences as load increases (38, 41). In the present dataset, the MLC3F:MLC1F ratio was not significantly associated with V_{max} (r = 0.300, P = 0.278) or absolute power (r = 0.232, P = 0.406) or normalized power (r = -0.055, P = 0.846), consistent with the small and variable nature of MLC3F in these human fibers. However, the broader compositional balance within the fast light chain pool, specifically the proportion of MLC1F relative to MLC2F did track variation in both V_{max} and absolute peak power. Because %MLC1F and %MLC2F were nearly perfectly anti-correlated (r = -0.995), this compositional signal cannot distinguish whether it is driven by the essential or regulatory light chain specifically, though it raises the possibility that the essential to regulatory light chain ratio may carry functional relevance in human fibers beyond what has been demonstrated for the ELC isoforms alone.

The tropomyosin results add a second layer of interpretation but also highlight an important methodological nuance. At the proteoform level, αTpm showed the strongest overall positive relationship with absolute peak power and was also positively associated with P_0 and V_{max}. Proteoform-level βTpm behaved in a more nuanced manner, its absolute abundance (quantified by deconvoluted peak intensity) was positively associated with P_0 and V_{max}, yet the βTpm/total Tpm ratio was negatively associated with absolute peak power and trended negatively with normalized peak

power. This pattern likely reflects the difference between total contractile protein content and relative phenotype dominance. A fiber with high overall sarcomeric protein abundance may exhibit more absolute βTpm signal simply because it contains more thin-filament protein, but a fiber in which βTpm dominates the tropomyosin pool may occupy a slower molecular phenotype that limits peak power. This interpretation is also consistent with the heatmap (Figure 2), where the most slow-associated fibers were strongly βTpm-dominant.

A notable discrepancy emerged between the two analysis levels, at the isoform level, βTpm (quantified by AUC of the extracted ion chromatogram) was negatively associated with Vmax ($r = -0.592$), whereas at the proteoform level, βTpm (quantified by deconvoluted peak intensity) was positively associated with Vmax ($r = 0.667$). This apparent reversal is attributable to the different quantification methods. The isoform level AUC integrates signal across all co-eluting molecular forms of β-tropomyosin in the chromatographic peak, whereas the proteoform level intensity resolves individual intact species after mass deconvolution. In fibers containing substantial total thin filament material but a lower βTpm-dominant phenotype, these two metrics can diverge. Consistent with this, the isoform AUC and proteoform intensity measurements of βTpm were not positively correlated after fiber matching ($r = -0.462$, $P = 0.083$). This methodological discrepancy does not invalidate either measurement, rather it underscores that isoform-level and proteoform-level quantification can capture different aspects of protein expression and should not be assumed interchangeable. Future work should explicitly compare these quantification approaches to determine which more faithfully reflects functionally relevant βTpm abundance.

Exploratory Age-Related Patterns in the Paired Subset

Direct fiber-level comparisons between younger and older fibers added a complementary perspective to the within-fiber correlations. Sarcomeric α-actin was significantly reduced in older fibers (~54% lower; $P = 0.024$), and MLC2F total phosphorylation trended higher with age (~3.6-fold; $P = 0.088$), while several fast-associated isoforms and proteoforms (MLC1F, MLC2F, MLC3F, fsTnC, MLC2F proteoform, pMLC2F) showed non-significant numerical reductions of approximately 24% to 47% in older fibers. The convergence between these direct contrasts and the within-fiber correlations is biologically coherent: the molecular features that tracked higher P_0, V_{max}, and absolute peak power within fibers were also numerically lower in the older subset, where mechanical performance was reduced. The reduction in sarcomeric α-actin is particularly noteworthy because thin-filament protein content directly constrains the number of available cross-bridge attachment sites, providing a plausible structural mechanism for the lower absolute force and power observed in older fibers. Similarly, the trend toward elevated MLC2F total phosphorylation in older fibers is consistent with the negative within-fiber association between MLC2F total phosphorylation and both P_0 and V_{max}, raising the possibility that age-related shifts in regulatory light chain phosphorylation contribute to the contractile phenotype. The non-significance of most other comparisons should not be interpreted as evidence against age-related differences in these proteins, given that the older group included only five fibers and that the confidence intervals for the mean differences encompass biologically meaningful effect sizes. Notably, the present analysis is comparable in scale to prior published top-down proteomics work in skeletal muscle (20).

The pMLC2F findings require careful interpretation because the direction of association depended on how phosphorylation was indexed. Gregorich et al. (2016) showed in aging rat fast-twitch muscle that declining regulatory light-chain phosphorylation was linked to lower force, Ca^{2+} sensitivity, velocity, and power (7). In the present human paired-fiber dataset, absolute pMLC2F abundance was positively associated with absolute peak power and trended positively with normalized peak power, which is directionally compatible with that rodent literature.

At the same time, total MLC2F phosphorylation was negatively associated with P_0 and trended negatively with V_{max}, and Teigen et al. (2020) previously reported no clear age-related difference in human regulatory light-chain phosphorylation (23). Taken together, these observations argue against a simple one-to-one translation of the rodent regulatory-light-chain story to human muscle fibers. Instead, they suggest that the functional meaning of phosphorylation depends on the exact proteoform context, species, fiber phenotype, and analytic level being examined. A positive relationship for the phosphorylated species itself does not necessarily imply that a ratio style total phosphorylation variable will behave identically. This is precisely the type of nuance that intact-proteoform analysis can reveal.

Brocca et al. (2017) and Li et al. (2015) both emphasized that qualitative remodeling of the sarcomeric apparatus can influence function without a simple reduction in myosin quantity (5, 12). The absence of significant molecular correlations with specific force is therefore equally important. In many aging studies, specific force is treated as a central readout of intrinsic contractile quality. Yet in the present paired subset, none of the isoform or proteoform variables significantly tracked specific force.

Several interpretations are possible. The most parsimonious is partly arithmetic, because the absolute isoform abundances were significantly correlated with fiber CSA (r = 0.65–0.70) and P_0 was strongly correlated with CSA (r = 0.759), the CSA-mediated component of the absolute abundance-to-P_0 relationship is removed when force is normalized to CSA. The second interpretation is biological, the molecular features quantified in this fiber subset may modulate absolute force-generating capacity, shortening velocity, and power more strongly than they modulate force normalized to CSA. A third possibility is that SF is determined by additional factors not captured in this assay, such as myofibrillar packing, ultrastructural organization, lattice spacing, oxidative modifications at sites not represented in the quantified proteoforms, or the cumulative effects of habitual activation patterns and physical activity history on myofilament structure in the subject muscle. The present data are consistent with that broader view, but they suggest that the measured qualitative features mapped more cleanly onto absolute contractile function than onto specific force, per se.

The slow-associated signals require careful interpretation because their detection was sparse. Two fibers showed dominant slow-associated troponin signatures, and one additional fiber exhibited a mixed pattern. Some slow-associated light-chain proteoforms were present in only a handful of fibers. As a result, the absence of strong slow-proteoform correlations should not be overinterpreted as evidence that slow-associated biology is unimportant. Rather, the current dataset had limited power to resolve those relationships. Even so, the heatmap is valuable because it demonstrates that the approach can detect mixed molecular phenotypes within individual human fibers after mechanics. This is especially relevant in human muscle, where hybridization and

continuum-like phenotypes are common. In that sense, one of the study's most important methodological messages is that future work should resist overly rigid classification when direct MHC typing is unavailable and instead use multi-marker interpretation.

From a sarcopenia perspective, the present findings support a model in which age-related dysfunction in this selected subset is linked more strongly to molecular determinants of absolute contractile output than to a uniform loss of size-normalized contractile quality. The lower P_0, lower V_{max}, and lower absolute peak power in older subject fibers suggest impairment of both the force and the velocity sides of the power equation. The molecular correlates that emerged most clearly, MLC1F, MLC2F, fsTnC, αTpm, βTpm, and pMLC2F are all plausible contributors to that integrated phenotype. This does not establish causality, but it does prioritize specific targets for future mechanistic studies. In particular, the convergence of light-chain and tropomyosin signals suggests that age-related decline may reflect coordinated remodeling of both thick- and thin-filament regulation rather than a defect confined to a single protein family. These observations also have biomarker implications. Current sarcopenia biomarker frameworks rely largely on circulating, imaging, or whole-muscle signals that are biologically informative but only indirectly connected to the contractile phenotype itself (42). The present pairwise design suggests a complementary strategy in which candidate proteoform markers are prioritized precisely because they covary with force, shortening velocity, or power in the same fiber. In the longer term, such markers could help distinguish mechanistically defined sarcopenic phenotypes, monitor response to

intervention, or inform multi-target therapeutic strategies that combine exercise with molecularly guided treatment (42, 43).

Strengths, Limitations, and Future Directions

Several limitations should be acknowledged explicitly. The most important is sample size. Only fifteen fibers completed both workflows successfully, and effective sample size for some slow-associated features was smaller still. Consequently, rare proteoforms or subtle age-related molecular changes may have been missed, and the age-related patterns reported here should be viewed as hypothesis-generating rather than definitive population-level conclusions. Second, the fibers were selected from a much larger mechanical dataset and were enriched for high-quality higher-power fibers. This proof-of-concept strategy was necessary to ensure mechanically interpretable paired fibers, but it likely underrepresented more compromised fibers and may therefore have attenuated or obscured molecular features associated with lower-performing sarcopenic phenotypes. Third, direct MHC isoform typing was not available for these same fibers. We therefore intentionally avoided definitive fast-versus-slow labeling and relied instead on marker-based interpretation. However, this necessarily leaves ambiguity about canonical fiber classification and limits direct comparison with the extensive literature built around MHC typed human fibers (8, 15). Fourth, two fibers displayed molecular signatures consistent with slow dominant phenotypes (zero αTpm, zero MLC2F, βTpm/total Tpm ratio of 1.0) and functioned as high-leverage observations in several correlations. Post hoc sensitivity analyses indicated that excluding these two fibers weakened or eliminated certain proteoform associations, most notably MLC2F

proteoform vs PPO, pMLC2F vs PPO, and βTpm/total Tpm ratio vs PPO, while other key relationship (αTpm, βTpm, and MLC2F with P_0 and V_{max}) remained significant.

These limitations are balanced by substantial strengths. The study used human tissue, paired contractile and molecular measurements within the same individual fibers, and top-down proteomics capable of resolving intact proteoforms rather than peptide surrogates. It also examined force, velocity, and power together, allowing the molecular data to be interpreted against a richer mechanical phenotype than force alone. Finally, by preserving ambiguity where the data warranted it, most notably regarding fiber typing, the study provides a framework for rigorous interpretation rather than forcing a false precision.

Future work should expand this design in a few directions. Larger studies should pair direct MHC typing with mechanics and proteomics in the same specimen, ideally by mechanically characterizing a fiber and then dividing it (i.e., dissect in half) for complementary top-down proteomics and SDS-PAGE MHC determination so that marker-based inference can be anchored to canonical fiber classification data. Larger subject level designs should use mixed-effects or hierarchical models to partition within- and between-subject variance and determine whether the molecular correlates identified here remain significant after accounting for clustering and relevant covariates. Also, future studies should combine this paired design with emerging higher-throughput single fiber proteomics workflows to increase scale without losing fiber-resolved biological context (22), and should test whether the present signatures are reproducible across broader cohorts that differ in sex, activity, disease status, and muscle group. Finally, intervention studies should determine whether these molecular correlates are

modifiable with resistance training, nutrition, or combined anti-sarcopenic therapies, because that would move them from associative signatures toward actionable therapeutic targets (43). If validated, proteoform-level panels derived from such work could eventually complement existing biomarker strategies by identifying functional sarcopenic endotypes rather than relying exclusively on bulk or circulating measures (42).

Conclusion

In conclusion, pairwise analysis of contractile mechanics and top-down proteomics in the same human single muscle fibers is feasible and biologically informative. In this selected human vastus lateralis subset, aging was associated with lower absolute contractile performance, and multiple isoform/proteoform features associated with faster-contracting phenotypes tracked force, shortening velocity, and power. These findings refine the mechanistic interpretation of age-related single fiber dysfunction by showing that molecular heterogeneity at the intact protein level can be linked directly to contractile phenotype in human muscle. More broadly, they establish a framework for discovering proteoform signatures that are not merely associated with aging but anchored to the specific functional deficits most relevant to sarcopenia.

TABLES AND FIGURES

Table 1. Subject characteristics and mechanical properties of the paired-analysis fiber subset

Variable	Young	Older	Exploratory *P* value
Subjects, *N*	6	4	—
Fibers, *n*	10	5	—
Age, years	28.1 ± 1.8	61.1 ± 3.8	—
Men/Women	3/3	1/3	—
P_0 (mN)	1.27 ± 0.25	0.78 ± 0.20	**0.003**
Specific force ($kN \cdot m^{-2}$)	179.0 ± 39.5	157.2 ± 50.2	0.373
CSA (μm^2)	7428 ± 2109	5482 ± 2469	0.134
V_{max} ($fl \cdot s^{-1}$)	0.75 ± 0.12	0.58 ± 0.08	**0.014**
Absolute peak power ($\mu N \cdot fl \cdot s^{-1}$)	54.8 ± 21.9	34.7 ± 7.6	**0.023**
Normalized peak power ($W \cdot L^{-1}$)	7.72 ± 3.40	7.27 ± 3.22	0.808

Fifteen permeabilized single muscle fibers from ten adults were selected from a larger mechanically tested pool for paired top-down proteomic analysis. Peak isometric force (P_0), specific force, cross-sectional area (CSA), maximum shortening velocity (V_{max}), absolute peak power, and normalized peak power were measured in each fiber prior to proteomic analysis. P values are from exploratory Welch's two-tailed t-tests comparing fibers from younger (*n* = 10 fibers, 6 subjects) and older (*n* = 5 fibers, 4 subjects) groups. Because the paired-analysis subset was small, unbalanced, and purposively enriched for technically successful, higher-power fibers, age-group contrasts should be interpreted as exploratory rather than definitive. Data are presented as the mean ± SD.

Table 2. Isoform marker correlations with single fiber mechanics

Outcome	Isoform Marker	*r*	*P value*	*n*
PPO	MLC1F[a]	0.620	0.014	15
PPO	fsTnI[a]	0.598	0.019	15
PPO	%MLC2F[b] (% of MLCF pool)	0.584	0.022	15
PPO	MLC2F[a]	0.582	0.023	15
PPO	%MLC1F[b] (% of MLCF pool)	-0.581	0.023	15
PPO	fsTnC[a]	0.569	0.027	15
P_0	MLC1F[a]	0.666	0.007	15
P_0	MLC2F[a]	0.630	0.012	15
P_0	fsTnC[a]	0.555	0.032	15
V_{max}	MLC1F[a]	0.747	0.001	15
V_{max}	MLC2F[a]	0.684	0.005	15
V_{max}	fsTnC[a]	0.655	0.008	15
V_{max}	βTpm (AUC)	-0.592	0.020	15
V_{max}	MLC3F[a]	0.584	0.022	15
V_{max}	%MLC1F[b] (% of MLCF pool)	-0.556	0.031	15
V_{max}	%MLC2F[b] (% of MLCF pool)	0.551	0.033	15

[a]Absolute abundance of fast-associated isoforms (MLC1F, MLC2F, MLC3F, fsTnI, fsTnC) were highly intercorrelated ($r > 0.85$) and correlated with CSA ($r = 0.65–0.70$), reflecting a shared fast-phenotype signal.

[b]%MLC1F and %MLC2F were nearly perfectly anti-correlated ($r = -0.995$) due to the small, invariant fraction of %MLC3F (~4%), these represent complementary expressions of the same compositional signal, not independent predictors.

Table 3. Proteoform marker correlations with single fiber mechanics

Outcome	Proteoform Marker	*r*	*P* value	*n*
PPO	αTpm	0.738	0.002	15
PPO	MLC2F	0.667	0.007	15
PPO	pMLC2F	0.621	0.013	15
PPO	βTpm / Total Tpm Ratio	-0.532	0.041	15
P_0	βTpm	0.687	0.005	15
P_0	MLC2F	0.582	0.023	15
P_0	αTpm	0.575	0.025	15
P_0	MLC2F Total Phosphorylation	-0.553	0.033	15
V_{max}	βTpm	0.667	0.007	15
V_{max}	MLC2F	0.655	0.008	15
V_{max}	αTpm	0.653	0.008	15

Proteoform quantification used deconvoluted peak intensity (see Methods). βTpm at this level was positively associated with P_0 and V_{max}; note that isoform-level βTpm (quantified by AUC) showed the opposite direction with V_{max}, attributable to the different quantification methods (see Discussion).

Table 4. Direct comparisons of isoform and proteoform abundance between younger and older fibers in the paired-analysis subset

Variable	Younger (*n* = 10)	Older (*n* = 5)	Mean difference (95% CI)	*P* value
MLC1F	12.92	8.92	-4.00 (-10.69, 2.69)	0.218
MLC2F	9.49	5.98	-3.51 (-10.02, 3.01)	0.266
MLC3F	1.03	0.55	-0.48 (-1.20, 0.24)	0.176
fsTnC	0.83	0.54	-0.29 (-0.82, 0.25)	0.267
sa-actin	2.14	0.98	-1.16 (-2.14, -0.18)	**0.024**
pMLC2F proteoform	1.37	1.04	-0.34 (-1.52, 0.85)	0.551
MLC2F total phosphorylation	0.027	0.098	+0.071 (-0.012, 0.154)	0.088

Values shown are fiber-level mean abundances within each age group. Isoform abundances are reported as extracted ion chromatogram area-under-the-curve values (arbitrary units), proteoform abundances are reported as deconvoluted peak intensities (arbitrary units), and total phosphorylation is reported as a unitless ratio. Comparisons were performed using unpaired two-tailed t-tests. Bold values indicate statistical significance ($P < 0.05$). Mean difference is presented as older minus younger; negative values indicate lower abundance in older fibers.

Figure 1. Exploratory mechanical profile of the paired-analysis fiber subset

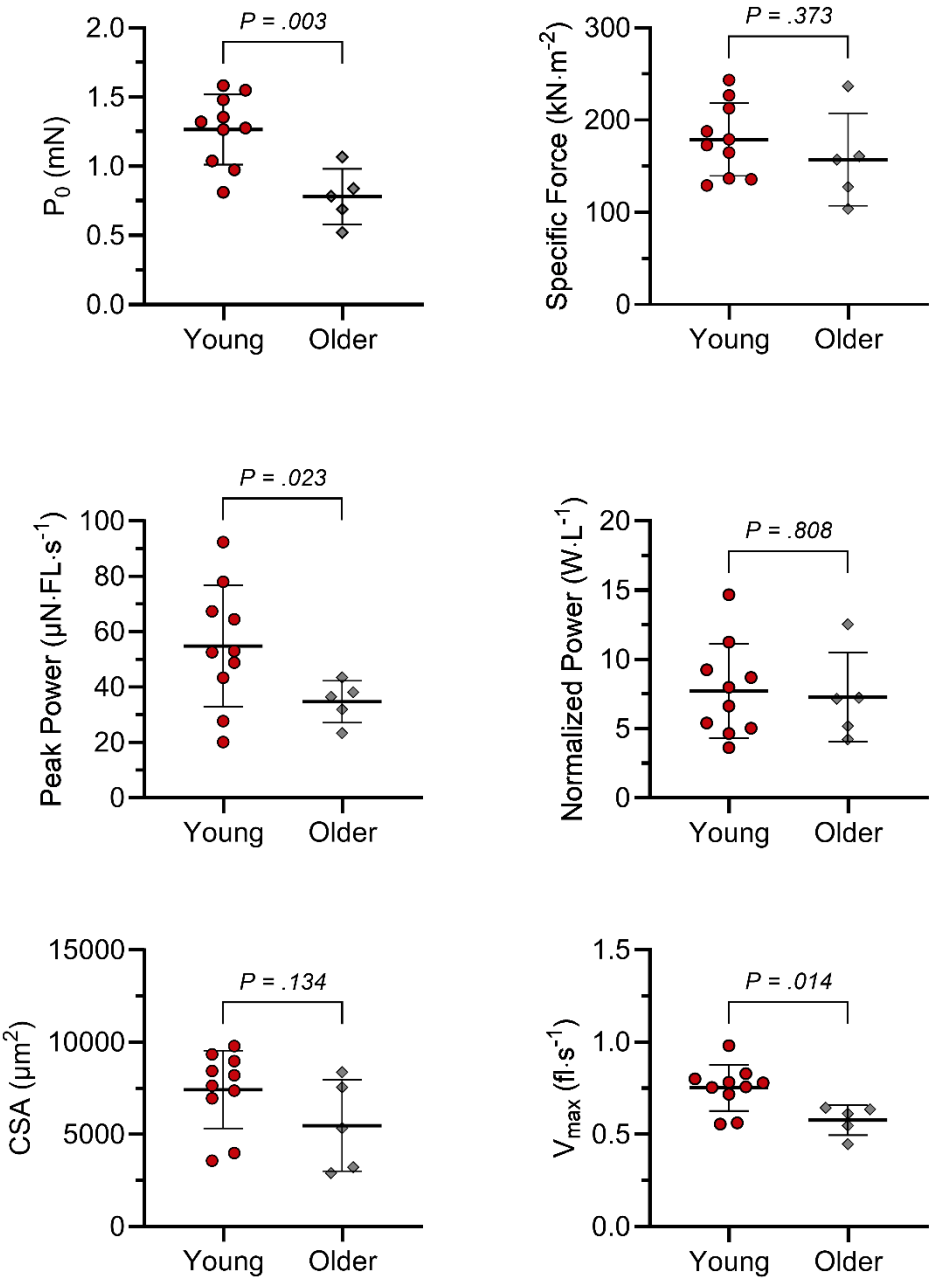

Figure 1. Exploratory mechanical profile of the paired-analysis fiber subset. Contractile properties of the 15 fibers selected for paired mechanical and top-down proteomic analysis, grouped by subject age category. Older-subject fibers exhibited lower peak isometric force (P_0), maximal shortening velocity (V_{max}), and absolute peak power, whereas specific force, cross-sectional area (CSA), and normalized peak power were comparatively preserved. Symbols represent individual fibers; horizontal bars indicate mean ± SD. Exact P values are shown for exploratory fiber-level comparisons.

Figure 2. Relative isoform and proteoform marker landscape of the analyzed fibers

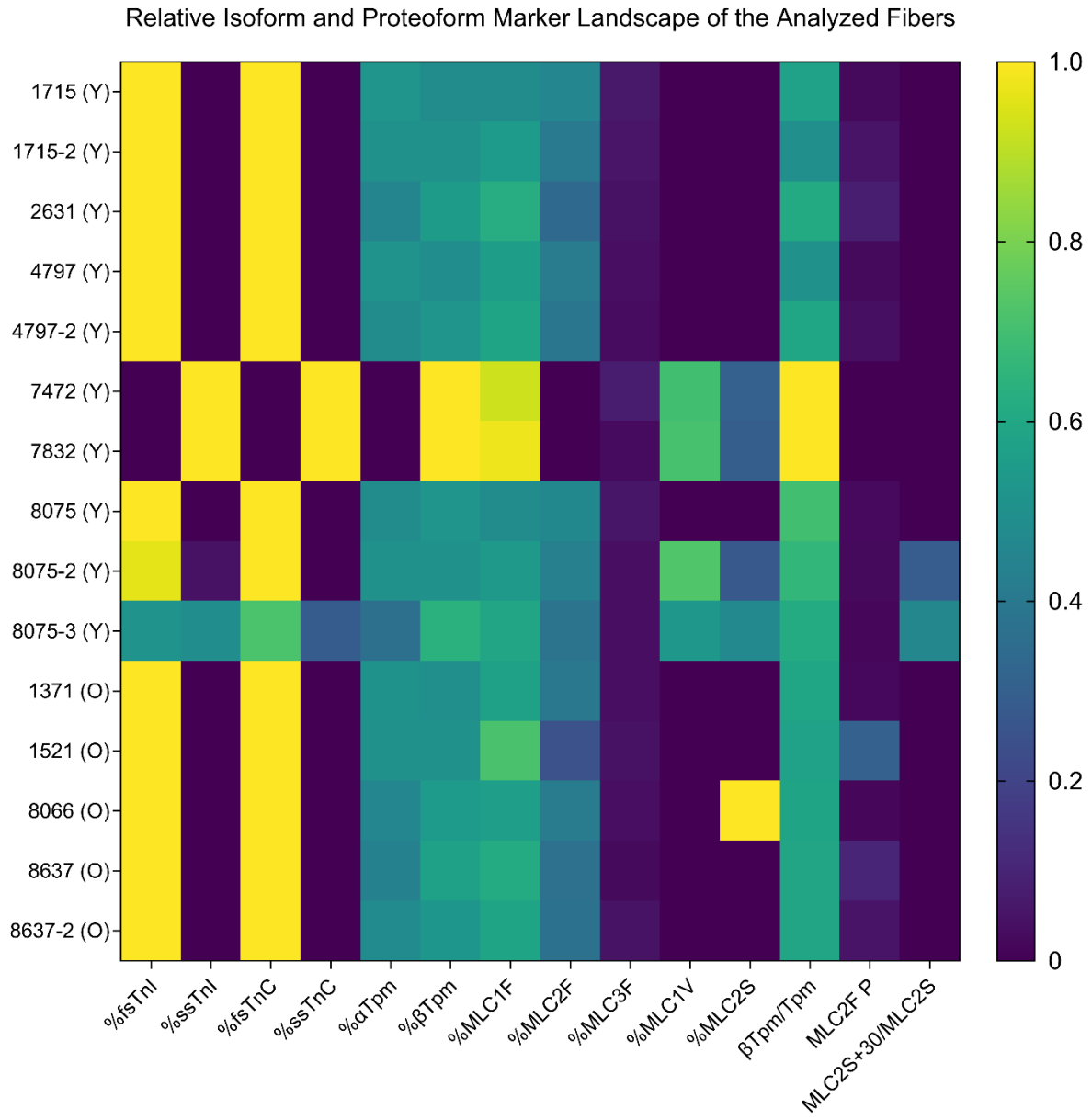

Figure 2. Relative isoform and proteoform landscape of the paired-analysis fibers. Heatmap showing the relative abundance of selected molecular markers across the 15 mechanically tested fibers that underwent top-down proteomic analysis. Rows represent individual fibers and columns represent isoform- or proteoform-level variables associated with faster- or slower-contracting phenotypes, including troponin, tropomyosin, and myosin light-chain features. Values are displayed after within-variable normalization to highlight relative between-fiber heterogeneity. The analyzed subset was enriched for fast-associated markers, but several fibers exhibited mixed molecular profiles.

Figure 3. Representative pairwise correlations between molecular features and single-fiber mechanics

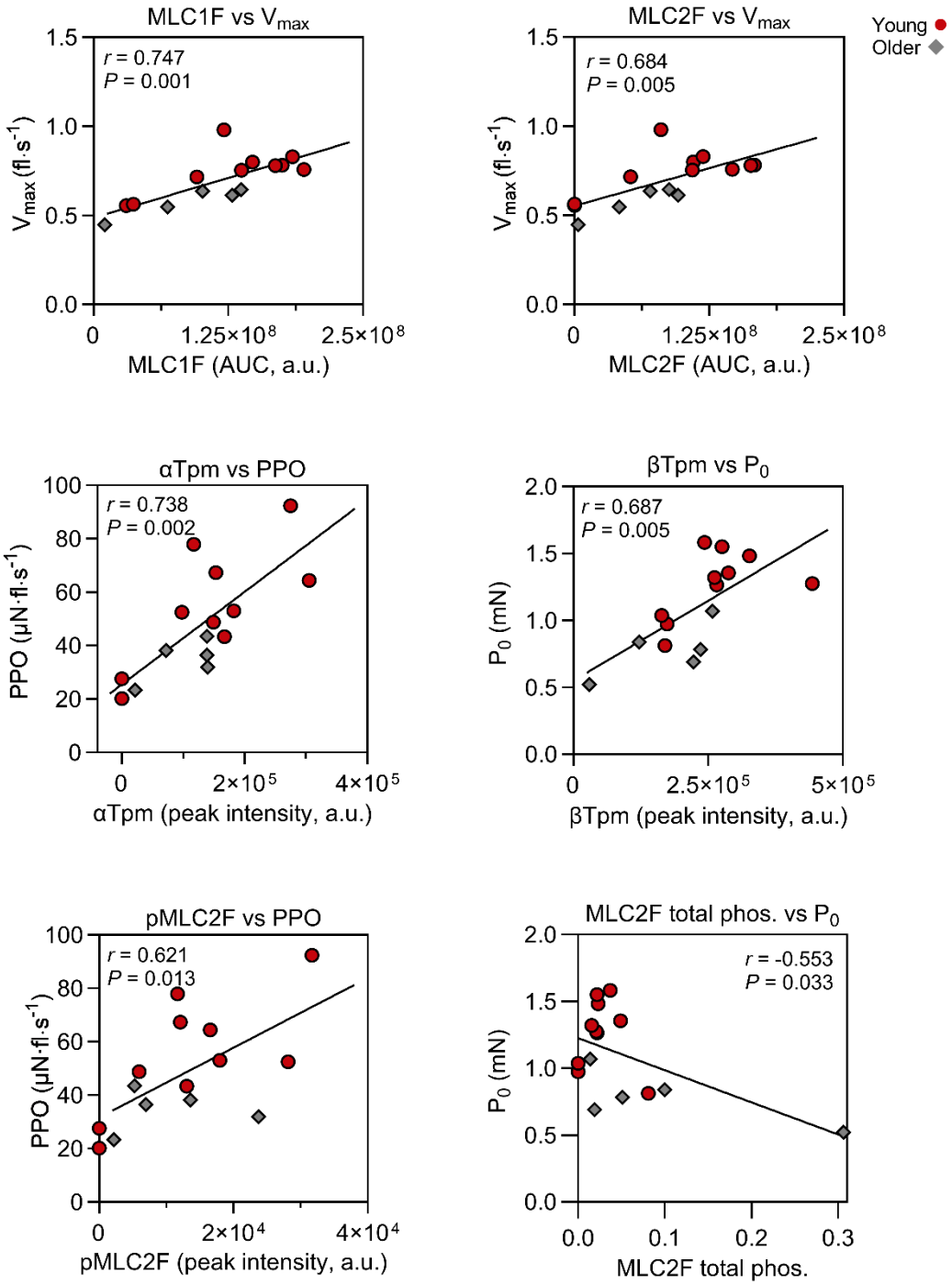

Figure 3. Representative pairwise correlations between molecular features and single muscle fiber contractile properties. Scatterplots showing significant Pearson correlations between selected isoform- and proteoform-level variables and single fiber mechanics across the paired-analysis subset (n = 15 fibers).

Figure 4. Direct comparisons of selected isoform and proteoform abundances between younger and older fibers.

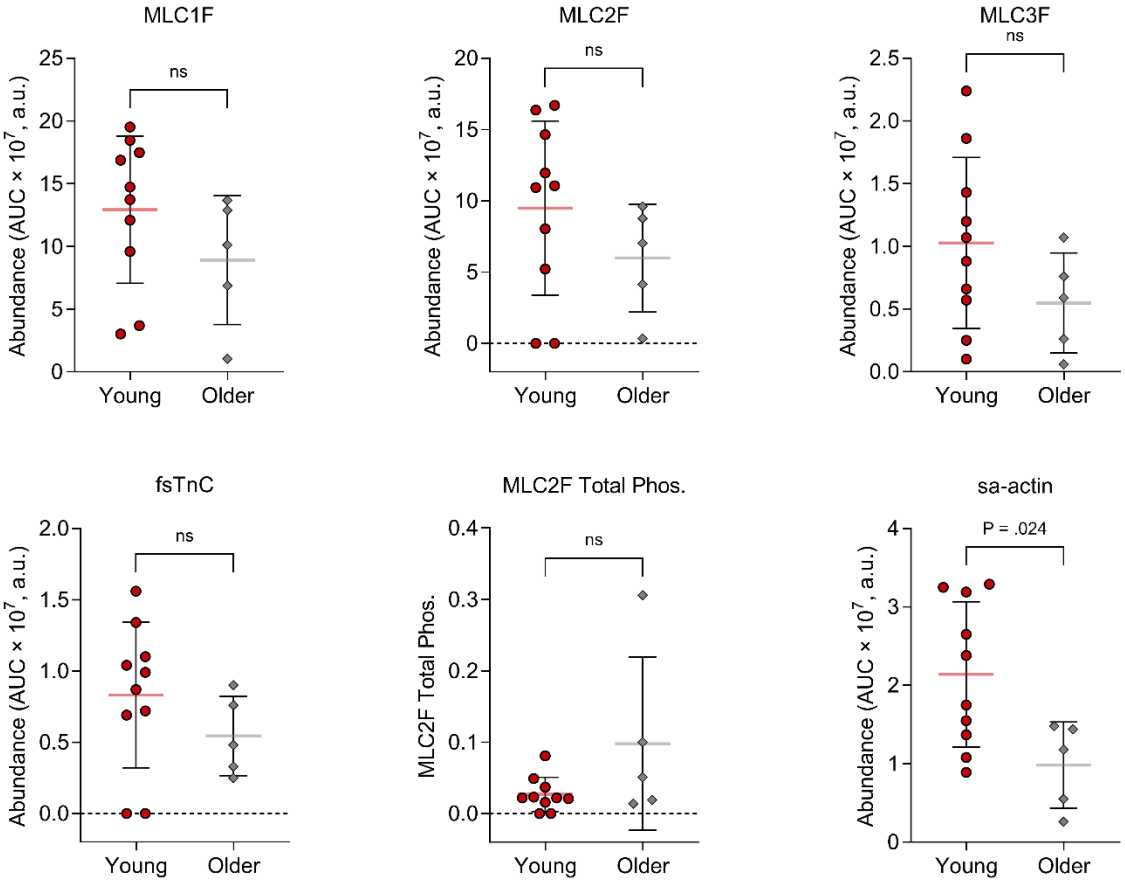

Figure 4. Direct comparisons of selected isoform and proteoform abundances between younger and older fibers. Exploratory fiber-level comparisons of selected fast-associated isoforms and proteoforms between fibers from younger (*n* = 10) and older (*n* = 5) subjects in the paired-analysis subset. Panels include MLC1F, MLC2F, MLC3F, fsTnC, MLC2F total phosphorylation, and sarcomeric α-actin (sa-actin). Symbols represent individual fibers; horizontal bars indicate mean ± SD. Exact *P* values are shown.

REFERENCES

1. **Cruz-Jentoft AJ, Bahat G, Bauer J, Boirie Y, Bruyère O, Cederholm T, Cooper C, Landi F, Rolland Y, Sayer AA, Schneider SM, Sieber CC, Topinkova E, Vandewoude M, Visser M, Zamboni M, Writing Group for the European Working Group on Sarcopenia in Older People 2 (EWGSOP2) and the EG for E.** Sarcopenia: revised European consensus on definition and diagnosis. *Age and Ageing* 48: 16–31, 2019. doi: 10.1093/ageing/afy169.

2. **Reid KF, Fielding RA.** Skeletal Muscle Power: A Critical Determinant of Physical Functioning in Older Adults. *Exercise and Sport Sciences Reviews* 40: 4–12, 2012. doi: 10.1097/JES.0b013e31823b5f13.

3. **Grosicki GJ, Zepeda CS, Sundberg CW.** Single muscle fibre contractile function with ageing. *The Journal of Physiology* 600: 5005–5026, 2022. doi: 10.1113/JP282298.

4. **Ochala J, Frontera WR, Dorer DJ, Hoecke JV, Krivickas LS.** Single Skeletal Muscle Fiber Elastic and Contractile Characteristics in Young and Older Men. *The Journals of Gerontology: Series A* 62: 375–381, 2007. doi: 10.1093/gerona/62.4.375.

5. **Brocca L, McPhee JS, Longa E, Canepari M, Seynnes O, De Vito G, Pellegrino MA, Narici M, Bottinelli R.** Structure and function of human muscle fibres and muscle proteome in physically active older men. *The Journal of Physiology* 595: 4823–4844, 2017. doi: 10.1113/JP274148.

6. **Lin Z, Wei L, Cai W, Zhu Y, Tucholski T, Mitchell SD, Guo W, Ford SP, Diffee GM, Ge Y**. Simultaneous Quantification of Protein Expression and Modifications by Top-down Targeted Proteomics: A Case of the Sarcomeric Subproteome. *Mol Cell Proteomics* 18: 594–605, 2019. doi: 10.1074/mcp.TIR118.001086.

7. **Gregorich ZR, Peng Y, Cai W, Jin Y, Wei L, Chen AJ, McKiernan SH, Aiken JM, Moss RL, Diffee GM, Ge Y.** Top-Down Targeted Proteomics Reveals Decrease in Myosin Regulatory Light-Chain Phosphorylation That Contributes to Sarcopenic Muscle Dysfunction. *J Proteome Res* 15: 2706–2716, 2016. doi: 10.1021/acs.jproteome.6b00244.

8. **Murgia M, Toniolo L, Nagaraj N, Ciciliot S, Vindigni V, Schiaffino S, Reggiani C, Mann M.** Single Muscle Fiber Proteomics Reveals Fiber-Type-Specific Features of Human Muscle Aging. *Cell Reports* 19: 2396–2409, 2017. doi: 10.1016/j.celrep.2017.05.054.

9. **D'Antona G, Pellegrino MA, Adami R, Rossi R, Carlizzi CN, Canepari M, Saltin B, Bottinelli R.** The effect of ageing and immobilization on structure and function of human skeletal muscle fibres. *The Journal of Physiology* 552: 499–511, 2003. doi: https://doi.org/10.1111/j.1469-7793.2003.00499.x.

10. **Trappe S, Gallagher P, Harber M, Carrithers J, Fluckey J, Trappe T.** Single Muscle Fibre Contractile Properties in Young and Old Men and Women. *The Journal of Physiology* 552: 47–58, 2003. doi: 10.1113/jphysiol.2003.044966.

11. **Prochniewicz E, Thompson LV, Thomas DD.** Age-Related Decline in Actomyosin Structure and Function. *Exp Gerontol* 42: 931–938, 2007. doi: 10.1016/j.exger.2007.06.015.

12. **Li M, Ogilvie H, Ochala J, Artemenko K, Iwamoto H, Yagi N, Bergquist J, Larsson L.** Aberrant post-translational modifications compromise human myosin motor function in old age. *Aging Cell* 14: 228–235, 2015. doi: 10.1111/acel.12307.

13. **Bottinelli R, Schiaffino S, Reggiani C.** Force-velocity relations and myosin heavy chain isoform compositions of skinned fibres from rat skeletal muscle. *The Journal of Physiology* 437: 655–672, 1991. doi: 10.1113/jphysiol.1991.sp018617.

14. **Bottinelli R, Canepari M, Pellegrino MA, Reggiani C.** Force-velocity properties of human skeletal muscle fibres: myosin heavy chain isoform and temperature dependence. *The Journal of Physiology* 495: 573–586, 1996. doi: 10.1113/jphysiol.1996.sp021617.

15. **Schiaffino S, Reggiani C**. Fiber Types in Mammalian Skeletal Muscles. *Physiological Reviews* 91: 1447–1531, 2011. doi: 10.1152/physrev.00031.2010.

16. **Schiaffino S, Chemello F, Reggiani C.** The Diversity of Skeletal Muscle Fiber Types. *Cold Spring Harb Perspect Biol* 17: a041477, 2025. doi: 10.1101/cshperspect.a041477.

17. **Toby TK, Fornelli L, Kelleher NL.** Progress in Top-Down Proteomics and the Analysis of Proteoforms. *Annu Rev Anal Chem (Palo Alto Calif)* 9: 499–519, 2016. doi: 10.1146/annurev-anchem-071015-041550.

18. **Brown KA, Melby JA, Roberts DS, Ge Y.** Top-down Proteomics: Challenges, Innovations, and Applications in Basic and Clinical Research. *Expert Rev Proteomics* 17: 719–733, 2020. doi: 10.1080/14789450.2020.1855982.

19. **Wei L, Gregorich ZR, Lin Z, Cai W, Jin Y, McKiernan SH, McIlwain S, Aiken JM, Moss RL, Diffee GM, Ge Y.** Novel Sarcopenia-related Alterations in Sarcomeric Protein Post-translational Modifications (PTMs) in Skeletal Muscles Identified by Top-down Proteomics. *Mol Cell Proteomics* 17: 134–145, 2018. doi: 10.1074/mcp.RA117.000124.

20. **Melby JA, Brown KA, Gregorich ZR, Roberts DS, Chapman EA, Ehlers LE, Gao Z, Larson EJ, Jin Y, Lopez JR, Hartung J, Zhu Y, McIlwain SJ, Wang D, Guo W, Diffee GM, Ge Y.** High sensitivity top–down proteomics captures single muscle cell heterogeneity in large proteoforms. *Proceedings of the National Academy of Sciences* 120: e2222081120, 2023. doi: 10.1073/pnas.2222081120.

21. **Wilson MC, Gao Z, Lopez JR, Zhu Y, Olszewski SS, Konopka AR, Diffee GM, Ge Y.** Top–Down Proteomics of Skinned Human Muscle Fibers Reveals Proteoform-Resolved Fiber-to-Fiber Variability. *Journal of Mass Spectrometry* 61: e70040, 2026. doi: 10.1002/jms.70040.

22. **Momenzadeh A, Jiang Y, Kreimer S, Teigen LE, Zepeda CS, Haghani A, Mastali M, Song Y, Hutton A, Parker SJ, Van Eyk JE, Sundberg CW, Meyer JG.** A Complete Workflow for High Throughput Human Single Skeletal Muscle Fiber Proteomics. *J Am Soc Mass Spectrom* 34: 1858–1867, 2023. doi: 10.1021/jasms.3c00072.

23. **Teigen LE, Sundberg CW, Kelly LJ, Hunter SK, Fitts RH.** Ca2+ dependency of limb muscle fiber contractile mechanics in young and older adults. *Am J Physiol Cell Physiol* 318: C1238–C1251, 2020. doi: 10.1152/ajpcell.00575.2019.

24. **Fabiato A.** Computer programs for calculating total from specified free or free from specified total ionic concentrations in aqueous solutions containing multiple metals and ligands. In: *Methods in Enzymology*. Elsevier, p. 378–417.

25. **Moss RL.** Sarcomere length-tension relations of frog skinned muscle fibres during calcium activation at short lengths. *J Physiol* 292: 177–192, 1979. doi: 10.1113/jphysiol.1979.sp012845.

26. **Schneider CA, Rasband WS, Eliceiri KW.** NIH Image to ImageJ: 25 years of image analysis. *Nat Methods* 9: 671–675, 2012. doi: 10.1038/nmeth.2089.

27. Edman KA. The velocity of unloaded shortening and its relation to sarcomere length and isometric force in vertebrate muscle fibres. *The Journal of Physiology* 291: 143–159, 1979. doi: 10.1113/jphysiol.1979.sp012804.

28. **Trappe S, Williamson D, Godard M, Porter D, Rowden G, Costill D.** Effect of resistance training on single muscle fiber contractile function in older men. *Journal of Applied Physiology* 89: 143–152, 2000. doi: 10.1152/jappl.2000.89.1.143.

29. **Trappe S, Godard M, Gallagher P, Carroll C, Rowden G, Porter D.** Resistance training improves single muscle fiber contractile function in older women. *American Journal of Physiology-Cell Physiology* 281: C398–C406, 2001. doi: 10.1152/ajpcell.2001.281.2.C398.

30. **Hill AV.** The heat of shortening and the dynamic constants of muscle. *Proc R Soc Lond B* 126: 136–195, 1938. doi: 10.1098/rspb.1938.0050.

31. **Sundberg CW, Teigen LE, Hunter SK, Fitts RH.** Cumulative effects of H+ and Pi on force and power of skeletal muscle fibres from young and older adults. *The Journal of Physiology* 603: 187–209, 2025. doi: 10.1113/JP286938.

32. **Widrick JJ, Trappe SW, Costill DL, Fitts RH.** Force-velocity and force-power properties of single muscle fibers from elite master runners and sedentary men. *Am J Physiol* 271: C676-683, 1996. doi: 10.1152/ajpcell.1996.271.2.C676.

33. **Harber MP, Konopka AR, Undem MK, Hinkley JM, Minchev K, Kaminsky LA, Trappe TA, Trappe S.** Aerobic exercise training induces skeletal muscle hypertrophy and age-dependent adaptations in myofiber function in young and older men. *Journal of Applied Physiology* 113: 1495–1504, 2012. doi: 10.1152/japplphysiol.00786.2012.

34. **Wilson MC, Josvai M, Walters JK, Lawson J, Rossler KJ, Gao Z, Zhu Y, Kamp TJ, Crone WC, Eckhardt LL, Ge Y.** High-Sensitivity Top-Down Proteomics Reveals Enhanced Maturation of Micropatterned Induced Pluripotent Stem Cell-Derived Cardiomyocytes. *J Proteome Res* 24: 4335–4343, 2025. doi: 10.1021/acs.jproteome.5c00505.

35. **Ramirez-Sagredo A, Sunny AT, Cupp-Sutton KA, Chowdhury T, Zhao Z, Wu S, Chiao YA.** Characterizing age-related changes in intact mitochondrial proteoforms in murine hearts using quantitative top-down proteomics. *Clin Proteom* 21: 57, 2024. doi: 10.1186/s12014-024-09509-1.

36. **Rossler KJ, Lange WJ de, Mann MW, Aballo TJ, Melby JA, Zhang J, Kim G, Bayne EF, Zhu Y, Farrell ET, Kamp TJ, Ralphe JC, Ge Y.** Lactate- and immunomagnetic-purified hiPSC–derived cardiomyocytes generate comparable engineered cardiac tissue constructs. *JCI Insight* 9, 2024. doi: 10.1172/jci.insight.172168.

37. **Melby JA, de Lange WJ, Zhang J, Roberts DS, Mitchell SD, Tucholski T, Kim G, Kyrvasilis A, McIlwain SJ, Kamp TJ, Ralphe JC, Ge Y.** Functionally Integrated Top-Down Proteomics for Standardized Assessment of Human Induced Pluripotent Stem Cell-Derived Engineered Cardiac Tissues. *J Proteome Res* 20: 1424–1433, 2021. doi: 10.1021/acs.jproteome.0c00830.

38. **Zhong S, Thompson LV.** The roles of myosin ATPase activity and myosin light chain relative content in the slowing of type IIB fibers with hindlimb unweighting in rats. *American Journal of Physiology-Cell Physiology* 293: C723–C728, 2007. doi: 10.1152/ajpcell.00009.2007.

39. **Hvid LG, Ørtenblad N, Aagaard P, Kjaer M, Suetta C.** Effects of ageing on single muscle fibre contractile function following short-term immobilisation. *The Journal of Physiology* 589: 4745–4757, 2011. doi: 10.1113/jphysiol.2011.215434.

40. **Sundberg CW, Hunter SK, Trappe SW, Smith CS, Fitts RH.** Effects of elevated H+ and Pi on the contractile mechanics of skeletal muscle fibres from young and old men: implications for muscle fatigue in humans. *The Journal of Physiology* 596: 3993–4015, 2018. doi: 10.1113/JP276018.

41. **Bottinelli R, Reggiani C.** Force-velocity properties and myosin light chain isoform composition of an identified type of skinned fibres from rat skeletal muscle. *Pflugers Arch* 429: 592–594, 1995. doi: 10.1007/BF00704166.

42. **Kalinkovich A, Livshits G.** Sarcopenia--The search for emerging biomarkers. *Ageing Res Rev* 22: 58–71, 2015. doi: 10.1016/j.arr.2015.05.001.

43. **Dent E, Morley JE, Cruz-Jentoft AJ, Arai H, Kritchevsky SB, Guralnik J, Bauer JM, Pahor M, Clark BC, Cesari M, Ruiz J, Sieber CC, Aubertin-Leheudre M, Waters DL, Visvanathan R, Landi F, Villareal DT, Fielding R, Won CW, Theou O, Martin FC, Dong B, Woo J, Flicker L, Ferrucci L, Merchant RA, Cao L, Cederholm T, Ribeiro SML, Rodríguez-Mañas L, Anker SD, Lundy J, Gutiérrez Robledo LM, Bautmans I, Aprahamian I, Schols JMGA, Izquierdo M, Vellas B.** International Clinical Practice Guidelines for Sarcopenia (ICFSR): Screening, Diagnosis and Management. *J Nutr Health Aging* 22: 1148–1161, 2018. doi: 10.1007/s12603-018-1139-9.

CHAPTER V

Summary and Conclusions

The central premise of this dissertation was that age-related muscle dysfunction reflects integrated impairments across biological scales, such that whole-muscle contractile deficits are linked to fiber-type-specific alterations in single muscle fiber mechanics, and those cellular deficits are in turn associated with molecular changes within the sarcomeric contractile apparatus. To test this premise, a multiscale experimental approach was employed in younger and older men and women, combining whole-muscle knee extensor function and body composition testing, fiber-type-stratified single muscle fiber mechanical experiments from the vastus lateralis, and paired top-down proteomic characterization of the same individual fibers that had completed mechanical testing. The three experimental chapters addressed this premise in sequence, progressing from the cellular phenotype (Chapter II) to its translation to whole-muscle function (Chapter III), and finally to its molecular correlates (Chapter IV).

Summary of Principal Findings

Aim 1 (Chapter II) identified age-related, fiber-type-specific alterations in single muscle fiber contractile properties. Peak power was approximately 32% lower in older adults in both Type I and Type II fibers, demonstrating that cellular power loss was not restricted to fast fibers alone. This reduction in power was not attributable to slower shortening velocity, as V_{max} was preserved with aging in both fiber types, indicating instead that impaired force generation was the primary driver of the deficit. The nature of the force impairment differed by fiber type. Older Type I fibers exhibited lower peak isometric force despite preserved specific force, consistent with a modest reduction in absolute force without clear evidence of intrinsic dysfunction. In contrast, older Type II fibers exhibited lower specific force and lower normalized power, which together

indicate impaired intrinsic contractile function. Notably, and contrary to the original hypothesis, aging was not associated with a significant reduction in Type II fiber cross-sectional area in this cohort. Thus, Type II deficits emerged in the absence of meaningful atrophy, providing direct evidence that intrinsic impairments in muscle quality can develop independently of fiber size. Chapter II therefore established that Type I fibers were not uniformly protected from age-related decline and that Type II fibers can exhibit intrinsic contractile impairment without measurable atrophy.

Aim 2 (Chapter III) determined the relationship between single muscle fiber contractile properties and whole-muscle knee extensor function and composition and identified the cellular contributors to age-related whole-muscle dysfunction. Type II fiber force, power, and size emerged as the principal cellular correlates of whole-muscle performance, while Type I fiber associations were weaker and largely explained by shared age-related decline. Whole-muscle peak power was the functional outcome most tightly coupled to Type II fiber mechanics and was the functional outcome at which aging modified the cellular-to-whole-muscle relationship, with the slopes of the Type II P_0–peak power and Type II CSA–peak power relationships attenuated approximately 4- to 8-fold in older adults compared to younger adults, indicating that the translation from fiber to muscle is itself altered with age, not merely the inputs to that translation. Critically, the absolute Type II properties (peak power, peak force, and cross-sectional area) retained independent predictive value after adjustment for age, demonstrating a genuine cellular contribution to whole-muscle function that cannot be dismissed as shared age-related covariation. Thigh lean mass was a meaningful contributor to absolute whole-muscle outputs, as expected, but did not supplant the independent

contribution of Type II fiber properties. Chapter III therefore provided a novel paired demonstration in humans that Type II single fiber mechanics translate to whole-muscle function across the age span, and that this translation is modified by aging.

Aim 3 (Chapter IV) identified molecular features of the sarcomeric proteome associated with single muscle fiber contractile properties, using top-down proteomics performed on the exact same fibers that had completed mechanical experiments. To our knowledge, this represented the first paired molecular-mechanical analysis of individual human muscle fibers. At the isoform level, the fast-associated regulatory proteins MLC1F, MLC2F, and fsTnC were strongly and positively correlated with maximal shortening velocity, with MLC1F exhibiting the strongest single relationship. These isoforms were highly intercorrelated, indicating that they reflect a shared fast-phenotype signal rather than independent molecular predictors of velocity. At the proteoform level, α-tropomyosin showed the strongest positive association with absolute peak power, whereas the β-tropomyosin to total tropomyosin ratio was negatively associated with peak power, a pattern consistent with the interpretation that tropomyosin isoform balance serves as a molecular readout of fiber phenotype along the fast-slow continuum, with slower, β-dominant fibers producing less power. MLC2F proteoform abundance and phosphorylated MLC2F were also positively associated with absolute peak power, consistent with the regulatory role of light-chain phosphorylation in modulating cross-bridge kinetics (2).

Direct fiber-level comparisons between younger and older fibers identified sarcomeric α-actin as significantly reduced in older fibers (~54% lower; $P = 0.024$), with non-significant but directionally consistent reductions in several fast-associated

isoforms, providing preliminary evidence that age-related reductions in thin-filament contractile protein content accompany the fiber-level impairments documented in Chapter II. Together, these results identified specific molecular features of the sarcomeric proteome, including fast regulatory light-chain and troponin isoform composition and tropomyosin proteoform balance, that track with contractile function at the single-fiber level. Notably, the measured molecular features mapped more clearly onto absolute force, shortening velocity, and power than onto specific force, thereby providing a molecular footing for understanding the cellular impairments documented in Chapters II III.

Integrated Synthesis Across Biological Scales

Taken together, the three experimental chapters of this dissertation support the central premise that age-related muscle dysfunction is an integrated, multiscale phenomenon that cannot be explained by any single level of biological organization in isolation. Whole-muscle deficits in the older adults of this cohort were not attributable to muscle mass alone, and the cellular chapters revealed why. At the single-fiber level, these functional deficits were mirrored by reduced cellular power output, and in Type II fibers they occurred without significant atrophy, localizing an important portion of age-related dysfunction to impaired intrinsic contractile function rather than to simple atrophy of the fiber. (Chapter II). At the whole-muscle level, those Type II fiber deficits tracked with knee extensor peak power, and the cellular-to-whole-muscle scaling itself was altered with age, meaning that the same unit of Type II fiber function did not produce the same unit of whole-muscle output in older adults as in younger ones (Chapter III). At the molecular level, isoform composition and proteoform balance of the regulatory thin-

filament and light-chain proteins were associated with fiber mechanics in ways that map onto the fast-slow phenotype continuum and implicate the sarcomere as the center of intrinsic dysfunction (Chapter IV). The unifying picture is one in which age-related whole-muscle dysfunction cannot be explained by any single scale of biological organization in isolation, and in which Type II fiber mechanics and the sarcomeric proteoforms that shape them stand out as inviting targets for studies designed to establish causality linking cellular dysfunction to clinical functional decline.

A secondary but consequential contribution of this work is methodological. The paired design of Chapters III and IV matching single fiber mechanics to whole-muscle function in the same individuals, and matching molecular to mechanical phenotypes in the same individual fibers addressed a longstanding limitation of the aging muscle literature, in which cellular, whole-muscle, and molecular findings have largely accumulated in parallel rather than being linked within participants. The proteoform-level findings in particular demonstrate that top-down proteomics at single-fiber resolution is feasible in human aging studies and that it yields information about regulatory protein balance that is not accessible through bottom-up approaches or MHC-based fiber typing alone (3, 4).

The integrated picture that emerges is one in which age-related whole-muscle dysfunction reflects the combined influence of structural, cellular, and molecular factors, with Type II fiber mechanics occupying a central linking role between sarcomeric biology and whole-muscle function. The findings further indicate that intrinsic dysfunction can develop in the absence of overt atrophy and that age-related decline in whole-muscle performance reflects not only reduced cellular contractile capacity, but

also altered translation of cellular function to muscle-level output. In this framework, the sarcomeric contractile apparatus is not simply a downstream consequence of aging muscle dysfunction; it is a mechanistically meaningful site at which age-related impairment is expressed.

Contributions to Knowledge

This dissertation makes several contributions to the study of human skeletal muscle aging. First, it demonstrates that age-related cellular power deficits are not restricted to Type II fibers alone, as older adults exhibited lower peak power in both Type I and Type II fibers. Second, it shows that intrinsic Type II contractile dysfunction can occur in the absence of significant fiber atrophy, thereby strengthening the case that muscle quality declines independently of muscle size in healthy aging. Third, it provides an integrated human demonstration that Type II single-fiber mechanics are the principal cellular correlates of whole-muscle performance and that these associations persist beyond shared age-related decline. Fourth, it shows that the cellular-to-whole-muscle relationship itself is altered with aging, particularly for whole-muscle peak power. Finally, it establishes the feasibility of paired top-down proteomics and contractile mechanics in the same human single fibers and identifies candidate sarcomeric isoform and proteoform features associated with force, shortening velocity, and power. Together, these contributions move the field from parallel descriptions at separate biological scales toward a more integrated mechanistic account of age-related muscle dysfunction.

Limitations

Several limitations should be acknowledged. First, the cohort studied across the experimental chapters was modest in size, which constrained precision for subgroup analyses, particularly those stratified by sex. Second, the older adults were healthy and community-dwelling, and the findings may not generalize to frail, mobility-limited, or clinically sarcopenic populations in whom atrophy and whole-muscle dysfunction may be more advanced. Third, the molecular analysis in Chapter IV was performed on a small subset of 15 fibers selected from a larger mechanically tested pool, and direct myosin heavy chain typing was not available for those same fibers, requiring interpretation of phenotype from other molecular markers. Fourth, the dissertation was cross-sectional in design, which limits inference regarding the temporal ordering through which molecular, cellular, and whole-muscle deficits develop. Finally, although the paired and multiscale design is a major strength, the observational nature of the work does not establish causality; rather, it identifies mechanistically plausible associations that now require targeted experimental testing.

Future Directions

The integrated findings reported here motivate several lines of future work. First, the observation that Type II intrinsic dysfunction can occur without significant atrophy suggests that interventions targeting muscle function, rather than muscle mass alone, may yield meaningful functional benefits in older adults. Direct comparisons of the cellular and molecular responses of aging muscle to resistance training, power training, nutritional strategies, and pharmacological interventions therefore represent a logical next step. Second, the paired molecular-mechanical approach developed in Chapter IV

should be extended to a larger number of fibers with direct MHC typing, enabling formal age-group comparisons at the proteoform level and permitting tests of whether specific proteoform signatures precede overt mechanical deficits. Third, the integrated design should be expanded longitudinally so that whole-muscle, single-fiber, and proteoform-level measurements can be followed within the same participants over time, enabling the temporal ordering of decline to be established. Fourth, future work should determine whether the sarcomeric features identified here, including regulatory light-chain state and tropomyosin proteoform balance, are modifiable with intervention and whether they can serve as mechanistically meaningful biomarkers of functional aging (5, 6). More broadly, the multiscale framework developed in this dissertation provides a platform for testing whether distinct molecular and cellular endotypes of sarcopenia exist and whether those endotypes differ in prognosis or treatment responsiveness.

Conclusion

In summary, this dissertation demonstrates that age-related muscle dysfunction in healthy older adults is an integrated, multiscale phenomenon in which cellular, whole-muscle, and molecular impairments are meaningfully linked. Single muscle fiber contractile dysfunction, particularly in Type II fibers, contributed to whole-muscle performance deficits independently of muscle size, and candidate molecular features of the sarcomeric proteome tracked force, shortening velocity, and power at the fiber level. By linking whole-muscle, cellular, and molecular measurements within the same individuals and, in the case of Chapter IV, within the same individual fibers, this work provides an integrated mechanistic framework for understanding aging muscle that moves beyond any single level of organization. More broadly, it identifies the

sarcomere, and especially the Type II fiber contractile phenotype and its molecular regulators, as a promising focal point for future work aimed at understanding and ultimately mitigating the functional consequences of sarcopenia.

REFERENCES

1. **Grosicki GJ**, **Zepeda CS**, **Sundberg CW**. Single muscle fibre contractile function with ageing. *J Physiol* 600: 5005–5026, 2022. doi: 10.1113/JP282298.

2. **Stull JT**, **Kamm KE**, **Vandenboom R**. Myosin light chain kinase and the role of myosin light chain phosphorylation in skeletal muscle. *Arch Biochem Biophys* 510: 120–128, 2011. doi: 10.1016/j.abb.2011.01.017.

3. **Melby JA**, **Brown KA**, **Gregorich ZR**, **Roberts DS**, **Chapman EA**, **Ehlers LE**, **Gao Z**, **Larson EJ**, **Jin Y**, **Lopez JR**, **Hartung J**, **Zhu Y**, **McIlwain SJ**, **Wang D**, **Guo W**, **Diffee GM**, **Ge Y**. High sensitivity top–down proteomics captures single muscle cell heterogeneity in large proteoforms. *Proc Natl Acad Sci* 120: e2222081120, 2023. doi: 10.1073/pnas.2222081120.

4. **Wilson MC**, **Gao Z**, **Lopez JR**, **Zhu Y**, **Olszewski SS**, **Konopka AR**, **Diffee GM**, **Ge Y**. Top–Down Proteomics of Skinned Human Muscle Fibers Reveals Proteoform-Resolved Fiber-to-Fiber Variability. *J Mass Spectrom* 61: e70040, 2026. doi: 10.1002/jms.70040.

5. **Wei L**, **Gregorich ZR**, **Lin Z**, **Cai W**, **Jin Y**, **McKiernan SH**, **McIlwain S**, **Aiken JM**, **Moss RL**, **Diffee GM**, **Ge Y**. Novel Sarcopenia-related Alterations in Sarcomeric Protein Post-translational Modifications (PTMs) in Skeletal Muscles Identified by Top-down Proteomics *. *Mol Cell Proteomics* 17: 134–145, 2018. doi: 10.1074/mcp.RA117.000124.

6. **Kalinkovich A**, **Livshits G**. Sarcopenia--The search for emerging biomarkers. *Ageing Res Rev* 22: 58–71, 2015. doi: 10.1016/j.arr.2015.05.001.

Disclosure statement

Microsoft 365 Copilot (Microsoft, 2026), provided by the University of Wisconsin-Madison, was used only for minor sentence-level editing to improve grammar and clarity. This tool was not used to generate scientific content, interpret results, or influence conclusions.